Wnt7b and Its Direct Target *p57kip2* in Renal Medulla Development

LaToya Ann Roker
Philadelphia, Pennsylvania

Bachelor of Arts, Oberlin College, 2005

A Dissertation Presented to the Graduate Faculty
of the University of Virginia in Candidacy for the Degree of
Doctor of Philosophy

Department of Cell Biology

University of Virginia
May 2016

Abstract

The renal medulla is critical for urine concentration and maintaining the body's salt and water homeostasis. Its development and physiology are dependent on reciprocal signaling between different cell types. However, the way in which the various cells of the renal medulla orchestrate its development is not well understood. For this reason, my work focuses on Wnt7b, a Wnt ligand that is expressed in the ureteric bud (UB) epithelium that gives rise to the collecting ducts. Previous work demonstrated that Wnt7b promotes elongation of the medullary ureteric trunks through regulation of their oriented cell division, and elongation of the loop of Henle through regulation of their proliferation. Wnt7b was shown to signal through the canonical Wnt pathway to the renal interstitium. I set out to characterize the subset of interstitial cells in the medulla that are responsive to Wnt7b canonical Wnt pathway signaling, to identify the role of Wnt7b in their development, and to identify their roles in renal medulla formation. Here I present evidence that canonical Wnt target cells in the medulla are pericytes of the peri-UB capillaries, and that Wnt7b regulates the development of both these pericytes and of the endothelium these pericytes associate with in the renal medulla. In the nascent renal medulla, Wnt7b regulates the proliferation of peri-UB pericytes and endothelial cells, pericyte expression of *PDGFRβ*, and endothelial cell flattening and capillary lumen formation. To determine the mechanism by which Wnt7b directs renal medulla elongation, I also studied the role of p57kip2. Medullary peri-UB pericyte expression of p57kip2 is lost in *Wnt7b* mutants, and *p57kip2* mutants have a shorter renal medulla. Here I identify *p57kip2* as a direct transcriptional target of canonical Wnt signaling, and demonstrate that pericyte expression of p57kip2 is sufficient and necessary for renal

medulla elongation. Furthermore, I demonstrate that p57kip2 expression in the interstitium partially mediates Wnt7b's role in renal medulla elongation, likely via oriented cell division. My work shows that although p57kip2 is not a regulator of peri-UB capillary lumen formation, it does regulate proliferation of pericytes and endothelial cells. Importantly, my work on the function of p7kip2 that is expressed in the peri-UB capillary mural cells demonstrates the significance of this population of cells in renal medulla elongation, and the proliferation of the peri-UB capillaries, downstream of Wnt7b. Finally, I extended my work into the embryonic lungs to compare the functions of Wnt7b in capillary development in the kidney and lungs. My analysis of *Wnt7b* mutant lungs confirms the effect of Wnt7b on capillary lumen formation and on proliferation is tissue specific. Together, my work identifies additional cells types whose development is regulates by Wnt7b, and has begun to uncover the signaling pathways and tissue interactions regulating renal medulla formation.

Acknowledgements

This dissertation was made possible because of the support of many people. I would first like to thank my advisor, Jing Yu. The number of things she has taught me and the amount of support she has given me is too vast to fit on this page. I also thank my committee, Paul Adler, Todd Stukenberg, and Maria Luisa Sequeira Lopez, thank you for your insights and your support.

I would like to thank the past and present members of the Yu lab. Special thanks to Qun Ren, who generated the *R26Rp57kip2* mouse, and who generally helped me out a lot when I first joined the lab. Thank you to all of the undergraduate researchers who contributed to this work in large and small ways. Sam Kim, Katrina Nemri, Alexander Varzari, Isabella Liu, and Deborah Druckerman, thank you.

For their assistance, advice and equipment I thank The Advanced Microscopy Facility Staff, and the Gomez, Lu, Dwyer, and Yuan Labs. Thank you so much.

I acknowledge the financial support for this work; NIH Predoctoral Training Grant T32GM008136 and NIDDK 1R01DK085080S to L.A.R. and NIDDK 1R01DK085080 to J.Y.

I thank the Cell Biology department for their support. Thank you Mary Hall and the administrative staff members. Thank you Cell Biology graduate students, I couldn't have asked for a better group of people to travel with on this journey.

Dedication

For Mom. You were told that you weren't good enough to pursue the career you wanted to. In response you ignored that teacher and did it anyway. Thank you for teaching me perseverance despite the expectations of others.

For Dad. Losing you taught me a different kind of perseverance. I'm a stronger person now because of it, and I'm thankful for that. Thank you for all the time we had together.

List of Abbreviations

ADH	Antidiuretic hormone
ALK	Activin receptor-like kinase
APC	Adenomatous polyposis coli
AQP	Aquaporin
AVR	Ascending vasa recta
BMP	Bone morphogenetic protein
BMP	Bone Morphogenetic Protien
BWS	Beckwith Wiedemann Syndrome
CDK	Cyclin Dependent Kinase
CDKN1C	Cyclin Dependent Kinase Inhibitor 1C
ChIP	Chromatin Immuno-Precipitation
CKI	Cyclin Dependent Kinase Inhibitor
DVR	Descending vasa recta
E#	Embryonic day #
ECM	Extracellular Matrix
Epo	Erythropoetin
GBM	Glomerular Basement Membrane
GDNF	Glial cell line-derived neurotrophic factor
GFP	Green Flourescnet Protein
Gfrα	GDNF family receptor alpha
GSK3	Glycogen synthase kinase 3
HGF	Hepatocyte growth factor
Id2	Inhibitor of DNA binding 2
IMAGe	Intrauterine growth restriction, Metaphyseal dysplasia, Adrenal hypoplasia congenita and Genital anomalies
Itga3	Integrin α3
Itgα3	Integrin alpha 3
JG	Juxtaglomerular
Lef	Lymphoid enhancer-binding factor
LOH	Loop of Henle
LRP	Lipoprotien receptor-related protein
MT/MG	Membrane Tomato/ Membrane GFP
NO	Nitric oxide
OCD	Oriented Cell Division
P#	Postnatal day #
PCNA	Proliferating Cell Nuclear Antigen
PCR	Polymerase Chain Reaction
PDGFB/ PDGFRβ	Platelet derived growth factor B/receptor beta
RBPJ	Recombining binding protein suppressor of hairless
RSS	Russell Silver Syndrome
RV	Renal Vesicle
TCF	T-cell factor
TnC	Tenascin C

UB	Uretic Bud
VEGF	Vascular Endothelial Growth Factor
VEGF/VEGFr	Vascular endothelial growth factor
VEGFR	Vascular Endothelial Growth Factor Receptor
ZO-1	Zona Occludens 1

List of Figures

List of Tables

Chapter 1
Background

1.1 Physiology and structure of the adult kidney (the metanephric kidney)

The physiological function of the kidney includes removal of wastes and regulation of acid-base, salt, and water homeostasis.[1] The kidneys excrete excess water and waste from the blood into urine, while reabsorbing essential molecules such as glucose[2] and amino acids[3] into the blood stream. The renal epithelium organized into the renal tubules is essential for collection of the plasma filtrate and for reabsorption and secretion, while the renal vasculature delivers blood to the glomerulus for filtration and carries the reabsorbed nutrients to the rest of the body. Normal physiological function of the kidney requires specific organization of renal structures. This section provides an overview of kidney organization and physiology.

1.1.1 Organization of the kidney and the cortico-medullary axis

The structure of the kidney can be divided into two distinct regions histologically, the outer region is called the cortex and is recognizable by its light color. The inner region, which is darker in color, is called the medulla[4]. In humans, the medulla is divided into 8-12 pyramids, or papillae, which each extend into an opening termed the renal calyx.[4, 5] The calyces merge into the renal pelvis. Conversely, rodent kidneys house a single medullary pyramid which extends directly into the pelvis. The pelvis narrows as it reaches the hilum, defined as the opening at the medial surface of the kidney. The kidney is connected to the urinary tract via the transitional epithelium of the pelvis which connects to the ureter.[5]

The organization of the vasculature and the renal tubule system along this cortico-medullary axis is important for the kidney's physiological function. This organization

allows us to further classify the regions of the adult kidney based on the tubule components present (**Figure 1-1**). The cortex contains renal corpuscles which include glomeruli, convoluted tubules, and collecting ducts. The outer stripe of the outer medulla contains the thick limbs of the LOH and collecting ducts, while the inner stripe of the outer medulla contains some thick ascending limbs of the LOH, thin descending limbs and collecting ducts. Finally, the inner medulla is comprised of the thin limbs of the LOH and collecting ducts. The inner-most part of the medulla is sometimes also referred to as the papilla. The nephrons have varying LOH lengths based on their position along the cortico-medullary axis. The nephrons containing a cortical renal corpuscle, closer to the kidney surface, have shorter LOH that do not extend into the inner medulla. In humans there are some short cortical nephrons that do not extend into the medulla at all. The nephrons with their renal corpuscle located in the region of the cortex bordering the outer stripe of the renal medulla (juxtamedullary region) have long LOH that extend into the inner medulla. The renal corpuscles are the primary filtration units of the kidney, while each tubule segment has a different combination of ion channels to facilitate reabsorption and secretion. The collecting duct system is present in all compartments of the kidney, however the cellular composition and morphology of the collecting ducts is also organized along the cortico-medullary axis.[6]

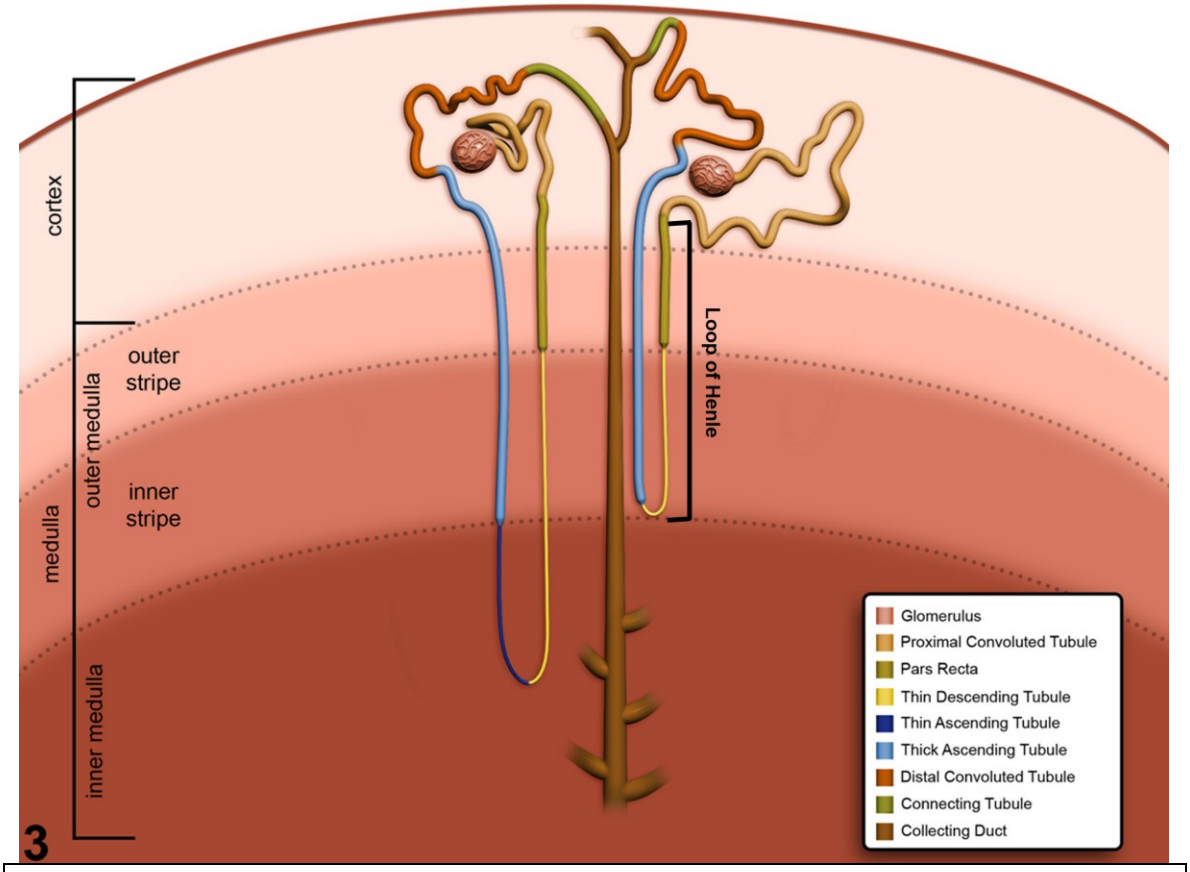

Figure 1-1 Organization of the kidney tubule structures along a cortico-medullary axis
This figure is adapted from Sands and Verlander, 2004[7]

1.1.2 Afferent vasculature and the glomerular filtration barrier

The renal vasculature, besides bringing nutrients to the organ tissues, must also direct blood to the renal filtration system. For this reason the kidney is heavily vascularized.[8] The renal artery is the major vessel which brings blood from the dorsal aorta into the kidney.[5, 8] In human kidneys, the renal artery branches into five segmental arteries before entering the kidney through the hilum. The segmental arteries enter the pelvic space and branch into lobar arteries then interlobar arteries. The interlobar arteries enter the kidney tissue at the cortico-medullary border. In unipapillate animals such as rodents, the renal artery branches once outside the kidney, giving rise to two or three renal arteries that enter through the hilum. These arteries branch at least once more

giving rise to interlobar arteries that enter the kidney tissue in rodents. For all of the species used to study the kidney, the arteries entering the kidney tissue are called interlobar, despite some of them only having one lobe.[8]

From this point the pattern of the arterial tree is conserved between species. The interlobar arteries produce the accurate arteries that run along the cortico-medullary border. The accurate arteries give rise to the interlobular arteries which extend upward toward the kidney surface. The smallest branches of the interlobular arteries produce afferent arterioles, which lead into the renal corpuscles (**Figure 1-2**).

The vascular component of the renal corpuscle is the glomerulus, where the endothelial cells form thin fenestrated capillary loops (**Figure 1-2**). The fenestrations are the pores through which the filtrate exits the bloodstream and enters the nephron tubules. The glomerular endothelial cells are supported by specialized mural cells called mesangial cells. Mesangial cells can regulate filtration through their contractile properties and maintenance of the extracellular matrix.[9] The glomerulus is surrounded by the glomerular basement membrane (GBM) which is the main barrier for filtration. The GBM has three layers of lamina visible by TEM and carries a negative charge.[10, 11]

Another key mediator of the filtration barrier is the podocyte (**Figure 1-2**). Podocytes are the visceral epithelial cells that extend foot processes into the GBM.[10, 11] The space in between each foot is bridged with a thin membrane called the slit diaphragm.[12] The slit diaphragm is a modified adherens junction that expresses tight junction marker ZO-1[13, 14], Nephrin, CD2AP, and Podocin[15] as part of a specialized junctional complex. Disruption of this complex is linked to proteinuria, highlighting the importance of the slight diaphragm for filtration.[15] The basal surface of the podocytes are

embedded in the GBM,[10, 11] while the apical surface is negatively charged due to negatively charged proteins which make up the glycocalyx layer.[16, 17] One major component of the glycocalyx is Podocalyxin.[18, 19] Podocytes also secrete VEGF, which promotes endothelial cell permeability by inducing the formation of fenestrae in the endothelial cells of the capillary loops.[20-24] The podocytes form one side, the visceral layer, of an epithelial structure termed the Bowman's capsule. The other side of Bowman's capsule is a sheet of the parietal epithelium that forms the outer border of the renal corpuscle. The lumenal space between the podocytes and the parietal epithelium is described as the Bowman's space.

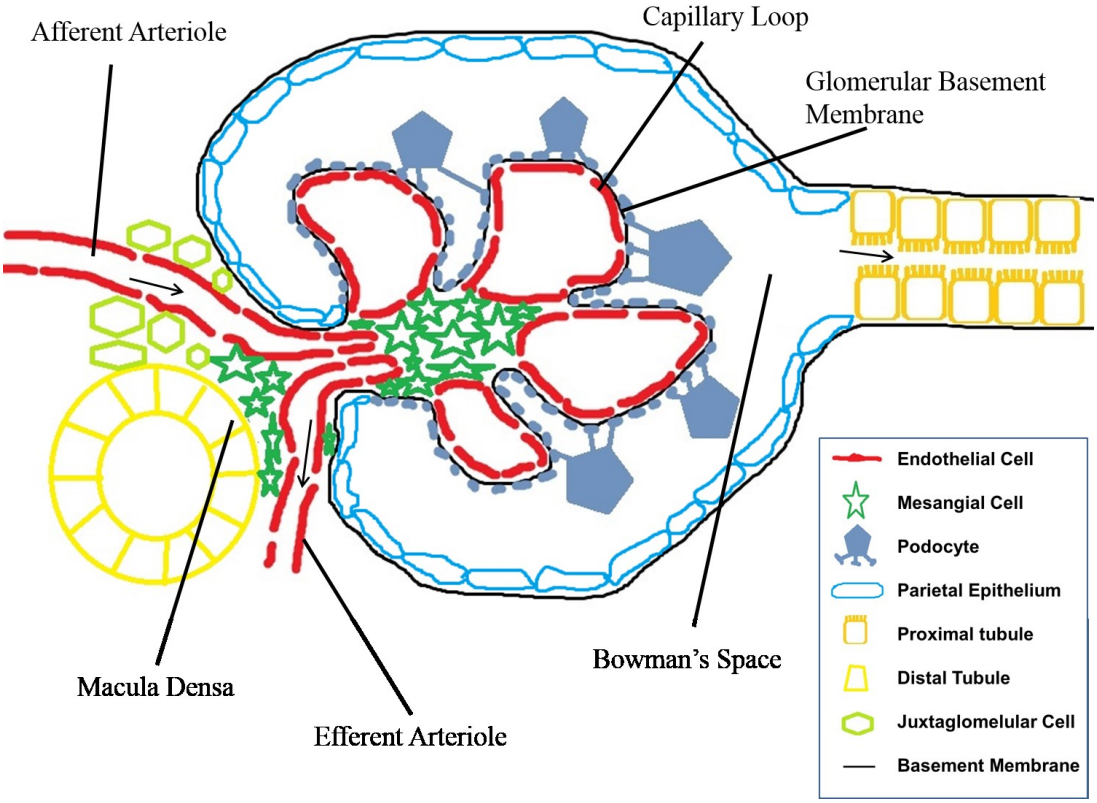

Figure 1-2 The renal corpuscle and its neighboring structures
The renal corpuscle includes the capillary loops (glomerulus), mesangial cells, podocytes, and parietal epithelium. Adjacent to the renal corpuscle on the left side of the figure, the macula densa, JG cells, and the extraglomerular mesangial cells comprise the Juxtaglomerular apparatus. The right side of the figure shows the proximal tubule, through which the filtrate exits the renal corpuscle.

1.1.3 The nephron epithelium

After primary filtration at the renal corpuscle, reabsorption and concentration of urine occurs via a series of tubules (**Figure 1-1**). The nephron tubule components of this system are; from the proximal (closest to the renal corpuscle) to the distal end; proximal tubule, loop of Henle (LOH), distal tubule, and connecting tubule. The connecting tubule leads to the collecting duct system which includes; the cortical collecting duct, the medullary collecting duct and the inner medullary collecting duct.

The first tubule that the primary filtrate passes through is the proximal tubule, which is directly connected to Bowman's capsule. The proximal tubule is comprised of cuboidal epithelium with numerous microvilli on their apical surface, collectively termed the brush border. The increased surface area provided by the brush border enhances the absorption and flow-sensing functions of the proximal tubule.[25] All of the glucose and amino acids are reabsorbed at the proximal tubules, as well as most of the Na+. Secreted molecules include ammonia,[26, 27] and creatinine. The brush border also has the ability to adjust the absorption rate of the proximal tubules based on the flow of filtrate from the glomerulus.[28] Pars recta (the proximal straight tubule) is a portion of the proximal tubule that descends into the outer medulla. The border between the pars recta and the thin descending LOH designates the border between the outer medulla and inner medulla.

The loop of Henle (LOH) runs from the proximal tubule to the distal tubule. It has a U-shape such that the structure extends down into the medulla then back up to the cortex. The descending thin limb of the LOH varies in length depending on the position of the loop turn along the cortico-medullary axis. Additionally, the cell shape of the descending thin limb epithelium depends on its location along the cortico-medullary

axis.[29] The thin descending limb passively absorbs water and is impermeable to the sodium ion, while the thin ascending limb is impermeable to water, but permeable to ions. In the thick ascending limb, sodium, potassium and chloride are actively reabsorbed via the Na-K-2Cl co-transporter.[30-32] Because the thick ascending limb is impermeable to water, only the ions move to the interstitial space, creating increased osmolality in the interstitial space. The thin descending limb neighbors the ascending limb in the medulla (**Figure1-1**). In response to the high osmolality in its environment, the thin descending limb draws water from the luminal space out into the interstitial space. As a result, the filtrate inside the thin descending limb becomes more concentrated and hyperosmotic. The medulla as a whole becomes hyperosmotic, and an osmolality gradient is established where the deeper the medulla, the higher the osmolality.[33]

The distal convoluted tubule consists of cuboidal epithelium with no brush border. It actively reabsorbs sodium via NaCl co-transporter.[34] Distal convoluted tubule cells are mitochondria-rich,[35] which belies their heavy transport activity. Absorption in the distal convoluted tubule can be regulated by hormones such as aldosterone and ADH.[36] The distal convoluted tubule is located in the cortex next to the renal corpuscle of the same nephron (**Figure 1-1**). The part of the distal convoluted tubule that abuts the renal corpuscle, the macula densa (**Figure 1-2**), and the closely associated juxtaglomerular (JG) cells, as well as the extraglomerular mesangium comprise the juxtaglomerular apparatus, which regulates blood flow. In this structure, the macula densa senses the salt concentration in the distal convoluted tubule and promotes vasodilation or vasoconstriction of the arteries to adjust glomerular filtration rate accordingly.[37] JG cells secrete Renin in response to low salt levels as a part of this feedback regulation.[38, 39]

1.1.4 The connecting tubule and collecting duct system

The connecting tubule is a heterogeneous structure that links the nephron epithelium to the collecting duct system. This tubule contains cells from the distal convoluted tubule and the collecting duct.

The collecting duct cellular morphology is more cuboidal in the cortex and columnar in the medulla. Additionally, the collecting duct contains two specialized cell types, principal and intercalated cells. Principal cells reabsorb sodium and secrete potassium via ENaC and reabsorb water via Aquaporin 2(AQP2).[40] ENaC is regulated by aldosterone[41] while AQP2 is regulated by vassopressin[42]. Intercalated cells, which are important for acid base balance,[43, 44] comprise 1/3 of the cortical collecting duct cell population. The proportion of intercalated cells decrease gradually to 10% in the papillary collecting duct.[6] The diameter of the collecting duct is also larger towards the papilla.

1.1.5 Efferent arterioles and the post-glomerular capillary beds

From the glomerulus, efferent arterioles of the cortical nephrons give rise to the peritubular capillaries surrounding the proximal and distal tubules. The cortical peritubular capillaries supply blood and nutrients to the cortical tissue. They also take up the fluids and ions that were reabsorbed by the tubules and reintroduce them in to the bloodstream. Efferent arterioles of the juxtamedullary nephrons give rise to the main blood supply for the medulla, the vasa recta. The vasa recta are straight capillaries running parallel to the LOH and collecting ducts. Like the LOH, they have a descending and ascending component. Descending vasa recta (DVR) and ascending vasa recta (AVR) are organized with the LOH in vascular bundles.[45, 46] The vasa recta is critical for

the maintenance of the osmolality gradient in the medulla. DVR are specialized endothelium because they express Aquaporin1 and Urea Transporter,[47-49] indicating they perform an active role in salt and water balance. Blood flow to the medulla is regulated by prostaglandins and nitric oxide, which control vasodilation. Without proper vasodilation, reduction of medullary blood flow leads to salt retention and hypertension.[50-54] In rodents, capillaries form interstitial nodal spaces throughout the inner medulla, but this structure is less frequent in humans.[55]

1.1.6 Interstitial cells

The renal interstitium is loosely defined as all of the space outside of tubules, blood vessels and glomeruli. Lymphatics and microvessels have been considered as part of the interstitium, but microvessels can also be considered as separate from the interstitium.[56] Dendritic cells are also considered part of the interstitium.[56, 57] The cortical interstitium and medullary interstitium are structurally distinct, but how that relates to a difference in function is not well understood.[56-58] In adult kidney much focus has been on interstitial cells as a source of fibrosis.[57, 59, 60] Several specialized cells in the cortical interstitium have also been described, a few examples of which are given below.

Erythropoietin (Epo) producing cells reside in the peritubular cortical interstitium.[61] Epo is a hematopoietic growth factor, responsible for the proliferation, differentiation, and survival of red blood cells. Transcription of Epo is promoted in hypoxic conditions,[62, 63] and Epo deficiency is linked with anemia in chronic kidney disease.[64, 65]

Another specialized cell type in the cortical interstitium is renin expressing cells.[66] Renin is expressed mainly by juxtaglomerular cells in response to a change in renal

homeostasis such as dehydration or hypertension.[38, 39] Renin is an enzyme that hydrolyzes angiotensinogen to angiotensin I, which regulates blood pressure and fluid homeostasis.[67] Renin cells can differentiate and contribute to smooth muscle, mesangial cells, Bowman's capsule, and proximal tubules; and when homeostasis is disturbed, the former renin cells can de-differentiate and express renin again.[68]

1.2 Kidney development

Kidney development is a complex process involving two separate tubulogenic events; branching morphogenesis of the uretic bud to establish the renal collecting duct system and mesenchymal to epithelial transition to generate the nephron epithelium.[69] Kidney development also involves migration and differentiation of the interstitial cells,[70-72] a cell population that has not been fully characterized. Signaling between the various progenitor compartments is essential for normal kidney development.[73] This section broadly describes renal development, with a brief introduction of some of the signaling pathways involved.

1.2.1 The ureteric bud: branching and elongation

Kidney development starts in mice at E10.5 when the ureteric bud epithelium protrudes from the Wolfian duct and invades the neighboring metanephric mesenchyme.[74-76] The metanephric mesenchyme induces a process called branching morphogenesis at the tip of the UB epithelium.[77] The first branching event forms a T-shaped structure, now with two tips. The UB continues to branch, increasing the number of tips, while elongation occurs of the UB trunks (**Figure 1-2A**). This process, branching

morphogenesis, establishes the collecting duct network and the sites of nephron differentiation.

The major signaling pathway for UB branching Morphogenesis is GDNF-Ret signaling. GDNF is expressed in the metanephric mesenchyme and signals to its receptors Ret and Gfrα in the ureteric tips.[78-81] Gdnf, Ret, or Gfrα1 mutant exhibited failed branching morphogenesis and kidney agenesis.[82-86] Furthermore, Wnt11 and Ret double heterozygotes have less glomeruli than the Wnt11 mutant,[87] indicating a synergistic genetic interaction between Wnt11 and GDNF-Ret signaling.

At E13.5 the lengths of the UB trunks between branch points are consistent throughout the kidney, however at E14.5, the interbranch regions of the more distal UB epithelium (closer to the ureter and future pelvic space) elongate.[70, 88] Concurrently, the ureter swells in the region where it meets the UB epithelium. At E15.5 a pelvic space has started to form and the UB trunks from the first few branching events are positioned so that they open into the pelvic space. This designates the onset of renal medulla formation (**Figure 1-2B**). From E15.5 until several days after birth, the medullary UB continues to elongate along a cortical-medullary axis.

Defects in branching morphogenesis can lead to renal medulla dysplasia or hypoplasia. Mice with the expression of BMP receptor ALK3 removed from the UB exhibited increased branching at earlier stages, followed by decreased tertiary branching at later stages and a decreased number of collecting ducts.[89] Adult kidneys had dilated collecting ducts and the medulla was absent.[89] This mouse model highlights how the initial branching events are important for subsequent growth and patterning of the collecting ducts.

Proper oxygenation from the vasculature is also important for normal renal medulla development. Mice lacking *Cited1* expression in the placenta have renal medullary dysplasia due to hypoxia induced apoptosis.[90] *Sox17; Sox18* double mutants have an atrophied outer medulla, due to loss of vasa recta in that region.[91]

The basement membrane is important for collecting duct development.[92, 93] Mice deficient in laminin in their UBs had defects at multiple stages of UB development and maturation, including branching, proliferation, and water transport postnatally.[93] The collecting ducts of *Wnt5a* mutant mice have various UB branching defects in conjunction with thicker basal lamina and lowered expression of several basement membrane components.[92]

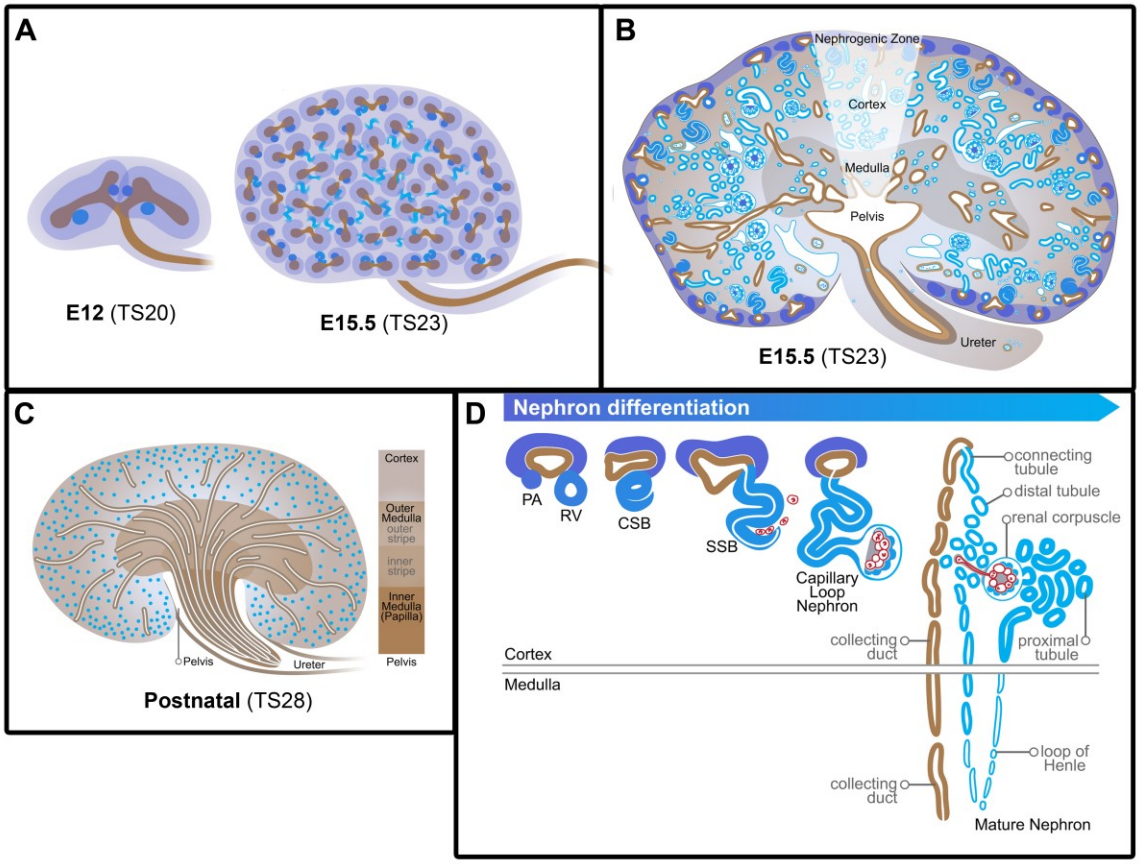

Figure 1-3 Development of the murine renal epithelia

Images were obtained from the GUDMAP database (http://www.gudmap.org/Schematics).[94] Originally designed by Kylie Georgas, University of Queensland

(A) The ureteric bud epithelium, in brown, undergoes multiple branching events. Pretubular aggregates, blue, are also visible from E12.5. (B) At E15.5 the UB epithelia, in brown, open into the pelvic space. The medulla contains UB trunks and loops of Henle, the cortex contains mature glomeruli closer to the medulla and immature glomeruli farther away from the medulla. The most cortical region is the nephrogenic zone. (C) Postnatally, the medulla extends out of the kidney, and can be divided into three regions (see also fig1-1). (D) Nephron differentiation. The condensed mesenchyme progenitor population is represented in purple, the induced nephron epithelium in blue. Endothelial cells are red. UB epithelium is brown.

1.2.2 Induction and differentiation of the nephron epithelium

Upon contact at E10.5, the ureteric bud epithelium induces the Six2+ subset of the metanephric mesenchyme to condense around the UB tips.[95] This population of the metanephric mesenchyme, which has also been referred to as the condensed mesenchyme or the cap mesenchyme, is a multipotent, self-renewing population that gives rise to all epithelial components of the nephon.[95] The cap mesenchyme that is Six2+ and Cited1+ remain in the nephron progenitor pool.[96] In contrast, the Six2+ Wnt4+ cells in the cap mesenchyme are committed to nephrogenesis.[95] In response to *Wnt9b* signal from the UB tips, the committed cells then down-regulate *Six2*, upregulate *Wnt4* and many other factors, and condenses further under the UB tips to make a structure called the pretubular aggregate.[97-102] The structure undergoes a mesenchyme to epithelial transition (MET) to become the renal vesicle, and after a series of morphological changes differentiates into the nephron.[77] Although the earliest differentiation from pretubular aggregate is at E12.5, as the UB continues to branch new nephrons continue to differentiate at the newly formed UB tips, in a process that continues throughout development.[88, 95, 103]

The earliest nephron epithelial structure, the renal vesicle (RV), expresses different gene combinations along a proximal to distal axis, specifying the different segments of the future nephron.[104, 105] The distal end of the RV and the UB epithelium merge along with some Six2+ cells to make the connecting tubule.[106] The proximal

portion of the renal vesicle elongates, changing the shape of the epithelial structure from renal vesicle to a comma shape and then S-shape. The S-shaped body has a proximal, medial and distal segment. The proximal segment becomes the glomerular epithelium and the proximal tubule, while the medial and distal segments become the distal tubule and the Loop of Henle (LOH). Notch signaling in conjunction with RBP-J mediates specification of the proximal portion of the nephron.[107, 108] Lgr5+ cells in the medial segment of the S-shaped body give rise to the thick ascending LOH as well as the distal convoluted tubule.[109] The first nephrons with capillary loops are visible at E15.5, but new nephrons continue to be induced throughout development. The cap mesenchyme is gone by P3.[110]

1.2.3 The stroma and its descendant interstitial cells

Upon the initiation of UB branching morphogenesis, the metanephric mesenchyme consists of two distinct progenitor compartments; the Six2+ cells (discussed in section 1.2.2) and the Foxd1+ stromal cells.[95, 111] While Foxd1 expression itself is restricted to the stromal cells surrounding the cap mesenchyme the descendant cells of the Foxd1+ stroma are found throughout the kidney and include: PDGFRβ+ mesangial cells in the glomerulus, PDGFRβ+ pericytes in the cortex, the vascular smooth muscle cells, the renin cells, the cortical interstitium, p57kip2 expressing interstitial cells in the medulla and p57kip2 negative interstitial cells in the medulla.[111, 112] Lineage tracing of Foxd1+ cells with tamoxifen induced labeling at different developmental stages indicate the Foxd1+ stromal cells are a continuously renewing stem cell population.[111] Further, they contribute to stromal lineages in a temporally restricted manner, such that the

earliest labeled cells contribute to the distal-most region (the medulla tip) and the latest labeled cells contribute to the cortex.

The Foxd1+ stroma is important for branching morphogenesis and nephrogenesis. Stromal expression of retinoic acid modulates GDNF-Ret signaling and promotes branching morphogenesis.[113] Stroma expressed angiotensin II also promotes GDNF-Ret signaling.[114] Foxd1 itself is important for nephron differentiation.[115] When *Foxd1* was deleted in mice, the stroma lost expression of progenitor markers and gained expression of differentiation markers such as PDGFRβ.[115] This indicates Foxd1 is important for maintenance of the stromal progenitor state, and that the progenitor stromal cells are necessary for nephron maturation. Supporting this conclusion, ablation of the stroma with diphtheria toxin A (*Foxd1Cre;DTA*) leads to arrested nephrogenesis.[72]

Foxd1Cre;DTA mice also exhibit ectopic vasculature in the nephrogenic zone,[72] and *Foxd1* null mutants had endothelial cells in the capsule, as well as fully differentiated arteries.[112, 116] This indicates that stromal cells are required for vascular patterning. The mural cells in the kidney, which are descendants of the stromal cells, are also required for normal development of the vasculature (discussed in section 1.2.4 and section 1.3.3).

The medullary interstitium expresses several genes that are important for renal medulla development, including *β-catenin*, *Pod1*, and *p57kip2*.[70, 117-119] Chapter 4 further discusses the role of p57kip2 in renal medulla development.

1.2.4 Renal endothelial cells and glomerulus maturation

The vascular network develops concurrently with the epithelium, and is established through vasculogenesis and later refined via angiogenesis.[120-125] Vessels are detected as early as E12.5, before the arterioles are detected, indicating that

vasculogenesis occurs in the kidney.[123] In fact, a recent study has shown that SCL/Tal1+ cells present in the metanephric mesenchyme at E12.5 give rise to endothelial cells in the renal artery, veins, glomerular capillaries, arterioles, and peritubular capillaries.[126] At E18.5 the arterial network is visible, and it continues to grow via branching and elongation until about one week postnatally.[123] Postnatal branching is regulated by the renin-angiotensin system.[127]

When nephron precursors are at the S-shaped body stage, angioblasts invade the vascular cleft to eventually differentiate into the capillary loops. The vascular cleft is located in the lower region of the S-shaped body, next to the podocytes. VEGF secreted by the podocytes acts as a chemoattractant for the migrating endothelial cells.[128] Maturation of the endothelial cells into a capillary loop requires signaling to and from the mesangial cells. Deletion of the Notch pathway effector, *RBPJ*, in FoxD1+ renal stromal progenitors leads to the absence of mesangial cells from the glomerulus and dilated glomerular capillaries.[71, 129] Deletion of *pdgfb* from the endothelial cells or *pdgfrb* from the mesangial cells also leads to a deformed glomerular capillary, due to the failure in the migration of mesangial cells into the vascular cleft.[130-132]

The development of the vasa recta is likely dependent on signals from the neighboring epithelial tubules. VEGF secretion from renal tubules mediates AngiotensinII dependent vasa recta development postnatally.[133] However, vasa recta development in embryonic stages has not been studied.

1.3 Development of endothelial cells and mural cells

The vasculature is important for distributing oxygen, nutrients, hormones, and immune cells throughout the body. The two major categories of vasculature are lymphatic vessels and blood vessels. Lymphatic vessels function to drain excess fluid from interstitial spaces.[134] In the adult kidney they are present abundantly in the cortex, around the nephron tubule and the glomerulus, and sparingly in the outer medulla neighboring the cortex.[135] Lymphatics are absent in the inner medulla, where fluid is absorbed into the vasa recta instead.[135, 136] This section will focus on development of the blood vessels and their support cells or mural cells.

1.3.1 Angiogenesis and vasculogenesis

The two main processes through which blood vessels form are vasculogenesis and angiogenesis. Vasculogenesis is the de novo formation of blood vessels from endothelial progenitor cells, termed angioblasts. The initial vascular plexus forms through vasculogenesis from angioblasts located in the yolk sac islands[137] and in the mesoderm.[138] VEGFR2 (also known as Flk1) is expressed in angioblasts and is required for vasculogenesis.[138-141] The angioblasts cluster together and form cords. Each cord then becomes a tube by forming a lumen and a basal lamina.[142] In addition to formation of the vascular plexus, vasculogenesis has been shown to occur within organs such as the liver, spleen and lung.[142, 143]

Angiogenesis describes the growth of new vasculature from preexisting vessels. In response to an angiogenic signal, the basement membrane of the existing vessel is broken down, and specialized endothelial cells called tip cells migrate toward the signal.[144] For example in hypoxia, cells will express VEGFA to induce angiogenesis, while VEGFR2 is expressed at the filopodia of the tip cells, making then sensitive to

changes in VEGF concentration.[145-147] Stalk cells are attached to the tip cell and trail behind. The stalk cells undergo proliferation to extend the new vessel. Notch signaling downstream of VEGF represses the VEGFR2 expression in the stalk cells.[145, 148, 149] Tube formation, mural cell association and finally basement membrane deposition mark the formation of the new vessel.

1.3.2 Vascular lumen formation

Angioblasts must undergo tubulogenesis, or vascular lumen formation to form a functional, mature blood vessel. During this stage, angioblasts change shape from cuboidal to flattened, and rearrange their junctions to the lateral sides of the cells.[150] Tubulogenesis was historically considered to occur mainly though vesicle or vacuole fusion,[151] however a number of studies describe a mechanism of membrane repulsion and/or junction remodeling. In mouse dorsal aorta cell flattening is VE-cadherin dependent, and lumen formation is driven by recruitment of negatively charged sialomucins to the luminal surface.[152] A similar mechanism is present in *Drosophila* heart tube formation, where Slit-Robo signaling mediates repulsion at the luminal surface.[153] Ras interacting protein 1 (Rasip1) is also required for lumen formation in mouse. Depletion of Rasip in culture leads to an abnormal increase in RhoA/ROCK/MyosinII signaling, mislocalization of Par3, and ectopic apical junctions.

1.3.3 Endothelial-mural cell communication

Several signaling pathways are known to be important for mural cell recruitment to the endothelium. The ligand platelet-derived growth factor B (PDGFB) is expressed in the endothelial cells while its receptor PDGF receptor beta (PDGFRβ) is expressed in

mural cells.[132, 154] Lack of either molecule causes loss of mural cells, and blood vessel instability.[131] The Angiopoetin (Ang) family of growth factors is expressed in the mural cells, while its receptor, Tie2, is expressed in endothelial cells.[155-158] *Tie2* mutant blood vessels lack mural cell associations, and mice have hemorrhage and die at E9.5.[159, 160]

Maturation of the endothelial cells and mural cells is also regulated by many different factors. TGFβ signaling can promote or inhibit endothelial cell migration, proliferation and differentiation depending on expression levels and receptors.[161] Removal of *Alk1*, a TGFβ receptor that is specifically expressed in endothelial cells,[162] causes defects in vessel remodeling and hematopoiesis.[163] *Notch3* mutants have altered morphology of vascular smooth muscle cells (VSM), and poor association of VSM cells to vessels.[164] Interestingly, Notch3 also promotes PDGFRβ expression.[165]

1.4 Known roles of Wnt7b

Wnt7b is a secreted Wnt ligand that has been shown to act via canonical,[166, 167] non-canonical PCP (Planar Cell Polarity),[168] and non-canonical G-protein coupled pathways.[169] *Wnt7b* has three isoforms that share a common exon 2 and 3, one of the isoforms has a different exon 1.[170] The other two isoforms' mRNA share the exon1 sequence but have a different translation start site, causing difference in the region of the protein translated from exon1.[171] Wnt7b regulates the development of multiple tissues, with striking diversity in target cells and cellular mechanisms.[70, 166, 168-170, 172-182] In this section I will discuss in detail Wnt7b role in kidney, lung and other systems.

1.4.1 Wnt7b is required for renal medulla formation

Wnt7b is expressed in the non-branching uretic trunk epithelium, which gives rise to the ureter and collecting duct system of the kidney. Conditional knockouts of *Wnt7b* exhibit defective oriented cell division in the UB trunks, decreased proliferation in the LOH and failure to form the renal medulla.[70] Starting from the onset of renal medulla development, E15.5, mutant kidneys displayed dilated UB in the nascent medulla, and from E16.5 onward cortical structures were observed directly abutting the renal pelvis.[70] The histology of the cortex was normal, and analysis of several markers of cortical development showed that uretic branching, nephron induction, and nephron patterning were normal in *Wnt7b* mutant kidneys despite the absence of a renal medulla.[70] At P10 *Wnt7b* mutant urine osmolality was 56% that of control mice; within the next few days the mice die, most likely from dehydration.[70]

Wnt7b expression in the kidney is regulated by Integrin α3 (Itα3) in conjunction with c-Met.[171] When *Itα3* expression was removed from the entire kidney or conditionally from collecting ducts, the inner medulla did not fully elongate.[171, 183] Interestingly, this is a less severe phenotype than *Wnt7b* mutants. This is likely because Itα3 only regulates two of the three isoforms of *Wnt7b*. c-Met binds to integrin, and treatment with HGF (the ligand for c-met) promoted transcription of all three *Wnt7b* isoforms.[171] On the other hand, Itα3 expression did not change in *Wnt7b* mutants, indicating the absence of a feedback loop.

Wnt7b regulates renal medulla elongation by activation of canonical Wnt signaling in the neighboring medullary interstitial cells.[70] In the canonical Wnt pathway the Wnt ligand binds to its receptor Frizzled, which is a multipass transmembrane

receptor.[184] In vertebrates Frizzled forms a complex with co-receptor LRP5 or LRP6,[185] resulting in the stabilization of β-catenin. In the absence of Wnt signal, β-catenin is recruited by the "destruction complex" consisting of Axin, Glycogen Synthase Kinase-3 (GSK3) and Adenomatosis Polyposis Coli (APC). β-catenin enters the nucleus and binds transcription factors of the TCF/Lef family[186-189] and activates target genes. Wnt7b-depentent expression of the canonical Wnt pathway components and targets Lef1 and *Axin2* are detected in the medullary interstitium, and when *β-catenin* was removed from the interstitial cells, renal medulla failed to form.[70] Conversely, deletion of canonical Wnt pathway agonist *Dkk1* led to increased expression of Lef1 in the interstitium and a longer medulla.[178]

Another gene that causes a shorter renal medulla when lost is *p57kip2*.[117] In *Wnt7b* mutants, p57kip2 expression was lost in the medullary interstitium yet unchanged in the podocytes.[70] These data suggest p57kip2 is a downstream mediator of Wnt7b role in renal medulla elongation (p57kip2 is discussed in section 1.5).

1.4.2 Wnt7b regulates lung proliferation and vessel stability

In the lung, *Wnt7b* is expressed in the tips of the branching lung bud epithelium (future airway epithelium).[190, 191] Similar to the kidney, the lung is an organ that undergoes branching morphogenesis, and the branching epithelium exchanges signals with its surrounding mesenchyme to coordinate lung growth.[192] Lung development starts at E9.5, when the primary lung buds emerge from the foregut endoderm, into the mesodermally derived mesenchyme.[193] E9.5 to E16.5 (pseudoglandular stage) is marked by highly stereotyped branching.[194, 195] E16.5 to E17.5 marks the canalicular stage, defined by the narrowing of the terminal buds. During this time the distal airway

epithelium begins to differentiate into specialized alveolar cells.[196] The saccular stage, when the alveoli mature, starts at E18.5 and continues postnatally.[197] Branching morphogenesis does not continue after birth, but the epithelial tubes increase in both length and diameter, thus increasing the organ size postnataly.[197, 198] The mesenchyme is not as well studied as the endothelium, but it is thought to give rise to vascular smooth muscles[199] and endothelial cells.[200, 201] Wnt7b's role in lung development was examined by detailed characterization of two mouse models. In the *Wn7b*$^{LacZ-/-}$ mouse, one of the two alternative exon1 was replaced by *LacZ*.[179] This mouse is likely a hypomorph, due to alternative splicing.[170] A mouse generated with exon3 deleted (D3) was a true null and died at E9.5 due to a placental defect.[170] Thus a conditional version of the gene, *Wnt7bC3*, was generated and used to study *Wnt7b* functions in several tissues, including in the lung.[170]

1.4.2.1 *Wnt7b*$^{LacZ-/-}$ mouse exhibits defects in vascular differentiation, airway differentiation, and proliferation

Wnt7b$^{LacZ-/-}$ mice were born with smaller lungs that exhibited hemorrhage and collapsed distal airways that failed to fill with air, causing neonates to die shortly after birth.[179] Examination of lungs during the pseudoglandular stage revealed abnormally small lungs at E12.5.[179] E12.5 mutant lungs also had reduced proliferation of the mesenchyme surrounding the lung bud tip, but not the tip itself, resulting in a thinner mesenchyme layer that was evident at both E12.5 and E14.5.[179] Examination of the canalicular/saccular stages revealed failed differentiation of the alveolar epithelial type I cells, the major cell type responsible for gas exchange, at E18.5.[179, 193] The major blood

vessels at E18.5 had no change in proliferation, but exhibited a thicker vessel wall compared to wildtype as well as dilation of the vessels and decreased branching.[179]

Analysis of the molecular mechanism of Wnt7b function in *Wnt7b*$^{LacZ-/-}$ mice demonstrated that Wnt7b regulates the development of smooth muscle precursors.[202] In the lung, smooth muscle cells support major arteries as well as surround the airway epithelium.[193] Wnt7b expression in the epithelium and β-catenin expression in the smooth muscle cells were shown to promote expression of SM22a (a smooth muscle specific protein), PDGFRα and PDGFRβ in smooth muscle precursor cells.[202] Tenascin C (TnC), an ECM protein expressed in the mesenchyme, was shown to be a direct target of the canonical Wnt signal, and was both necessary and sufficient for PDGFRα and PDGFRβ expression in lung explants.[202]

1.4.2.2 *Wnt7bC3* mice with complete ablation of Wnt7b function in the embryo proper have decreased proliferation resulting in severe hypoplasia

Mice with *Wnt7b* completely removed from embryonic tissues but not the placenta (*Wnt7b*$^{c3/-}$*;Sox2Cre*) die shortly after birth.[170] Compared with the hypomorphic *Wnt7b*$^{LacZ-/-}$ mutants, they had less severe hemorrhage in major vessels. However hemorrhage was observed in alveolar capillaries, unlike *Wnt7b*$^{LacZ-/-}$ mutants.[170, 179] Compared to wildtype, *Wnt7b*$^{c3/-}$*;Sox2Cre* lungs were smaller and poorly inflated.[170] Smaller lungs were observed in the mutant from E12.5.[170] The mutant lungs exhibited decreased proliferation in both the mesenchyme and the epithelial cells, resulting in lungs with fewer epithelial tips and thinner mesenchyme surrounding the tips.[170] Interestingly no patterning defect, epithelial differentiation, or smooth muscle differentiation defect was detected.[170]

In wildtype lungs, canonical Wnt target Axin2 is expressed in both the epithelium tips and the mesenchyme surrounding the tips, while Lef1 is expressed only in the mesenchyme.[170, 203-205] Expression of Axin2 and Lef1 was lost in the *Wnt7b*$^{c3/-}$*;Sox2Cre* mutant lungs.[170] Furthermore, expression of Bmp4 and Id2 in the tips were lost in the mutants. BMP4 is a known regulator of proliferation in distal lung epithelial cells,[206] thus it is a likely mediator of Wnt7b's regulation of proliferation in the epithelium. In short, Wnt7b directs proliferation in lung through a canonical paracrine signal to the mesenchyme and a canonical autocrine signal to Bmp4 and Id2 in the epithelium.[170]

1.4.3 The diverse roles of Wnt7b in other tissues

Studies in the pancreas illustrate that the response to Wnt7b signaling is both cell type specific and dynamic.[172] In the pancreas, deletion of *Wnt7b* expressed in the epithelial cells causes reduced proliferation of the epithelial progenitor cells and decreased organ size, whereas overexpression of *Wnt7b* at the onset of pancreas development prevented specification of the epithelial tip and trunk progenitor cells, resulting in disrupted branching morphogenesis. At a later stage, extreme dilation of the epithelium was reported. When *Wnt7b* overexpression was induced later in pancreas development, the epithelial cell differentiation was rescued, but the organ size was smaller. Interestingly, the neighboring mesenchyme exhibited increased proliferation, and increased expression of Lef1, cFos and Desmin.[172]

Wnt7b signals to vascular endothelial cells in several tissues. In the brain, Wnt7b expressed in epithelium promotes angiogenesis and maintenance of the blood brain barrier.[182] In the eye, Wnt7b expressed in macrophages signals to endothelial cells of the hyaloid vasculature, inducing their programmed cell death that is necessary for vascular

remodeling.[166] Conversely, in breast cancer tumors, Wnt7b expressed in macrophages promotes angiogenesis and tumor growth.[207] Together, these studies show how Wnt7b can signal to the same cell type but have a different effect based on the tissue context.

1.5 p57kip2 structure and function

p57kip2 is a cyclin dependent kinase inhibitor (CKI)[208] that has been implicated in non-CKI related functions such as transcription, apoptosis and migration, and differentiation.[117, 209-211] p57kip2 is expressed in several organs during development, and it is the only CKI that has a developmental defects when knocked out, including defects in abdominal wall, bone, palate, eye adrenal gland, and kidney.[117, 212] This section is an overview of p57kip2 structure and function.

1.5.1 p57kip2 has conserved and unique domains

p57kip2 is transcribed from *Cdkn1c*, a maternally imprinted gene located on mouse chromosome 7 and human chromosome 11p15.[213-217] *Cdkn1c* mRNA undergoes alternative splicing and produces three transcripts.[214] This variant splicing is conserved from rodents to humans and produces heterogeneity in the amino terminus of p57kip2 protein.[214, 218] Downstream of the amino terminus, murine p57kip2 has 4 domains; (I) a cyclin dependent kinase (CDK) inhibitory domain similar to p21 and p27, (II) a proline rich domain containing a MAP kinase phosphorylation site, (III) an acidic domain containing tandem repeats of a 4 amino acid sequence, and (IV) a c-terminal domain similar to p27 containing a CDK phosphorylation site and a nuclear localization signal.[214,

[216] In humans, domains I and IV are conserved, but domains II and III are replaced with a single domain of proline-alanine repeats (PAPA domain).

1.5.2 p57kip2 in cell division

p57kip2 is a member of the CIP/KIP family of cell cycle inhibitors, which inhibit the G1 to S phase transition.[208, 214, 216] CIP/KIP broadly binds G1and S complexes; including cyclin E-CDK2, cyclin D2-CDK4, and cyclin A-CDK2.[214, 216, 219] At low levels, CIP/KIP family CKIs will promote CDK-cyclin assembly, and at high levels they inhibit CDK activity. The binding sites for cyclins and CDKs are in domain (I) of the p57kip2 protein, which is conserved between all CIP/KIP family members. Domain (I) alone, when transfected was able to arrest sarcoma osteogenic cells at G1 in vitro,[217] illustrating that it is sufficient for p57kip2's CKI activity.

Cell cycle exit is often accompanied by differentiation, a role that is supported by the spatial and temporal restriction of p57kip2 during development. Several studies demonstrate that p57kip regulates differentiation via its CKI functions. In the retina, p57kip inhibits cyclin D, promoting cell cycle exit in the differentiating lens fiber cells.[220] In placental development, p57kip2 binds to CDK1 and prevents the trophoblast cells from entering mitosis.[221] This allows the trophoblast cells to undergo endoreduplication, repeated G and S phase without mitosis, in order to differentiate into giant cells.[222-224] p57kip2 protein expression drops at the end of G phases which allows the trophoblast cells to proceed to S phase.[221, 225]

1.5.3 Non CKI roles of p57kip2

p57kip2 is most widely expressed during development,[226] and is the only CIP/KIP family CKI to have developmental defects when knocked out. Mouse mutants have several gross defects that cannot be explained solely by its CKI functions, including clef palate, renal medullary dysplasia, and defective bone formation which leads to smaller limbs.[117, 212]

p57kip2's central domain is unique among the CKIs, and is a candidate for elucidation of p57kip2's non-CKI roles.[214] Using human cDNA library a yeast two hybrid screen was performed to identify binding partners for the p57kip2 PAPA domain.[211] The study revealed that p57kip2 PAPA domain binds LIM kinase, and in cultured cells p57kip2 was shown to regulate actin dynamics through translocation of LIM kinase to the nucleus.[211] In rats, the proline rich domain of p57kip2 was also shown to interact with LIM kinase, indicating this function is conserved from rodents to humans despite differences in the protein structure.[227] p57kip2 inhibition induced actin stabilization, cell cycle exit, and myelination of the Schwann cells.[228] These results indicate that p57kip2's normal function in Schwann cells is inhibition of differentiation, which is contrary to its CKI function. p57kip2 control of actin dynamics can also promote apoptosis[229] and cell migration[230].

1.5.4 p57kip2 in human diseases

Two maternally inherited developmental diseases, RSS (Russel Silver Syndrome) and IMAGe (Intrauterine growth restriction, Metaphyseal dysplasia, Adrenal hypoplasia congenita and Genital anomalies) syndrome, have been linked to gain of function mutations in the PCNA binding domain of human CDKN1C.[231, 232] Mutations in the PCNA binding domain result in stabilization of p57kip protein so that cells are unable to

enter S-phase and proliferate.[233] Accordingly, both RSS and IMAGe syndrome are marked by growth retardation.[231, 232]

Conversely, loss of function of CDKN1C is linked to Beckwith-Wiedemann Syndrome (BWS). BWS has an incidence of 1:13,700 live births and is the most common overgrowth syndrome.[234, 235] Most cases of BWS are caused by an error in imprinting at chromosome 11p15.[235-238] However 5%-10% of sporadic cases[106, 239] and 40% of inherited BWS[240] are from point mutations in CDKN1C.

Chapter 2
Methods

2.1 Mice

All work on mice was approved by the Animal Care and Use Committee at the University of Virginia. *Wnt7b*^{c3},[70] *Wnt7b*$^{-}$,[177] *Sox2Cre*,[241] *HoxB7Cre*[242] *Foxd1GC*[59] and *p57kip2*$^{-}$[117] and *ROSA*$^{mT/mG}$*(Gt(ROSA)26Sor*$^{tm4(ACTB\text{-}tdTomato,\text{-}EGFP)Luo}$/J) [243] were previously published. *p57kip2NTAP* was obtained from Pumin Zhang. *R26Rp57* is described below.

2.2 Generation of R26p57 mice

R26Rp57 was generated from cloning the short isoform of *p57kip2* into a CAGGSpuro vector made in our lab. The CAGGSpuro vector contains a "floxed" dsRed CDS downstream of the CAGGS promoter, which is downstream of a splicing acceptor sequence. *p57kip2* CDS was amplified from an E15.5 kidney cDNA library and cloned downstream of the "floxed" dsRed between the NheI and XhoI sites to generate CAGGSpuro-p57kip2. Then the entire DNA fragment was cloned into the RosaPAS vector between the PacI and AscI sites to generate the targeting plasmid RosaPAS-p57kip2. RosaPAS-p57kip2 was linearized with SwaI and electroporated into ES cells for knock-in targeting into the *Rosa26* locus. The ES cell clones were screened with PCR for the 5' arm and confirmed with PCR for the presence of the p57Kip2 CDS. Primers used to amplify the *57kip2* short isoform and to screen for homologous recombination at the 5'arm are listed in **Table2-1**.

2.3 Histology and immunohistochemistry

Tissue preparation, histology, BrdU labeling, *in situ* hybridization and immunohistochemistry were performed as in Nagalakshmi et al.[244] For double staining

with two rabbit antibodies, a Zenon Kit (Invitrogen) was used on the antibody that produces stronger signals. A Tyramide Signal Amplification (TSA) kit (Invitrogen) was used to amplify signals for PDGFRβ. An Apoptag Red kit (Millipore) was used for TUNEL staining. High magnification images were collected with a CoolSnap HQ2 digital camera (Photometrix) attached to a Deltavison Microscope (Applied Precision). Images were deconvolved using the Applied Precision software and were projected as 1μm optical sections using Fiji[245]. Low magnification Images were collected with a DFC300 FX camera attached to a Leica MZ16F stereomicroscope. Antibodies used in this study were anti-Lef1 (Cell Signaling 1:200), anti-p57kip2 (Thermo Scientific 1:500), anti-Desmin (Epitomics 1:10K), anti-pan-Cytokeratin (Sigma 1:1K), anti- PDGFRβ (Cell Signaling 1:500), Streptavidin-conjugated DBA (sigma, 1:1K), anti-PECAM (BD Pharmingen 1:200), anti-BrdU (BD Pharmingen, 1:100), anti-VE-cadherin (Abcam 1:200), anti-CD34 (eBioscience 1:200), and anti-ZO1 (Invitrogen).

2.4 Cell proliferation measurements

2.4.1 Kidney

For the measurement of cell proliferation rates in epithelial cells, BrdU+ cells in the DBA+ or Cytokeratin+ cell population within the medulla were counted. For the measurement of cell proliferation rates in mural cells, BrdU+ cells in the Desmin+ mural cells located within the 6 μm distance from the basal surface of the medullary UB epithelium were counted. 150-206 cells were counted per embryo in 5 controls and 7 Wnt7b mutant embryos analyzed. For p57kip2 mutants, 4 mutants and 4 controls were analyzed. For the measurement of cell proliferation rates in endothelial cells, BrdU+ cells in the Pecam+ endothelial cells located within the 6 μm distance from the basal

surface of the medullary UB epithelium were counted. 150-250 cells were counted per embryo. For Wnt7b mutants, 4 mutants and 3 controls were analyzed. For p57kip2 mutants, 3 mutants and 4 controls were analyzed. The Student's t-test was used for the analysis of statistical significance.

2.4.2 Lung

For cell proliferation measurements in lungs, BrdU+ cells in 250 - 350 cells were counted per embryo in 4 controls and 3 Wnt7b mutants. The Student's t-test was used for the analysis of statistical significance.

2.5 Measurement of endothelial cell density in renal medulla

Endothelial cell density was represented as the number of endothelial cells per unit area. The area, was determined in each image by the length of medullary ureteric epithelium, and a width of 6μm from the basal surface of the ureteric bud epithelium, which covered the region that peri-UB capillaries resided. Immunostaining for Pecam together with Hoechst was used to identify endothelial cells within the region of interest (ROI). For each image, the number of Pecam-positive cells was normalized over the area of the ROI. The Student's t-test was used for the analysis of statistical significance.

2.6 Transmission electron microscopy

Freshly dissected kidney or lung samples were fixed in 4% paraformaldehyde (PFA) with 2.5% glutaraldehyde overnight, then post-fixed in 2% osmium tetroxide for 1 hr. After dehydration with ethanol, tissues were embedded in epoxy resin for 1 day at 65°C. Semi-thin sections were stained with Toluidine blue and used to determine the

suitable region for analysis. Ultra-thin sections were cut at 75 nm thickness and mounted on 200 mesh copper grids. The grids were contrast-stained with 0.25% lead citrate and 2% uranyl acetate and carbon-coated. Images were collected using a JEOL 1230 Transmission Electron Microscope.

2.7 Quantification of capillary morphology

TEM images were imported into Fiji,[245] and measurements were taken with the Line ROI Tool. Lumen width measurements were taken every 5 µm along a visible vessel length and averaged for each blood vessel. Cytoplasm length was measured from the nucleus to the lateral cell-cell junctions of each endothelial cell that could be identified as part of a blood vessel. Cells at the 'end' of a visible blood vessel were excluded. For the cytoplasm height measurement, the distance from the apical to basal boundaries of the endothelial cell was measured at 2 µm intervals along the lateral axis of the endothelial cell, from a point 2 µm from one lateral junction, to a point 2 µm from the nucleus, and measurements were then repeated at the other side of the nucleus. These distances were then averaged to get the cytoplasm height for each endothelial cell. Statistical analysis were was performed using the Mann-Whitney test (the U test). Color was added to TEM images in Photoshop.

2.8 Fluorescent dye injection into the embryonic circulation

Dye injection into the embryonic circulation was performed based on a protocol published by Ben-Zvi et al.[246] with modifications. Embryos were partially dissected from anesthetized dams with the umbilical cord remaining connected to the mother. An amount of 5 µl of 10 mg/ml 500 Kda Dextran Fluorescein, Lysine Fixable (Molecular

Probes) was injected into the embryonic liver. Five minutes after dissection, embryos were fixed in 4% PFA. The kidneys were then dissected in 4% PFA and fixed for 1 hr at 4°C before being processed for cryosectioning.

2.9 Generation of plasmids for luciferase assay

Intron 2 of p57kip2 was amplified by PCR from mouse genomic DNA (see **Table2-1** for primers) and first cloned into pGL3 using TA cloning kit from Invitrogen. It was then released from pGL3 using Nhe I and Xho I, and cloned into 8xFoflash.

Mutation of the two putative Lef/Tcf binding sites in the p57Kip2 intron 2 sequence site1B CTTTGTT to CTTGcg and site Q4 CCTTTAATGCC to CCTTTAcgGCC was performed on p57-Fof using a modified version of the quikchange site-directed mutagenesis protocol (Stratagene). Briefly, primers listed in **Table 2-1**were used to amplify the mutated site with PCR. Then the non-mutated, methylated plasmids were digested with Dpn1, and the mutated plasmid were gel purified and ligated.

Sequencing of p57kip2 intron 2, 1B*, Q4* and 1B*+Q4*was performed at the University of Virginia DNA sequencing facility. Since the plasmids were in a Fopfalash backbone, the reverse luciferase primer was used to sequence the plasmids.

2.10 Cell culture and Luciferase Assay

NIH3T3 cells were cultured in DMEM supplemented with 20% Calf serum, and incubated at 37C in a CO2 humidified atmosphere. The day before transfection cells were split into 24 well plate at a density of 1*10^5 cells per well. Cells at 50% to 60% confluency were transfected in OPTI-MEM with 0.8ug of DNA using 50ul of Lipofectamine transfection reagent. Each well included 40ng of pRL for normalization,

152ng of DA β-catenin, 304ng of DN-TCF or mCherry, and 304 ng of a firefly luciferase reporter construct (Topflash, Fopflash, p57-Fop with wild-type or mutant putative Lef/Tcf binding sites). After 48hrs, cells were lysed and luciferase activity was measured using Dual-Glo luciferase assay system from Promega. Plate reader used was a GloMax® 96 Microplate Luminometer w/Single Injectors (Promega).

2.11 Chromatin Immunopreciptation

GFP-positive interstitial cells were dissociated with Trypsin at 37C for 7 min, triturated to single cell suspension, and sorted from E15.5 Foxd1GC; ROSA$^{mT/mG}$. [243] kidneys with a Becton Dickinson FACSVantage SE Turbo Sorter with DIVA Option (BD Biosciences, San Jose, CA). Chromatin Immunoprecipitation was performed using a previously published protocol[101] A Misonix sonicator was used with settings of 10sec on and 15sec off for 25times, at level 5. For immunoprecipitation, rabbit anti β-catenin antibody (Invitrogen) was used and rabbit IgG was the control. Primers used for qPCR are listed in **Table 2-1**

Table2-1 Primers used

Name	Sequence	Application
p57Kip2s p57kip2as	5'-gggggctagcCCTCTCATCTCCGGTGAGC 5'-ggggctcgagAGAGACCCGCGAGGAGAC	Amplification of p57kip2 intron 2 for luciferase reporter assay
p57-1bmut top p57-1bmut bot	Phos - GCTACGTCGCCGCGCAATGTGCTGTGTA Phos - CAAAGCTGACCCGCCGCGGACCTC	Mutation of 1B site
p57-q4mut top p57-q4mut bot	Phos - GCCACGGGAGGAGGCGGGGACCGG Phos - GTCAAAGGGCCCGCGGCGCTTAGGG	Mutation of Q4 site
p57kip2 Negative Control	L - TCCCAGCGGTTCTGGTCCTC R – CGCTTGGCCTCCAGCGATAC	qPCR of ChIP product
p57 1B	L - CAGAGACCCGCGAGGAGACC R - GGCGACGTAAACAAAGCTGACC	qPCR of ChIP product
p57 Q4	L - CTTAGCTGCACCCCTACCAGT R - GGTGCGATCAAGAAGCTGTCG	qPCR of ChIP product
p57kip2fwd	5' -GGGGGCTAGCgccgccacc ATGGAACGCTTGGCCTCCTCCAG	Amplification of p57kip2 short isoform + NheI site
p57kip2rev	5' –GGGGCTCGAG TCATCTCAGACGTTTGCGCGGGGTCT	Amplification of p57kip2 short isoform + XhoI site
5armup 5armdwn	5'-CCTAAAGAAGAGGCTGTGCTTTGG 5'-CATCAAGGAAACCC TGGACTACTG	Screening for homologous recombination at 5' arm.

Table2-2 Plasmids used in luciferase reporter assay

Name	Description	Source
8xTopFlash	7 TCF/Lef binding sites upstream of Luciferase Reporter	Addgene12456 –from Randall Moon [247]
8xFopFlash	7 Mutated TCF/Lef Binding sites upstream of Luciferase Reporter	Addgene 12457 –from Randall Moon [247]
p57-Fof *1B, *Q4 *1B+Q4	p57kip2 intron 2 wildtype, and TCF/Lef sites mutants, upstream of Luciferase	Described in Section 2.9
pCS2+MT-xbCAT	Dominant Active β-catenin	Barry Gumbiner

Chapter 3

Wnt7b signaling from the ureteric bud epithelium regulates medullary capillary development

This chapter is based on work submitted for publication by:
LaToya Ann Roker, Katrina Nemri, and Jing Yu

3.1 Abstract

The renal vasculature is an integral component of the kidneys for its physiological function of regulating hemodynamics of the body, in addition to maintaining organ health. The close interrelationship of capillaries and the renal epithelium is key to renal physiology. In this study we uncovered a novel role of Wnt7b signaling and the ureteric bud epithelium in renal medullary capillary development. Our previous work has shown that Wnt7b is expressed in the ureteric trunk epithelium and activates canonical Wnt signaling in the surrounding medullary interstitium, where the capillaries reside. In this study, we demonstrate that the target interstitial cells of Wnt7b/canonical Wnt signaling are mural cells of peri-ureteric bud capillaries in the nascent renal medulla. Wnt7b inhibited proliferation of its target mural cells, at least in part due to its promotion of expression of PDGFRβ and p57Kip2 (*Cdkn1c*), a cyclin-dependent kinase inhibitor, in these cells. Furthermore, Wnt7b regulated lumen formation of the capillary endothelium in the renal medulla. In the absence of Wnt7b signaling, the peri-ureteric bud medullary capillaries displayed a narrower lumen that were lined with less flattened endothelial cells, and a significantly increased presence of luminal endothelial cell-cell junctions, a transient configuration in the forming blood vessels in the controls. Wnt7b achieved this function likely through modulation of VE-cadherin in the endothelial cells of these blood vessels, an upstream molecular player essential for blood vessel lumen formation.

3.2 Introduction

The kidney is a highly vascularized organ with an extensive capillary network. Its peritubular capillaries are key for the kidney's physiological role in removing metabolic waste and reserving nutrients in the bloodstream, and in maintaining body water and electrolyte homeostasis. Further, capillary rarefaction and regeneration is closely associated with pathogenesis of renal diseases. However, despite their physiological and pathological significance, the timing, morphogenesis, and molecular control of extraglomerular capillary formation in the kidney have been little explored. A tubulovascular cross-talk was recently discovered where the renal tubules maintain peritubular capillaries.[248] It remains to be identified what other aspects of capillary development renal tubules regulate and what specific segment(s) of the renal tubular epithelium is involved.

Wnt7b is a Wnt family ligand important for the proper formation of a number of organs and tissues including the placenta, the eye, the bones, the lungs, the kidney, the central nervous system (CNS), neurons, hair, the pancreas, and olfactory receptor neuron axon connectivity.[70, 166, 168-170, 172-182] Notably, *Wnt7b* has been reported to regulate vasculature development in the eyes, the brain, and the lungs, by different cellular mechanisms. In the eye, it signals to the endothelial cells of the hyaloid vasculature and activates their apoptosis.[166] In the CNS, it also acts on the endothelial cells but promotes angiogenesis and blood-brain barrier formation.[180, 182] In the lungs, it signals to the mesenchyme and regulates the differentiation/maintenance of vascular smooth muscles surrounding the major pulmonary vessels.[179]

In the embryonic kidneys, *Wnt7b* is expressed in the ureteric trunk epithelium and activates Wnt/β-catenin signaling in the surrounding medullary interstitium.[70, 170, 179, 202] It is required for collecting duct and loops-of-Henle elongation and renal medulla formation.[70, 170, 179, 202] Here we demonstrate that the medullary ureteric bud (UB) epithelium, through *Wnt7b*, regulates both the mural and the endothelial components of the capillaries that surround it. The *Wnt7b* target cells in the renal medullary interstitium are mural cells associated with peri-UB capillaries, and *Wnt7b* inhibits their cell proliferation. Further, *Wnt7b* regulates endothelial cell proliferation and lumen formation of the peri-UB capillaries in the renal medulla.

3.3 Results

3.3.1 A subset of renal interstitial cells in the nascent renal medulla responds to canonical Wnt signaling

We previously showed that Wnt7b activates canonical Wnt signaling (Wnt/β-catenin signaling) in the renal medullary interstitium, and Wnt/β-catenin signaling in the renal interstitial cells, like *Wnt7b*, is required for renal medulla formation.[70] To characterize this functionally important population of *Wnt7b*-responsive interstitial cells, we closely examined the distribution of these cells using Lef1, a readout of canonical Wnt signaling, as the marker (**Figure 3-1A**). At E15.5, the stage where a renal medulla defect was first observed in *Wnt7b* mutants,[70] in the wild-type renal medulla, not all the interstitial cells, but only the 1-3 layers of cells surrounding the UB epithelium were Lef1+ (**Figure 3-1A**). Their expression of Lef1 appeared to be in a gradient in which the strongest expression is closest to the UB epithelium (**Figure 3-1A**). Moreover, even

within these regions, not all interstitial cells were Lef1+. Consistent with our previous report, this expression of Lef1 was reduced to undetectable levels in *Wnt7b* mutants (**Figure 3-1A**).

Lef1 expression in interstitial cells surrounding the ureteric bud epithelium was not restricted to the renal medulla; rather, it extended into the renal cortex, around the entire length of the ureteric trunks (**Figure 3-2A**). However, in *Wnt7b* mutants, unlike the situation in the nascent medulla, Lef1 expression in the outer cortex was unaltered, and was only reduced in the deeper cortex abutting the renal medulla (**Figure 3-2A**). Taken together, this indicates that *Wnt7b* is specifically required for canonical Wnt signaling in the interstitium surrounding the medullary UB epithelium (the prospective medullary collecting ducts). Consistent with the less significant effect of *Wnt7b* on canonical Wnt signaling in the E15.5 renal cortex, canonical Wnt signaling in the *Wnt7b* mutant interstitium was unaltered in the outer region, and was reduced in the deeper region at E14.5, the stage right before a renal medulla emerges (**Figure 3-2B**). Lef1 expression at E13.5 was not altered in *Wnt7b* mutants (**Figure 3-3**). Therefore, the most dramatic disruption of canonical Wnt signaling in the *Wnt7b* mutant renal interstitium was initiated at E15.5, in the nascent renal medulla. This offers an explanation for the specific disruption of renal medulla development in *Wnt7b* mutants that we reported previously[70, 170, 179, 202] despite the fact that *Wnt7b* was ablated from the entire UB trunk epithelium.

3.3.2 *Wnt7b*/Canonical Wnt-responsive cells in the renal medulla are capillary mural cells

Given that the most *Wnt7b*-responsive interstitial cells are in the renal medulla, we focused our subsequent study on the renal medullary interstitium. At E15.5, we observed that endothelial cells, as identified by PECAM (CD31) staining, surrounded the medullary UB epithelium (**Figure 3-4A**). These endothelial cells form lumenized capillary blood vessels with cell-cell junctions appearing electron-dense by transmission electron microscopy (TEM) (**Figure 3-4B**). Mural cells and endothelial cells were observed interacting with each other with cytoplasmic extensions (**Figure 3-4B**).

Given the similar location of the *Wnt7b*-responsive interstitial cells and the capillaries surrounding the medullary UB, we set forth to determine whether the *Wnt7b*-responsive cells are a component of the peri-UB capillaries with markers for endothelial cells and mural cells. As shown in **Figure 1B**, the Lef1+ cells in the nascent renal medulla were PECAM-, demonstrating that they are not endothelial cells. However, they lay immediately adjacent to the PECAM+ endothelial cells (**Figure 3-1B**), suggesting that they are mural cells. Indeed, staining for mural cell markers PDGFRβ and Desmin[249] showed that the cells positive for Lef1 in the nucleus were also positive for PDGFRβ, which is localized to the cell surface, and for Desmin, which is an intermediate filament component in the cytoplasm (**Figure 3-1B, panels f–o**). Taken together, our analysis showed that the *Wnt7b*-responsive cells are mural cells of the peri-UB capillaries in the nascent renal medulla. Of note, we also observed that the interstitial cells close to the endothelium surrounding the loops of Henle (LOH) expressed PDGFRβ at a higher level than those surrounding the ureteric trunk epithelium (**Figure 3-5A**). The rest of the

nascent medullary interstitium expresses PDGFRβ at the basal level. Furthermore, the expression of PDGFRβ in the medulla is lower than that in the cortex (**Figure 3-5A**).

3.3.3 *Wnt7b* regulates PDGFRβ and p57kip2 expression in and proliferation of renal medullary peri-UB mural cells

To determine whether *Wnt7b* signaling regulates the fate of *Wnt7b*-reponsive mural cells during development, we examined their expression of mural cells markers in control and *Wnt7b* mutant mice at E15.5 (**Figure 3-6**). Desmin staining appeared unchanged in the interstitium adjacent to the UB epithelium in the nascent medulla of *Wnt7b* mutants, compared to the control counterpart (**Figure 3-6A**, panels b and g and **Figure 3-5B**), indicating that this population of mural cells was still present despite ablation of *Wnt7b* signaling. In contrast, PDGFRβ expression was drastically decreased in the *Wnt7b* mutant medullary interstitium surrounding the UBs (**Figure 3-6A**, panels a and f). *Pdgfrb* expression in this domain was decreased also at the mRNA level based on the *in situ* hybridization analysis (**Figure 3-6B**). The change in PDGFRβ expression was specific to the *Wnt7b*-responding cell population, since PDGFRβ expression in the interstitium surrounding loops of Henle remained unaltered (**Figure 3-5C**). The disruption of PDGFRβ expression in the *Wnt7b* mutant kidneys was restricted to the nascent renal medulla, whereas its expression in the E15.5 cortex (**Figure 3-5A**) or E14.5 kidneys (**Figure 3-7**) was not affected, even in regions where canonical Wnt signaling was reduced.

p57kip2 was first identified as a cyclin-dependent kinase inhibitor (CKI),[214, 216] but it can also function beyond cell cycle control.[250] In humans, its loss-of-function mutations are associated with Beckwith-Wiedemann syndrome[213, 235] and gain-of-

function mutations with IMAGe syndrome.[231] In mice, *p57kip2* mutant kidneys exhibited a shorter renal medulla.[117] We previously reported that p57Kip2 expression in the nascent medullary interstitium depends on *Wnt7b* signaling, such that in *Wnt7b* mutant kidneys the expression of p57kip2 in this domain was reduced to undetectable levels.[70] To determine whether p57kip2 is expressed in the *Wnt7b*-responding mural cells, we performed immunostaining for p57Kip2 together with either Lef1 or mural cell markers. As shown in **Figure 3-8**, in the medullary interstitium, p57Kip2-expressing cells were all Lef1+, demonstrating that p57Kip2 is expressed only in the subset of the medullary interstitium that responds to *Wnt7b*. Furthermore, p57kip2+ interstitial cells expressed PDGFRβ (**Figure 3-8**). Therefore, the p57 kip2+ cells in the medulla are the *Wnt7b* target mural cells.

As a cyclin-dependent kinase inhibitor, p57Kip2 inhibits cell proliferation. Consistent with p57Kip2 acting as a CKI in the *Wnt7b* target mural cells, the cell proliferation rate of these cells was increased in *p57Kip2* mutant kidneys as compared to that of controls, as assayed with BrdU incorporation (**Figure 3-9**). On the other hand, *PDGFRβ*, through its ligand PDGF-B, has been shown to promote mural cell proliferation.[251, 252] Since the *Wnt7b* target medullary mural cells exhibited great reduction in the expression of both *PDGFRβ* and p57kip2, we set out to determine whether and how cell proliferation in this population of mural cells was affected by loss of *Wnt7b* function. As shown in **Figure 3-9**, the cell proliferation rate of this cell population was increased in the *Wnt7b* mutants. However, this increase was less than that in the *p57Kip2* mutants. Interestingly, unlike the *Wnt7b* mutants, the expression of PDGFRβ in the peri-UB medullary mural cells in *p57kip2* mutants was not affected

(**Figure 3-10**). The difference in the PDGFRβ expression levels in *Wnt7b* and *p57kip2* mutant mural cells probably explains, at least in part, the difference in the cell proliferation rates of the two mutants.

3.3.4 *Wnt7b* regulates renal medulla microvascular lumen formation

PDGFRβ signaling is also involved in mural cell recruitment to the microvasculature, and in the regulation of microvasculature development and maturation.[132, 249, 253-255] To determine whether mural cell recruitment and capillary development were affected in *Wnt7b* mutants, we employed transmission electron microscopy to examine the capillaries surrounding the UB epithelium in the nascent medulla. As shown in **Figure 3-11A, B**, mural cells were seen close to the endothelial wall of the capillaries and making contacts with the endothelial cells in *Wnt7b* mutants similar to that in the controls. Thus, *Wnt7b* and PDGFRβ signaling is not required for mural cell recruitment and/or maintenance of mural cell association for this population of capillaries. Alternatively, the reduced expression of PDGFRβ is still sufficient for mural cell recruitment/maintenance of mural cell association for this population of blood vessels.

Our examination of E15.5 capillary morphology in the controls by TEM revealed that endothelial cells were organized into cords and vessels, representing multiple stages of active lumen formation (**Figure 3-12**). Endothelial cells were identified based on their similar histology in TEM to those in published reports, and the presence of electron-dense cell-cell junctions.[152, 256, 257] We observed endothelial cells with lateral junctions and only a slit between their luminal membranes, and flattened and unflattened

endothelial cells with a lumen and lateral junctions (**Figure 3-12**). When the peri-UB capillaries in the *Wnt7b* mutant medulla were examined, which was identified based on the presence of electron-dense cell-cell junctions between the cells lining them even when a lumen was absent (**Figure 3-11F**), we found that the endothelial component of these capillaries in *Wnt7b* mutants was visibly different from that in the controls (**Figure 3-11A**). Quantitative analysis confirmed that a higher percentage of endothelial cells were less flattened in *Wnt7b* mutants when cytoplasm height and length were measured (**Figure 3-11C, D**). More endothelial cells in the peri-UB medullary capillaries of *Wnt7b* mutants were taller (median, control=0.8 μm, mutant=1.2 μm, p=0.0024) and shorter (median, control=4.8 μm, mutant=3.9 μm, p=0.0004) than those of control kidneys (**Figure 3-11C** and **D**). Further, the lumen of the capillaries in the *Wnt7b* mutants was narrower (median, control=1.6 μm, mutant=1.0 μm, p=0.0139) (**Figure 3-11E**). Moreover, in the controls the vast majority of the endothelial cells had only lateral cell-cell junctions, with only a small fraction of endothelial cells (7%) with additional cell-cell junctions at the lumenal cell surface, whereas in *Wnt7b* mutants there was a significantly increased incidence of endothelial cells (25%) with additional junctions at the lumenal surface (**Figure 3-11F, G**).

Taken together, these results showed that capillary vessel lumen formation, in particular the resolution of cell-cell junctions (and/or apical membrane separation) and endothelial cell shape change, was disrupted from the loss of *Wnt7b* function. To determine the earliest time point at which the lumen formation defect of the peri-UB capillaries appeared, we examined capillary morphology at E14.5 with TEM (**Figure 3-13**). Since a nascent medulla is not present at this stage, we focused on the area adjacent

to the UB epithelium that is closest to the emerging pelvis. In the controls, there were far fewer endothelial tubes than at E15.5, and most of the endothelial cells were in clusters with or without a slit between the cells, suggesting that lumen formation of this population of capillaries likely commences at E14.5. Cells in clusters without a slit were identified as endothelial cells based on the presence of electron-dense cell-cell junctions[35] (**Figure 3-13**, arrowheads). Notably, in any of these configurations, we did not observe a prominent presence of vacuoles in the endothelial cells, suggesting that lumen formation in the population of capillaries does not involve vacuole fusion with the plasma membrane and may employ a mechanism similar to that of mouse dorsal aorta.[152] Examination of the counterpart in *Wnt7b* mutants identified no obvious difference from the controls (**Figure 3-13**), demonstrating that the earliest defect in lumen formation in *Wnt7b* mutants occurred at E15.5, after a slit between apposing endothelial cells started to form.

VE-cadherin has been shown to be an upstream player in vascular lumen formation. In its absence, endothelial cells failed to form a lumen or to flatten, and CD34 failed to localize to the apical membrane.[152, 258-261] To determine whether VE-cadherin is involved in *Wnt7b*-dependent capillary lumen formation, we examined VE-cadherin localization in the peri-UB capillaries in the nascent medulla. As shown in **Figure 3-14A**, in *Wnt7b* mutant peri-UB capillaries in the nascent medulla, VE-cadherin levels at the cell surface (marked by PECAM signals) was greatly diminished compared to that in the controls. As VE-cadherin is required for apical membrane localization of CD34 sialomucin,[152] which provides electrostatic repulsion for apical membrane separation during vascular lumen formation,[262] we examined CD34 localization in peri-UB

capillaries in *Wnt7b* mutant nascent medulla (**Figure 3-14B**). CD34 localization at the endothelial cell surface (labelled with PECAM) in *Wnt7b* mutant capillaries was also reduced and it appeared to be diffusely localized in the endothelial cells compared to the controls (**Figure 3-14B**). These results offer an explanation to the defects of the higher incidence of lumenal junctions and less elongation of the endothelial cells in *Wnt7b* mutants, and strongly suggest that the lumen formation defect in *Wnt7b* mutants is due to the deficiency of expression and/or proper localization of VE-cadherin in the endothelial cells. In contrast, at E14.5, VE-cadherin expression at the endothelial cell surface was patchy in controls, and this expression pattern was unchanged in *Wnt7b* mutants (**Figure 3-13**), in agreement with the observation that the majority of the endothelial cells were not lumenized and are consistent with the normal vascular phenotype of the *Wnt7b* mutants at this time point by TEM.

Despite the defective pattern of VE-cadherin at the endothelial cell surface, staining of ZO-1, a tight junction marker, identified its localization to the endothelial cell surface in the peri-UB capillaries in *Wnt7b* mutant nascent medulla (**Figure 3-15A**), consistent with the presence of electron-dense cell-cell junctions between endothelial cells in both controls and *Wnt7b* mutants by TEM. Taken together, these data suggest that the tight junctions can still form in these mutant capillaries. Consistent with this conclusion, injection of a fluorescence dye into the embryonic circulation showed that the integrity of these capillaries was not compromised in *Wnt7b* mutants, as the fluorescent dye was detected in the mutant capillaries at similar intensity to that in the controls (**Figure 3-15B**). Of note, that the fluorescent dyes injected into the embryonic liver can

be detected in the peri-UB capillaries in the nascent renal medulla demonstrated that these capillaries were open to the systemic circulation.

3.3.5 *Wnt7b* regulates renal medulla endothelial cell proliferation/density

The higher percentage of less flattened endothelial cells in *Wnt7b* mutants predicted a higher density of endothelial cells surrounding the mutant UB epithelium. Indeed, our quantification of PECAM+ endothelial cells adjacent to the UB epithelium in the nascent medulla clearly showed a higher density of endothelial cells in *Wnt7b* mutants as compared to that in the controls (**Figure 3-16A**). This suggests that there is either an increase in endothelial cell proliferation or a decrease in endothelial cell death. Our TUNEL staining did not reveal changes in apoptosis in these endothelial cells (data not shown). In contrast, the proliferation rate of endothelial cells surrounding the UB epithelium of the nascent medulla in the *Wnt7b* mutants was higher than that in the controls when examined with BrdU incorporation (**Figure 3-16B, C**).

3.4 Discussion

We have identified a new role for the ureteric bud epithelium and Wnt7b in the renal medulla during development, where the ureteric bud epithelium, via Wnt7b it secretes, regulates the development of the capillaries surrounding the ureteric bud epithelium of the nascent renal medulla (**Figure 3-17**).

In the developing kidney, *Wnt7b* is expressed along the entire length of the ureteric trunks, but the loss of canonical Wnt response in the interstitium from *Wnt7b*

ablation is only observed in the renal medulla. This suggests that other Wnt ligands expressed in the UB epithelium and/or other cortical structures performed redundant signaling functions in the renal cortex. Regardless, the normal canonical Wnt response in the *Wnt7b* mutant cortex explains the unaltered development of peri-UB capillaries in this compartment.

The proliferation of the peri-UB mural cells in the nascent renal medulla is increased in *Wnt7b* mutants as well as in *p57kip2* mutants. These results suggest that in the normal renal medulla, *Wnt7b* inhibition of mural cell proliferation is mediated by p57kip2. However, the increase in mural cell proliferation of the p*57kip2* mutants was greater than that of the *Wnt7b* mutants. This difference indicates that there is also a pro-proliferative signal acting downstream of *Wnt7b*. PDGF signaling is a likely candidate for the pro-proliferative signal in the renal medulla, since it has been previously shown to promote proliferation of renal mesangial cells. The fact that PDFGRβ expression was reduced in *Wnt7b* mutants, but not in *p57kip2* mutants, correlates with the difference in proliferation change between the two mutants.

Though PDGFRβ expression in *Wnt7b* mutants was greatly reduced in the *Wnt7b* target mural cells in the renal medulla, where canonical Wnt signaling was undetectable, it remained normal in the deeper cortex where canonical Wnt signaling was weak. This demonstrated that either the residual level of canonical Wnt signaling in the deeper cortical interstitium is sufficient for *Pdgfrb* expression, or other signaling pathways play a dominant role in regulating *Pdgfrb* expression in the cortex. On the other hand, for the peri-UB medullary capillaries, *Wnt7b*/canonical Wnt signaling is a dominant player in regulating *Pdgfrb* expression.

Pbx1 has been recently shown to negatively regulate *Pdgfrb* expression in renal interstitial cells and mural cell differentiation.[263] However, its expression in *Wnt7b* target mural cells was unaltered in *Wnt7b* mutant kidneys (**Figure 3-18**), suggesting that *Wnt7b* does not regulate *Pdgfrb* expression through inhibiting *Pbx1*. In the lungs, it has been reported that *Wnt7b* regulates *Pdgfrb* expression through Tenascin-C (TnC).[202] TnC expression was unaltered in the *Wnt7b* target mural cells in the developing kidneys (**Figure 3-19**), demonstrating organ-specific regulation of *Pdgfrb* by *Wnt7b*.

The importance of VE-cadherin in blood vessel lumen formation has been well documented in several animal models including the mice (see[259] for a recent review). In *Wnt7b* mutant kidneys, we observed a reduction in the cell surface (presumably cell-cell adherens junctions) localization of VE-cadherin in the peri-UB capillaries in the nascent medulla. This reduction is likely to cause the defective localization pattern of sialomucin CD34 in these endothelial cells, and to lead to disrupted lumen formation. On the other hand, the reduced abundance of VE-cadherin at the endothelial cell surface may be still sufficient to allow lumen formation to proceed in some regions of the developing capillaries, thus the variable severities of the lumen formation defect in the mutant capillaries. Though VE-cadherin expression/localization and thus adherens junctions were defective in the *Wnt7b* mutant renal medullary peri-UB capillaries, ZO-1 localization appeared normal. In a recent report where VE-cadherin was knocked down in Zebrafish embryos, some organized ZO-1 staining was still observed in the forming intersegmental vessels (ISV), suggesting some limited tight junctions can still form without (or with little) VE-Cadherin.[260] Thus it is possible that the reduced VE-cadherin

localization at the endothelial cell surface in *Wnt7b* mutant kidneys is still sufficient for tight junction formation.

The molecular mechanisms underlying the effect of *Wnt7b* on endothelial cell morphogenesis and proliferation in the developing kidney remain elusive, but likely lie in the effect of *Wnt7b* on its target mural cells. The fact that *Wnt7b* targets mural cells but endothelial cell morphogenesis and lumen formation was disrupted in the *Wnt7b* mutant peri-UB medullary capillaries during embryonic development implicates mural cells in capillary lumen formation, at least in the subpopulation of capillaries surrounding the medullary ureteric buds. The *Wnt7b* target mural cells is a population of mural cells that express unique markers, such as p57Kip2, which distinguish them from both the cortical mural cells and mural cells surrounding the loops of Henle. Future work on identifying the signals from these mural cells to the endothelium that regulate endothelial cell proliferation, morphogenesis and lumen formation in the peri-UB medullary capillaries should help identify the mechanism governing the regulation of capillary lumen formation by Wnt7b/canonical Wnt signaling.

The understanding of the regulation of extraglomerular capillary formation in the kidney is only beginning. In this study, we establishes a crucial role of the medullary ureteric bud epithelium, through *Wnt7b*, in the formation of the capillary bed surrounding it during embryonic development.

3.5 Figures

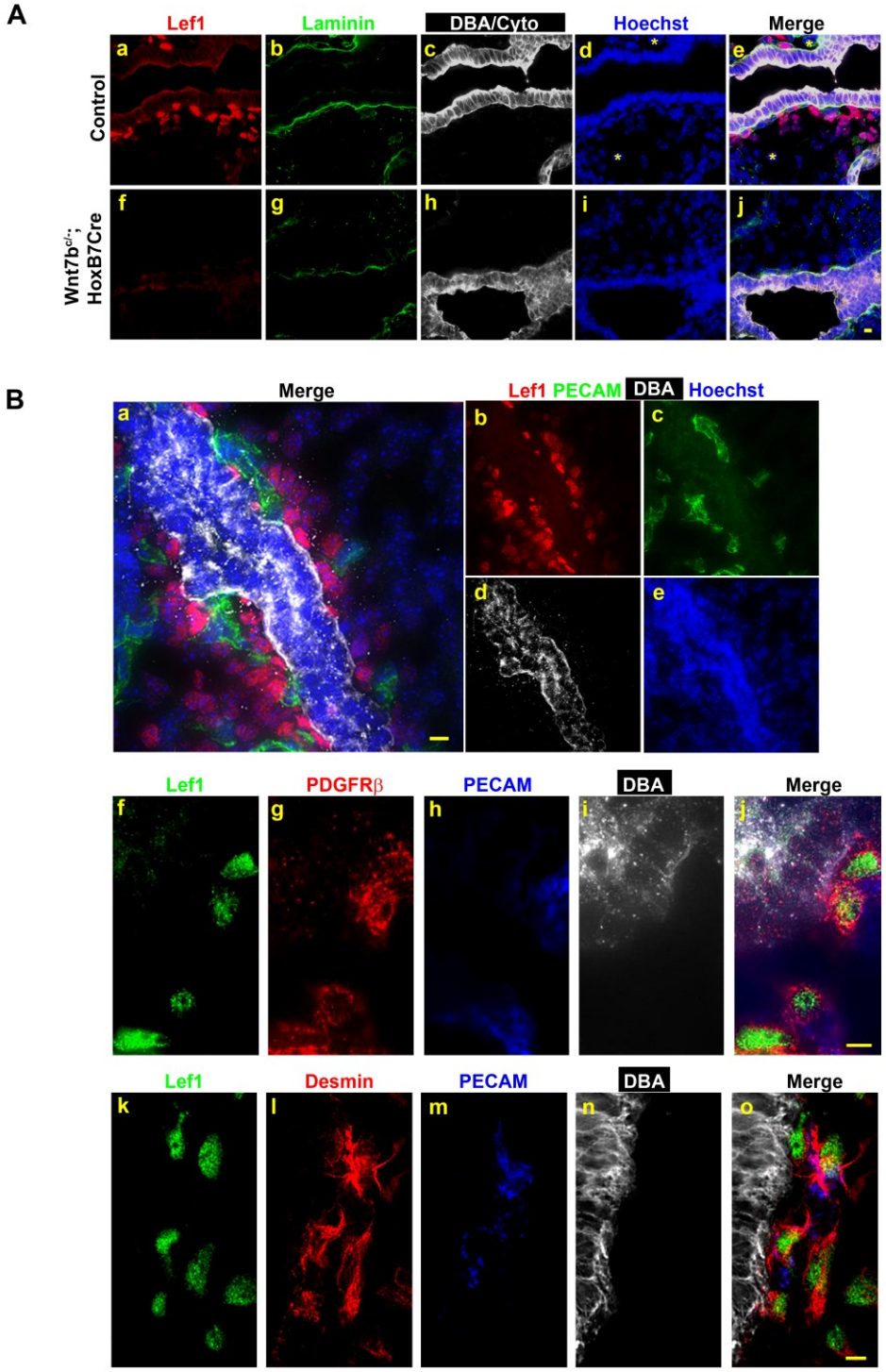
A
Lef1
Laminin
DBA/Cyto
Hoechst
Merge
Control
Wnt7b$^{c/-}$; HoxB7Cre
a
b
c
d
e
f
g
h
i
j
B
Merge
Lef1 PECAM DBA Hoechst
Lef1
PDGFRβ
PECAM
DBA
Merge
Lef1
Desmin
PECAM
DBA
Merge
k
l
m
n
o

Figure 3-1 *Wnt7b* target cells in the medullary interstitium are mural cells of peri-UB capillaries

(A) Lef1 expression in the control and *Wnt7b* mutant renal medulla. The renal epithelium is labeled with Laminin (green), and the UB epithelium is labeled with DBA and Cytokeratin (white). Interstitial cells are Laminin-. (a–e) Not all interstitial cells express Lef1 in the control. Instead, Lef1 is expressed in 1-3 layers of renal medullary interstitial cells surrounding the UB epithelium. Asterisk marks some of the Lef1- medullary interstitial cells. (f–j) Lef1 expression is reduced to undetectable levels in *Wnt7b* mutants. Scale bar=5 μm.

(B) *Wnt7b* target cells are mural cells of peri-UB capillaries. (a–e) *Wnt7b* target cells are not positive for endothelial cell marker PECAM, but are closely associated with endothelial cells. Mural cell markers PDGFRβ (f–j) and Desmin (k–o) are expressed in Lef1+ cells. Scale bar= 5 μm.

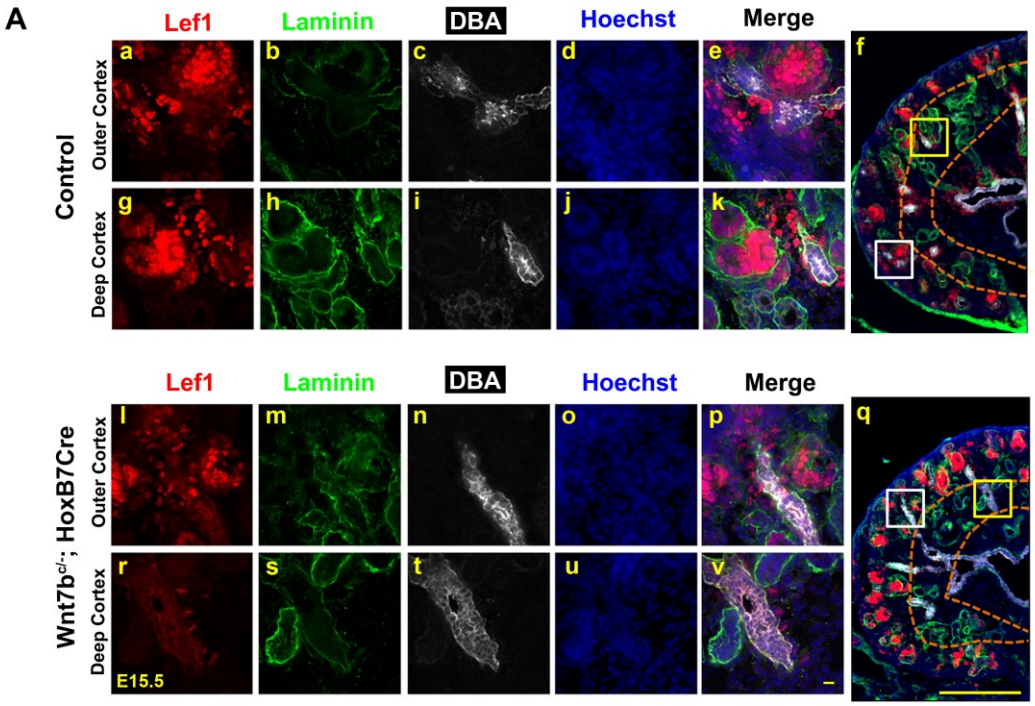
A
Lef1
Laminin
DBA
Hoechst
Merge
Control
Outer Cortex
Deep Cortex
a
b
c
d
e
f
g
h
i
j
k
Wnt7b$^{c/-}$; HoxB7Cre
l
m
n
o
p
q
r
s
t
u
v
E15.5

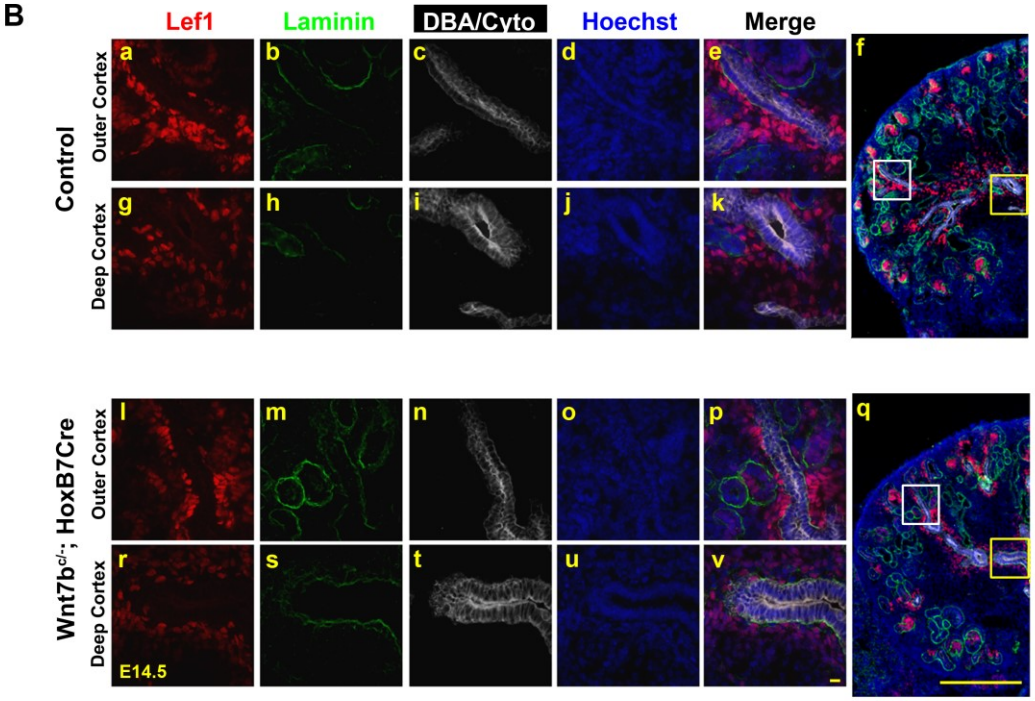
B
Lef1
Laminin
DBA/Cyto
Hoechst
Merge
Control
Outer Cortex
Deep Cortex
a
b
c
d
e
f
g
h
i
j
k
Wnt7b$^{c/-}$; HoxB7Cre
l
m
n
o
p
q
r
s
t
u
v
E14.5

Figure 3-2 Expression of Lef1 in the renal cortex of controls and *Wnt7b* mutants
(A) Lef1 expression in the control and *Wnt7b* mutant cortex at E15.5. (a–k) Lef1 is expressed in 1-3 layers of cells surrounding the UB in the control cortex. (l–v) In *Wnt7b* mutants, Lef1 expression in this domain is unaltered in the outer cortex, but reduced in the deep cortex close to the medulla. Scale bar=10 µm for panels a-e, g-k, l-p, and r-v. Scale bar=100 µm for panels f and q.
(B) Lef1 expression at E14.5. (a-k) peri-UB cells surrounding the UB trunk of control kidneys express Lef1 strongly. (l–v) In *Wnt7b* mutants this expression is unchanged in the outer cortex, but reduced in the deep cortex adjoining the pelvis. Scale bar=10 µm for panels a-e, g-k, l-p, and r-v. Scale bar=100 µm for panels f and q.

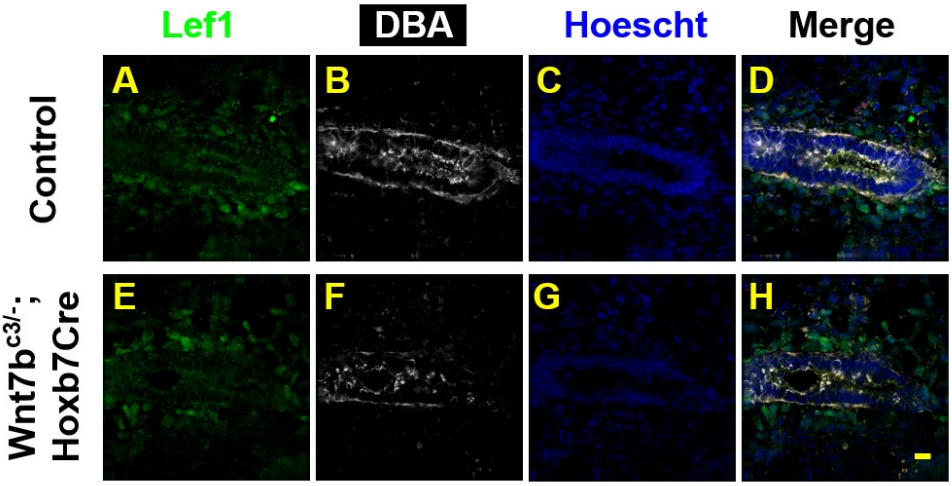

Figure 3-3 Lef1 expression is unchanged in *Wnt7b* mutants at E13.5
Scale bar=5µm.

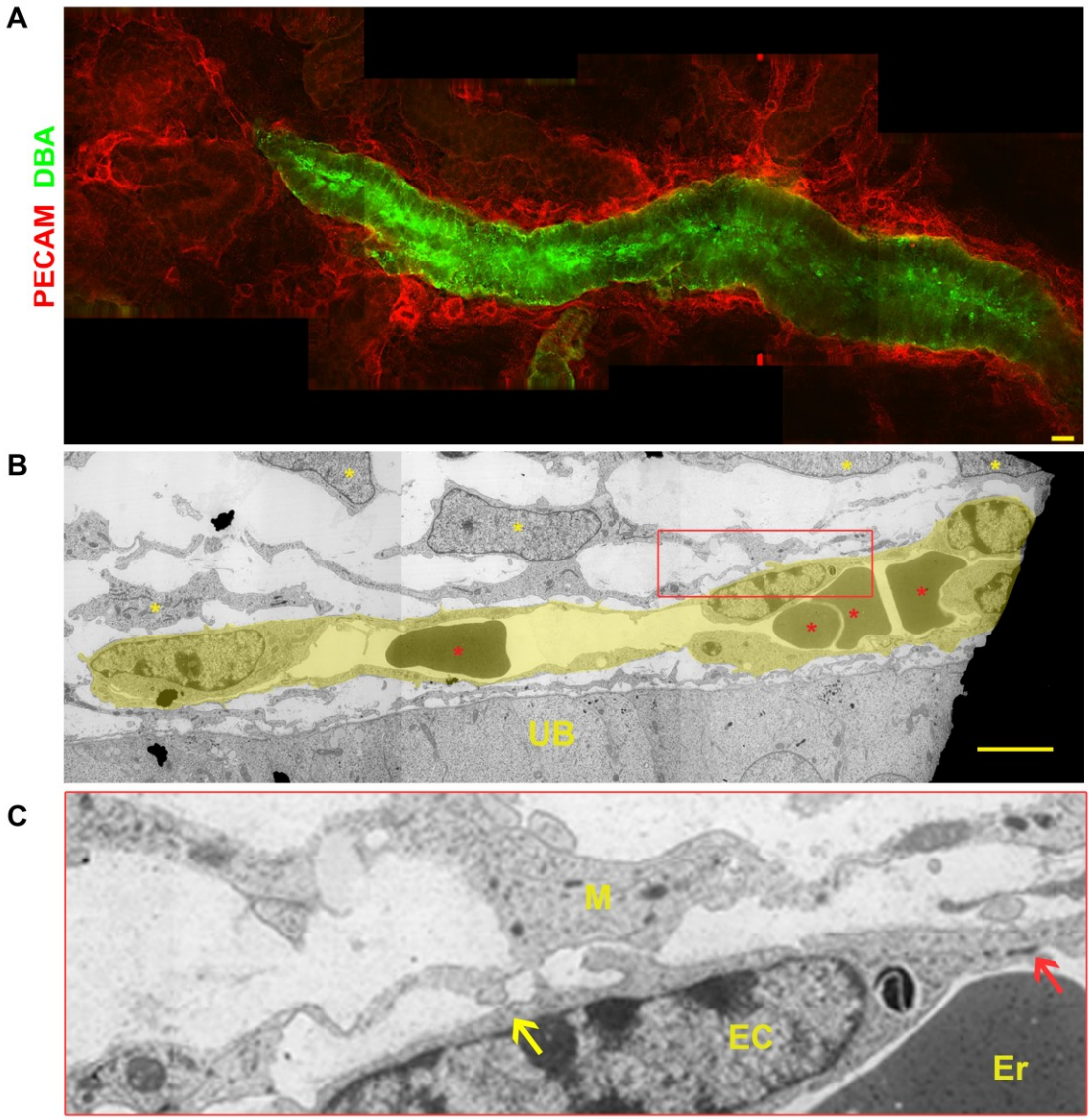

Figure 3-4 A network of capillaries surrounding the E15.5 UB in the nascent renal medulla

(A) An extensive network of Pecam-positive endothelial cells surrounding the UB at E15.5.

(B) Transmission electron microscopy (TEM) of a capillary vessel (highlighted in yellow) containing erythrocytes in the lumen (red asterisks) and in close contact with mural cells (yellow asterisks). Scale bar=5 µm.

(C) Cell-cell junctions (red arrow) are visible between the endothelial cells (EC). Endothelial cells and mural cells (M) interact through cytoplasmic extensions (yellow arrow).

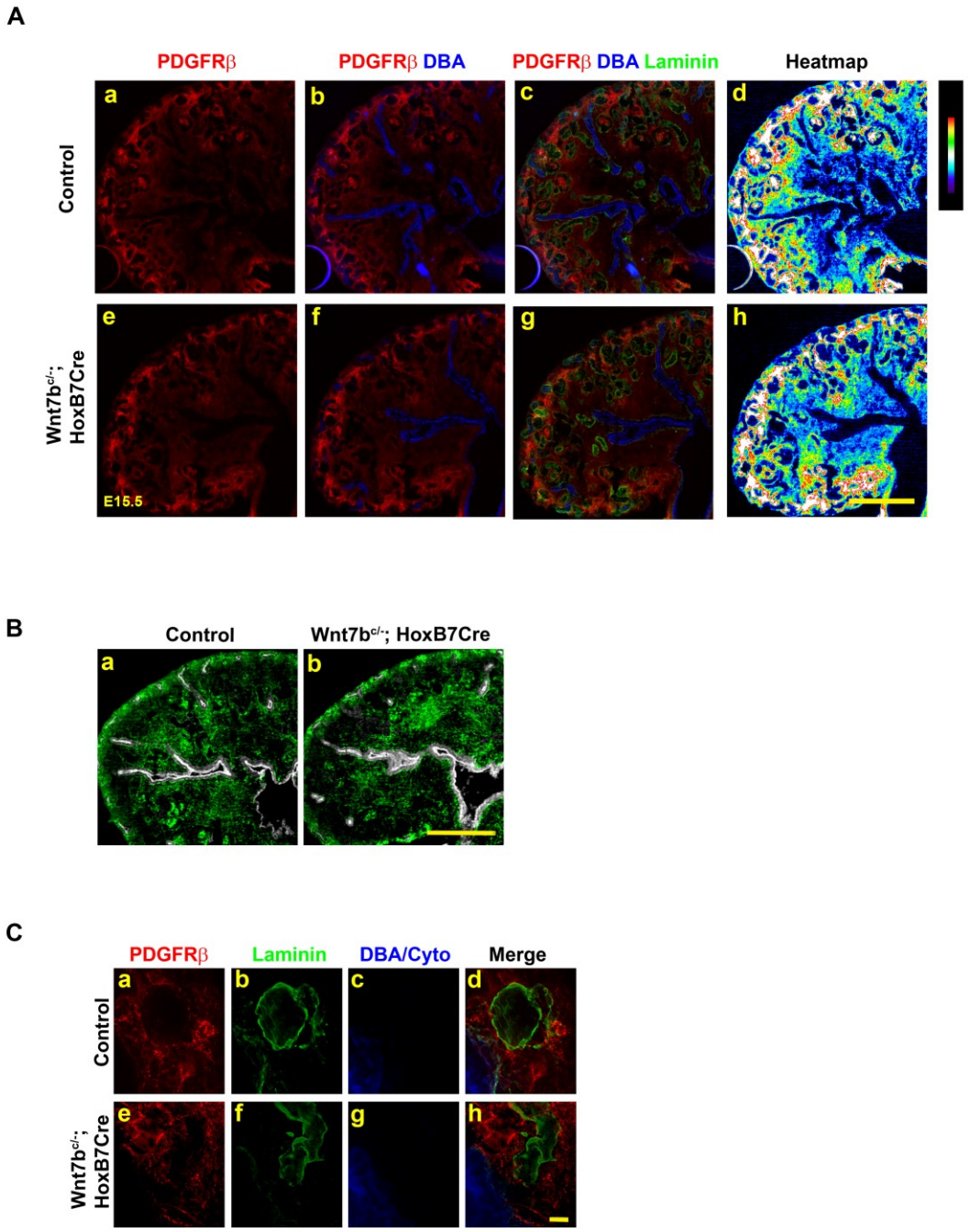

Figure 3-5 PDGFRβ and Desmin expression in the kidney
(A) PDGFRβ exhibits multiple levels of expression in the E15.5 kidney. PDGFRβ expression in the cortical interstitium is higher than that in the medulla. In the medulla, PDGFRβ expression in cells surrounding the UB is higher than basal levels, but lower than that in cells surrounding the loops of Henle. Scale bar= 100µm.
(B) Desmin expression is unchanged in *Wnt7b* mutants. Scale bar= 100µm.
(C) In *Wnt7b* mutants, PDGFRβ expression surrounding the loops of Henle is unchanged. Scale bar=10 µm.

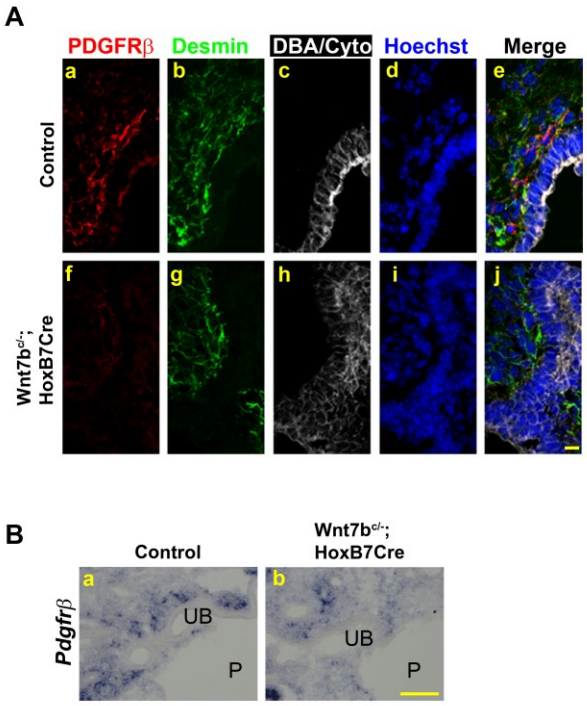

Figure 3-6 PDGFRβ expression is reduced to basal levels in the peri-UB mural cells in the *Wnt7b* mutant nascent medulla

(A) In *Wnt7b* mutants, expression of Desmin in mural cells surrounding the medullary UB epithelium is unchanged, but PDGFRβ protein levels in these cells are reduced. Scale bar=10 µm.

(B) The *Pdgfrb* mRNA level in interstitial cells adjacent to the UB epithelium is reduced in the *Wnt7b* mutant renal medulla. UB, ureteric bud; P, pelvis. Scale bar=100 µm.

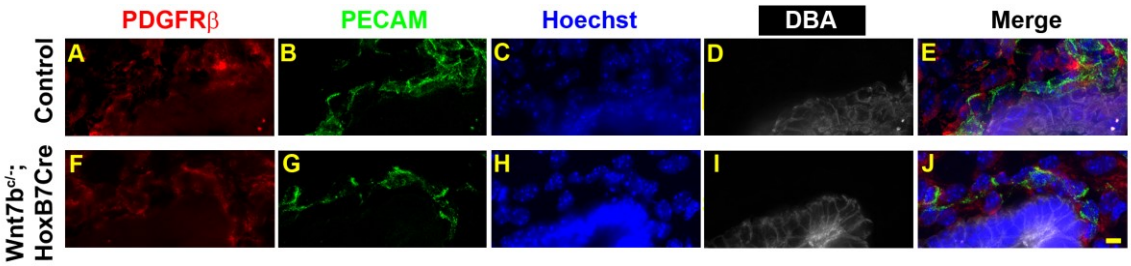

Figure 3-7 PDGFRβ expression is unchanged at E14.5
Scale bar=5 µm.

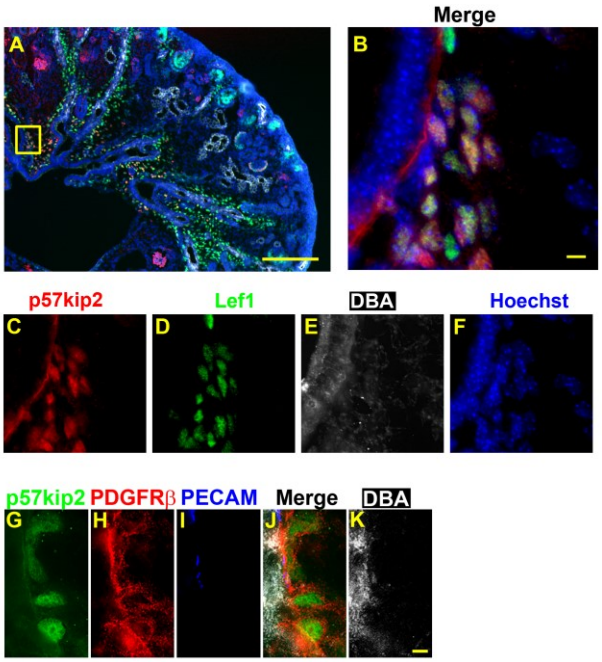

Figure 3-8 p57kip2-positive cells in the renal medulla are peri-UB mural cells
(A–F) p57kip2 co-localizes with Lef1 in the renal medulla. Scale bar=200 µm**.** (G–K) p57kip2+ cells in the renal medulla are PDGFRβ+. Scale bar=5 µm**.**

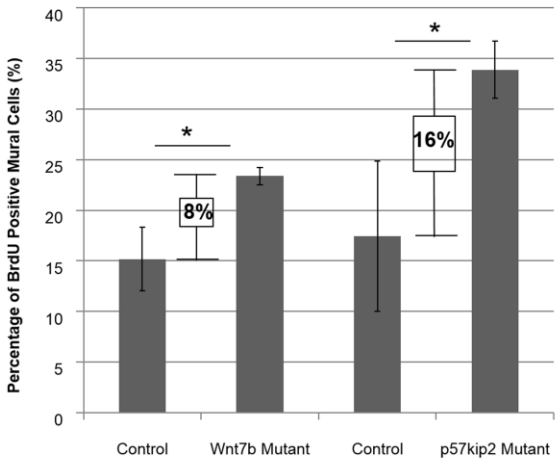

Figure 3-9 Peri-UB mural cell proliferation is increased in *Wnt7b* and *p57kip2* mutants

Cell proliferation was measured as the percentage of BrdU-positive cells in the population of Desmin-positive cells surrounding the nascent medullary UB epithelium of controls, *Wnt7b* mutants, and *p57kip2* mutants. At E15.5 proliferation is increased in *Wnt7b* mutants (p=0.0302). In *p57kip2* mutants, the increase in mural cell proliferation (p=0.0123) is greater than that in *Wnt7b* mutants.

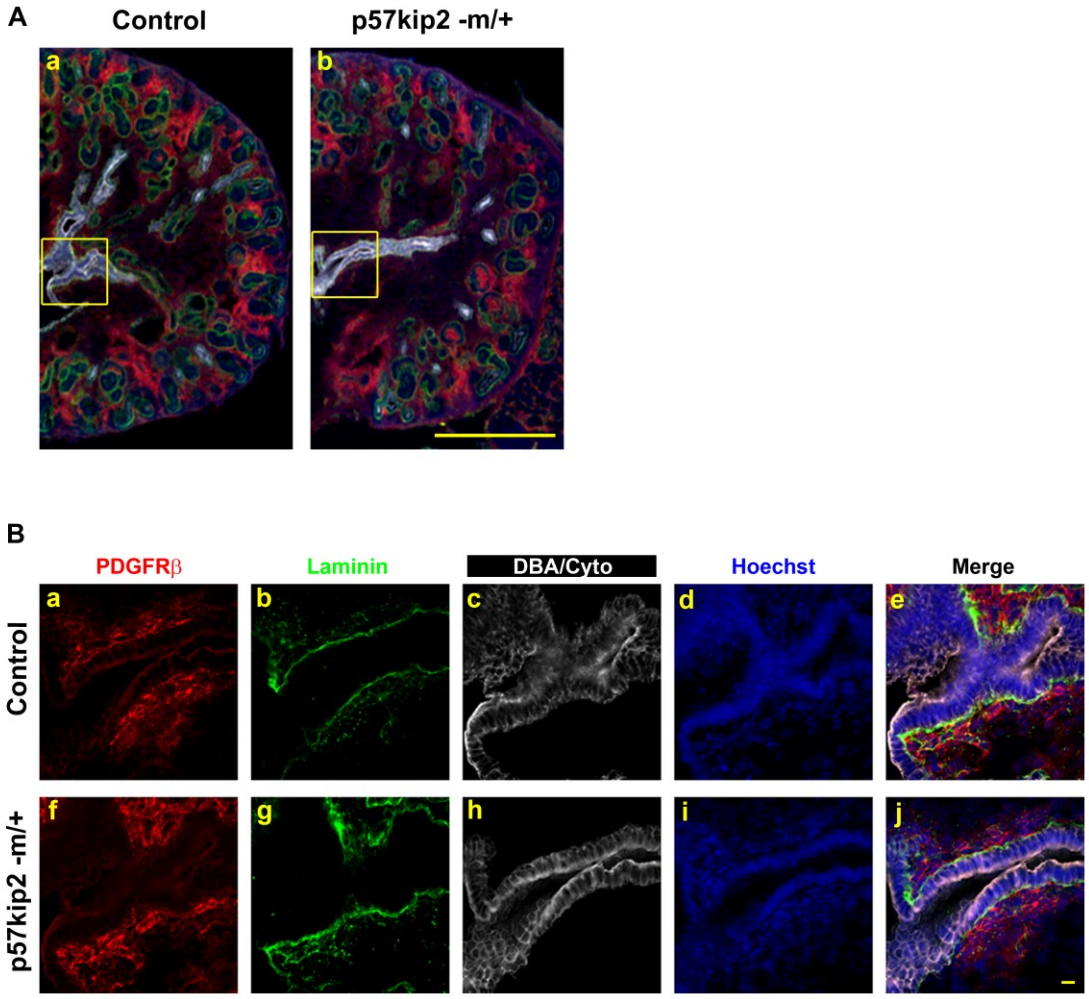

Figure 3-10 PDGFRβ expression is not changed in E15.5 *p57kip2* mutants
(A) The global view of PDGFRβ expression (red) in the E15.5 control and *p57Kip2* mutant kidneys. Scale bar=100 µm. (B) Expression of PDGFRβ in the mural cells surrounding the medullary UB epithelium is unchanged in *p57Kip2* mutant kidneys. Scale bar=5 µm.

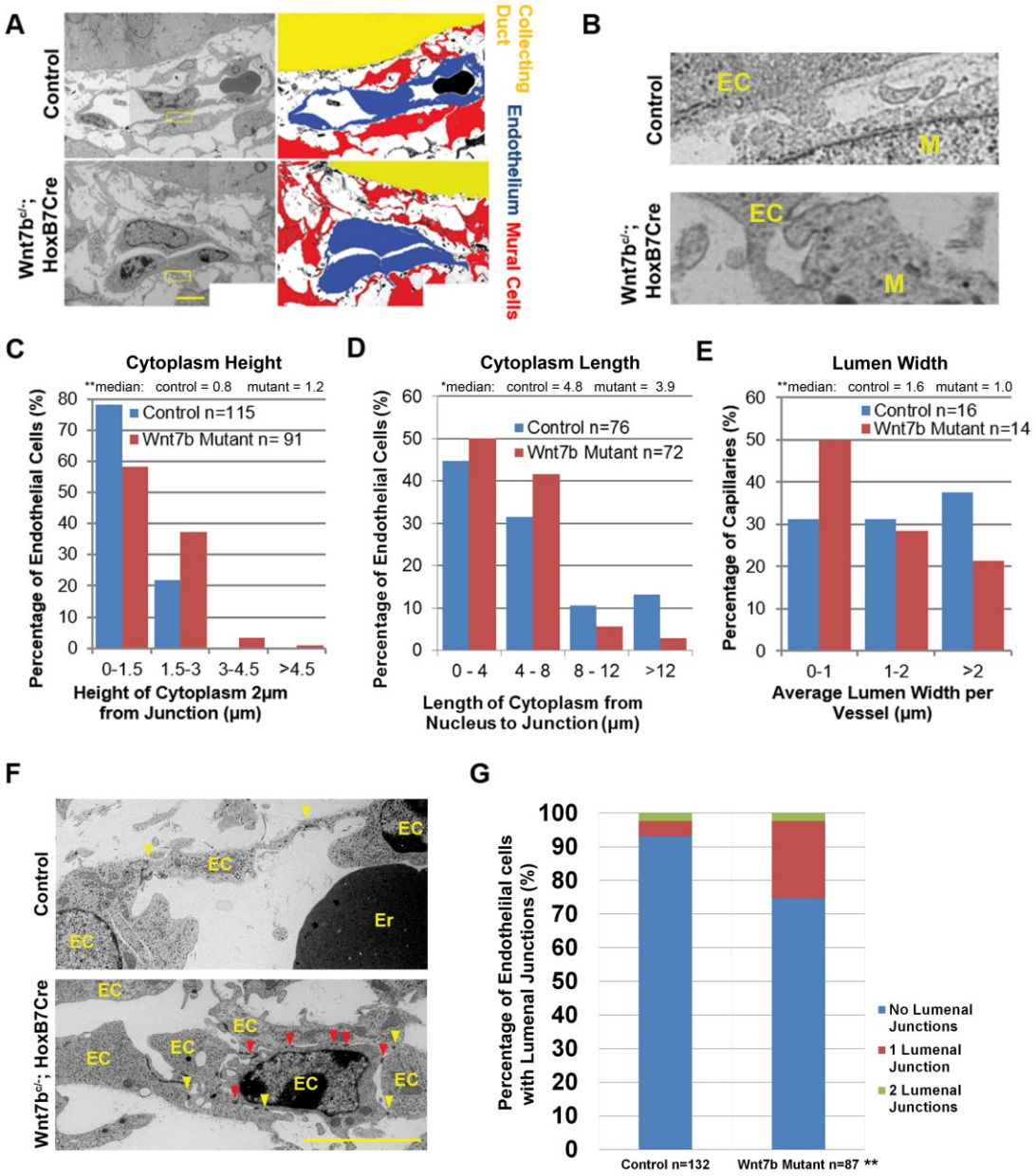
A
Control
Wnt7b$^{c/-}$; HoxB7Cre
Collecting Duct
Endothelium
Mural Cells
B
Control
EC
M
Wnt7b$^{c/-}$; HoxB7Cre
EC
M
C
Cytoplasm Height
**median: control = 0.8 mutant = 1.2
Control n=115
Wnt7b Mutant n= 91
Percentage of Endothelial Cells (%)
0-1.5
1.5-3
3-4.5
>4.5
Height of Cytoplasm 2µm from Junction (µm)
D
Cytoplasm Length
*median: control = 4.8 mutant = 3.9
Control n=76
Wnt7b Mutant n=72
Percentage of Endothelial Cells (%)
0 - 4
4 - 8
8 - 12
>12
Length of Cytoplasm from Nucleus to Junction (µm)
E
Lumen Width
**median: control = 1.6 mutant = 1.0
Control n=16
Wnt7b Mutant n=14
Percentage of Capillaries (%)
0-1
1-2
>2
Average Lumen Width per Vessel (µm)
F
Control
EC
Er
Wnt7b$^{c/-}$; HoxB7Cre
EC
G
Percentage of Endothelilal cells with Lumenal Junctions (%)
No Lumenal Junctions
1 Lumenal Junction
2 Lumenal Junctions
Control n=132
Wnt7b Mutant n=87 **

Figure 3-11 *Wnt7b* regulates endothelial cell flattening and capillary lumen formation

(A) A representative transmission electron microscopy (TEM) image of control and *Wnt7b* mutant capillaries surrounding the UB in the renal medulla with the box indicating the area showed in (B). Scale bar=5 µm. (B) High magnification transmission electron micrograph of endothelial cells (EC) of capillaries surrounding the UB epithelium and the mural cells (M) that interact with those endothelial cells. Mural cells and endothelial cells interact with each other with cytoplasmic extensions in both controls and mutants. (C) *Wnt7b* mutants have more endothelial cells with taller cytoplasm (p=0.0024). (D) *Wnt7b* mutants have more endothelial cells with shorter cytoplasm length (p=0.0004). (E) *Wnt7b* mutants have a higher number of capillary vessels with narrower lumens (p=0.0139). (F) A representative TEM image showing the lateral cell-cell junctions (yellow arrowheads) between ECs in a capillary surrounding the medullary UB and ectopic, lumenal cell-cell junctions (red arrowheads). Scale bar=5 µm. (G) Quantification of the percentage of endothelial cells with different numbers of lumenal junctions in the control and *Wnt7b* mutant medullary peri-UB capillaries (p=0.0002).

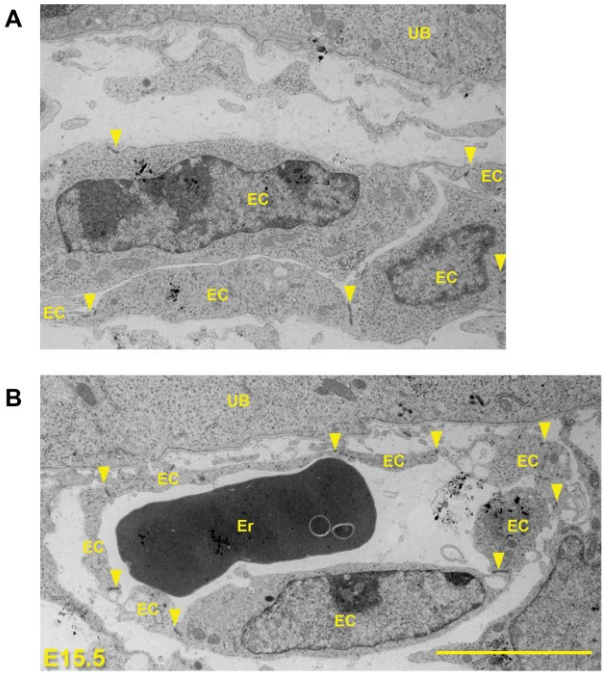

Figure 3-12 Transmission electron micrographs of the forming peri-UB capillaries in the E15.5 nascent renal medulla
(A) Early stages of peri-UB capillary development showing endothelial cells (EC) with lateral junctions (arrowheads) and a slit between lumenal membranes. (B) A lumenized peri-UB capillary with lateral junctions and a visible lumen, often with Erythrocyte (Er) inside. Scale bar=5 µm.

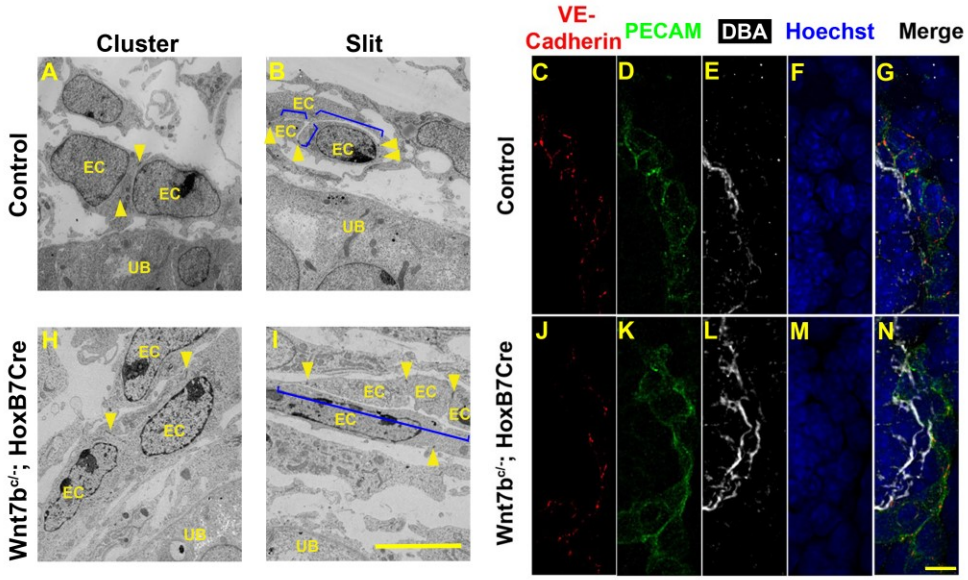

Figure 3-13 No lumen formation defect in Wnt7b mutant kidneys at E14.5
(A-B, and H-I) Transmission electron micrographs showing normal endothelial organizations in Wnt7b mutants. EC, endothelial cells. Arrowheads point to cell-cell junctions. Brackets mark the slits. (C-G and J-N) The VE-cadherin expression pattern in the peri-UB region in the deep cortex of Wnt7b mutants is similar to that of controls. Scale bar=5 µm.

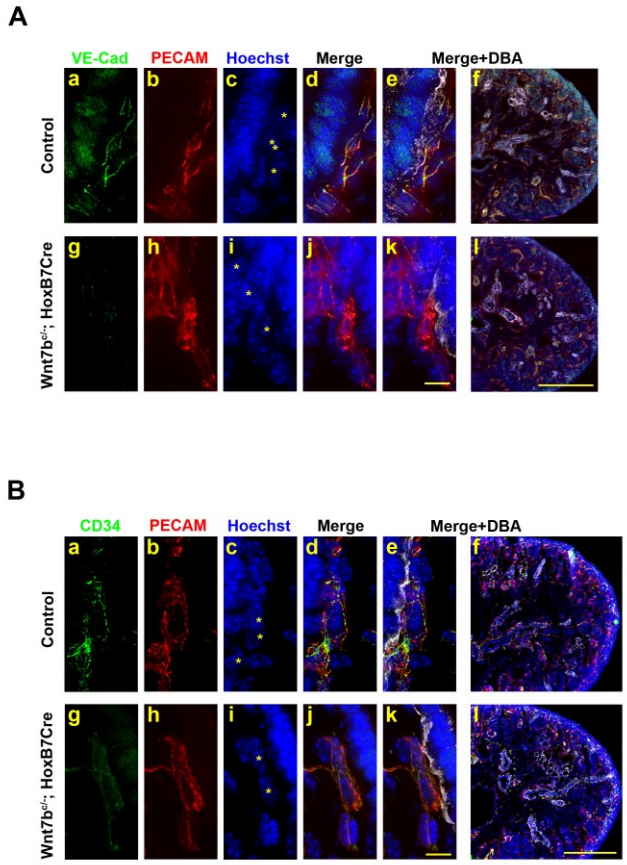

Figure 3-14 Decrease in the cell surface expression of VE-cadherin and CD34 in peri-UB capillaries in the Wnt7b mutant nascent medulla
(A) (a-f) VE-Cadherin co-localizes with PECAM on the surface of endothelial cells adjacent to the UB epithelium. Some endothelial cells are marked with asterisks. (g-k) In Wnt7b mutants, VE-Cadherin expression is reduced in the endothelial cells which still express PECAM. Some endothelial cells are marked with asterisks. (l) The loss of VE-Cadherin in Wnt7b mutants is restricted to the medulla. Panels a-e and g-k, scale bar= 10µm. Panels f and l, scale bar=500 µm.(B) (a-f) CD34 is localized to the cell surface of PECAM+ endothelial cells. Some endothelial cells are marked with asterisks. (g-l) CD34 is reduced at the cell surface of and diffused in the endothelial cells adjacent to the medullary UB epithelium. Some endothelial cells are marked with asterisks. Panels a-e and g-k, scale bar= 10µm. Panels f and l, scale bar=500 µm.

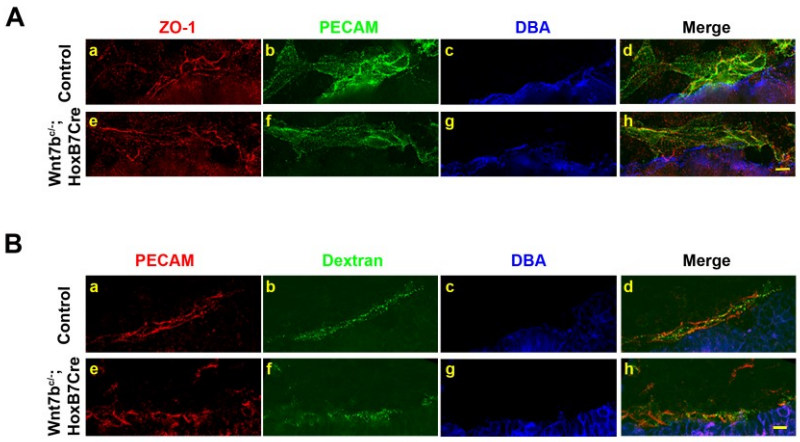

Figure 3-15 The integrity of peri-UB capillaries in the Wnt7b mutant nascent medulla is not compromised

(A) The normal ZO-1 expression pattern in the peri-UB endothelial cells in the Wnt7b mutant nascent renal medulla. Scale bar=5 µm. (B) Fluorescent Dextran injected into the blood circulation is retained at similar intensity in the peri-UB capillaries of Wnt7b mutant nascent renal medulla as in those of controls. Scale bar=10 µm.

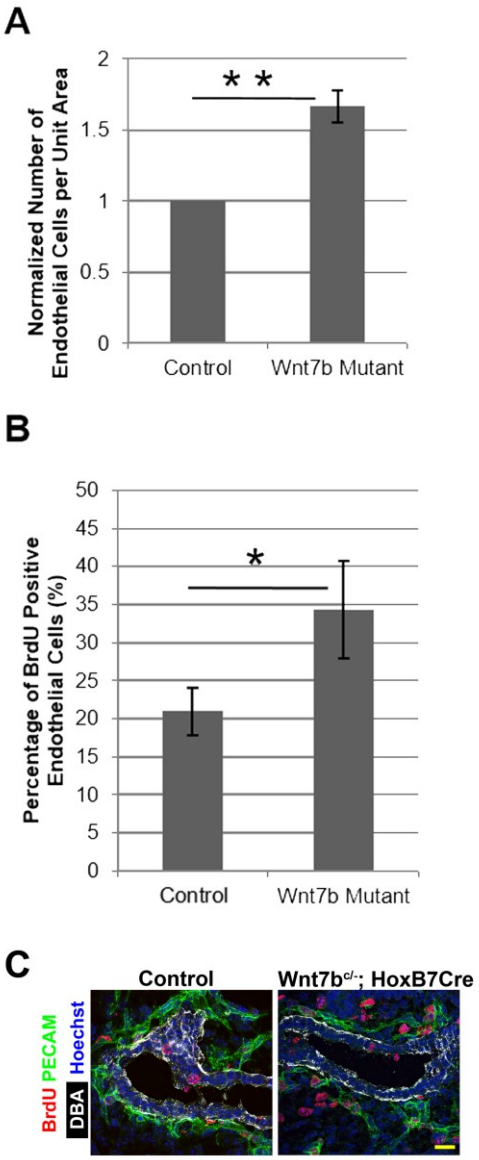

Figure 3-16 Quantification of density and proliferation of endothelial cells surrounding the UB epithelium in the nascent renal medulla
(A) Higher density of endothelial cells surrounding the UB epithelium in the Wnt7b mutant nascent renal medulla than in the controls (p=0.0014). (B) The cell proliferation rate in the endothelial cells surrounding the UB epithelium measured by BrdU incorporation is higher in the Wnt7b mutant nascent renal medulla than in the controls (p=0.0015). (C) Representative images of BrdU labeling in the endothelial cells surrounding the UB epithelium in the nascent renal medulla. Scale bar=10 µm.

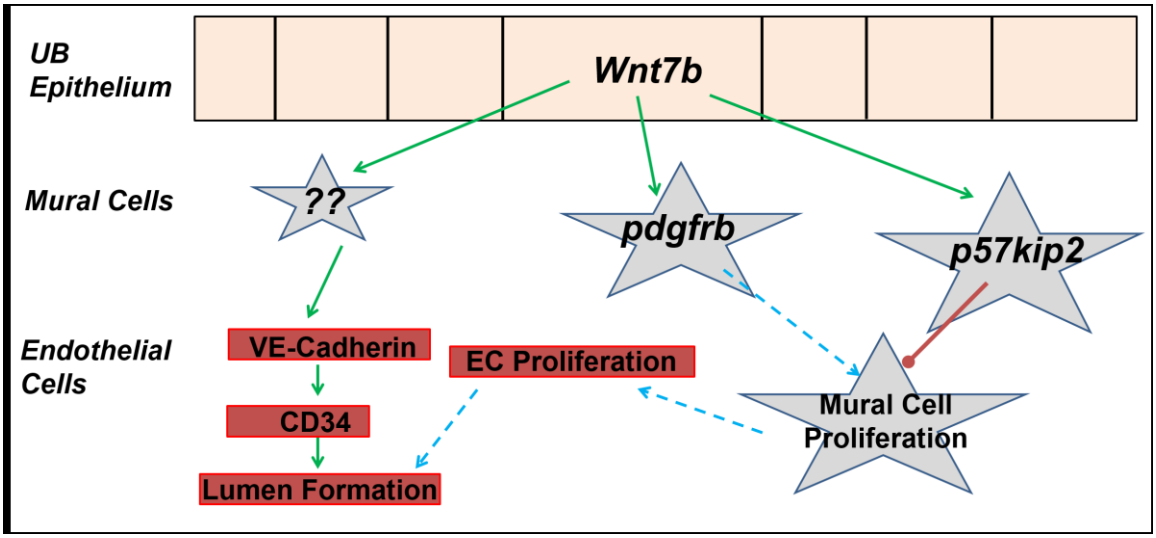

Figure 3-17 Wnt7b regulates vascular lumen formation and mural cell proliferation in the renal medulla

Wnt7b is secreted by the UB epithelium shown in yellow. Wnt7b promotes (green arrows) expression of *pdgfrb* and *p57kip2*. *p57kip2* mediates inhibition (red line) of mural cell proliferation. PDGFRβ likely promotes proliferation in mural cells (possible signaling represented by blue arrows). A signal from the Mural cells (stars) likely regulates proliferation and capillary lumen formation in endothelial cells (red).

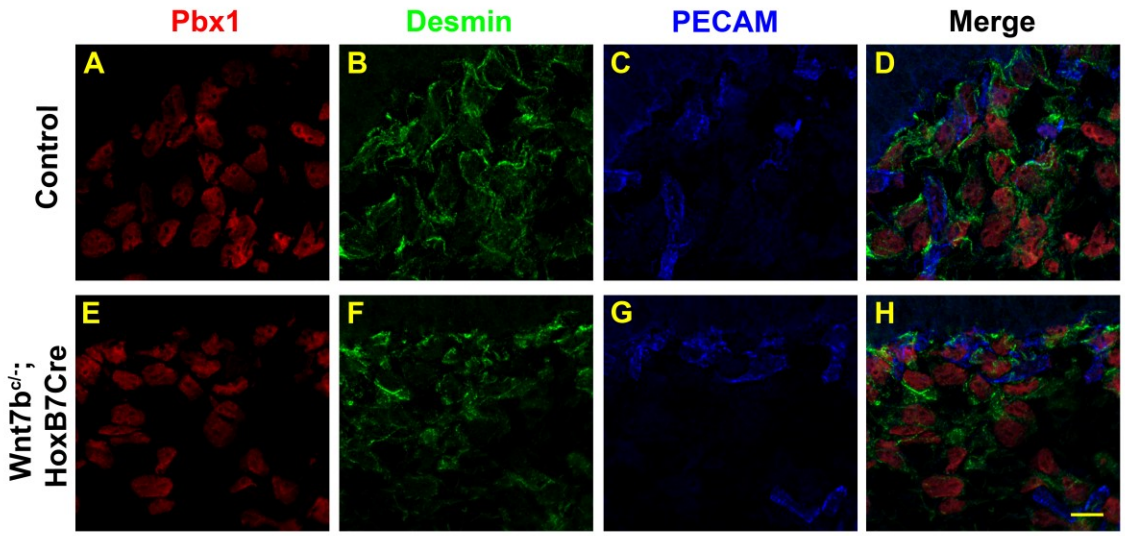

Figure 3-18 Pbx1 expression is unchanged in *Wnt7b* mutants
Scale bar=5 µm

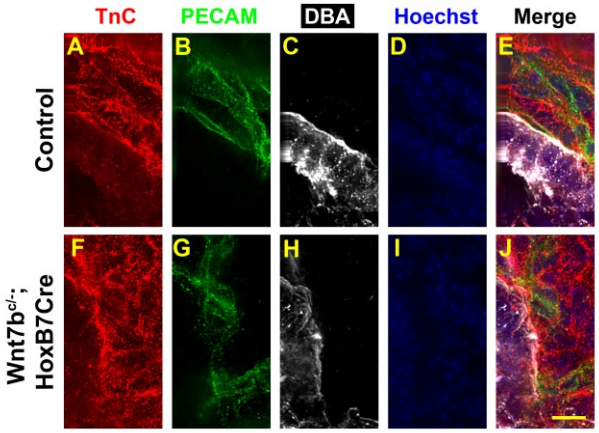

Figure 3-19 TenascinC expression is unchanged in *Wnt7b* mutants
Scale bar=5 µm

Chapter 4

Mural cell expression of *p57kip2* in the renal medulla is promoted by canonical Wnt signaling and regulates renal medulla elongation

4.1 Abstract

The renal medulla is essential for urine concentration and thus body salt and water homeostasis. Despite its role in renal physiological function, the mechanisms governing collecting duct elongation and renal medulla formation are not well understood. *Wnt7b* has been shown to mediate renal medulla formation, via activation of the canonical β-catenin pathway in the neighboring mural cells associated with the peri-UB capillaries, but the mechanism whereby the mural cells mediate Wnt7b action is unknown. Here we address the role of *p57kip2* as a mediator of Wnt7b signaling and effector of renal medulla formation. Results suggest that *p57kip2* expression in renal medullary mural cells is regulated by canonical Wnt signaling, through the binding of β-catenin with *p57kip2* intron 2. Furthermore, p57kip2 expressed in renal medullary mural cells is necessary for renal medulla elongation, and p57kip2 mediates Wnt7b's role in renal medulla elongation.

4.2 Introduction

The physiological function of the kidney is facilitated by organization of the renal structures along a cortical-medullary axis. The glomeruli and convoluted tubules are restricted to the cortex, while the loops of Henle (LOH) and collecting duct system extend from the cortex to the medulla.[264] The organization of collecting duct cells also varies from the cortex to the medulla.[265] The renal interstitium consists of mesenchymal cells descendent from the Foxd1+ stroma that are distributed throughout the kidney.[59, 115] Interstitial cells have been shown to be important for nephron formation, branching morphogenesis, and elongation of the presumptive collecting duct or ureteric bud (UB).[70, 115] The identities of various subsets of the interstitial cell populations, and the mechanisms by which they direct the development of kidney structures, are still being uncovered.

Wnt7b is a Wnt ligand which is important for development of various tissues, including the placenta, eye, bones, lungs, kidney, pancreas and neurons.[70, 166, 168-170, 172-182] In the kidney, Wnt7b is required for renal medulla formation. It promotes LOH elongation, regulates oriented cell division and elongation of the UB epithelium, inhibits proliferation in the peri-UB vasculature, and promotes peri-UB capillary formation.[70] (chapter3) Wnt7b is expressed in the ureteric trunk, and regulates renal medulla elongation through canonical Wnt signaling to cells in the neighboring interstitium.[70] My previous work shows the subset of interstitial cells in the medulla that receive a canonical Wnt signal from Wnt7b are mural cells associated with the peri-UB capillaries (chapter3). How peri-UB mural cells respond to canonical Wnt signaling, and what their role is in renal medulla elongation, is not studied.

p57kip2 is a member of the cip/kip family of cyclin dependent kinase inhibitors (CKI), which inhibit G1/S phase cyclins.[208] p57kip2 is a unique member of this family in that its expression is restricted to specific cells types, and it has been implicated in non-CKI related functions such as transcription, apoptosis and migration.[117, 209-211] Loss of *p57kip2* in mice causes defects in the abdominal wall, bone, palate, eye adrenal gland, and kidney.[117, 212] Defects seen in the mutant mice are similar to human patients with Beckwith-Wiedemann Syndrome. Patients with Beckwith-Wiedemann syndrome have renal medullary dysplasia; a smaller medulla with less epithelia than normal. In the embryonic kidney, p57kip2 is expressed in mural cells (Chapter 3) and also in podocytes. However when *Wnt7b* is ablated from the renal collecting ducts, only the mural cell expression of p57kip2 is lost.[70]

Here we provide evidence that *p57kip2* expressed in mural cells is a direct transcriptional target of canonical Wnt signaling, and is necessary and sufficient for renal medulla elongation. p57kip2 not only regulates the proliferation of the mural cells where it is expressed, but also regulates the proliferation of the adjacent endothelial cells. Additionally, p57kip regulates oriented cell division of the collecting ducts. Furthermore, p57kip2 partially mediates Wnt7b's regulation of renal medulla elongation.

4.3 Results

4.3.1 Wnt7b directly regulates expression of *p57kip2* in the peri-UB mural cells.

Previous work showed that Wnt7b signals through canonical pathway to the renal interstitium, specifically the mural cells in the renal medulla.[70](Chapter 3) In *Wnt7b*$^{c3/-}$

;Sox2Cre mice, where Wnt7b expression is ablated throughout the embryo, the medullary expression of p57kip2 is lost.[70] This suggests that *p57kip2* expressed in this domain is a target of canonical Wnt signaling. Examination of the *p57kip2* genomic sequence with ECR browser (**Figure4-1A**) revealed that *p57kip2* has two putative binding sites for TCF/Lef family members, which are canonical Wnt pathway effectors. Both sites, a LEF1B site (1B site) and a LEF1TCF1_Q4 site (Q4 site), were located in intron 2.

To determine if the 1B site and Q4 site are functional TCF/Lef response elements, we used a luciferase reporter assay in NIH3T3 cells (**Figure 4-1B**) where the expression of the luciferase reporter is controlled by canonical Wnt activity. We activated canonical Wnt pathway in these cells through transfection of a plasmid expressing a dominant active β-catenin, and compared their luciferase expression to that in the cells that had been transfected with plasmids expressing both a dominant active β-catenin and a dominant negative TCF. When the luciferase reporter 8xTopflash, which contains 7TCF/Lef binding sites, was co-transfected in these cells, we could detect a robust response to canonical Wnt signal. The negative control for Topflash, Fopflash, which contained only mutant TCF/Lef binding sites, did not produce luciferase in the presence of canonical Wnt signaling. I amplified *p57kip2* intron 2 from mouse genomic DNA with PCR, and inserted it upstream of the luciferase cDNA in the Fopflash vector. Site-directed mutagenesis was used to generate 3 mutant versions of the p57kip2 intron 2 sequence; one with the 1B site mutated (*1B), one with the Q4 site mutated (*Q4) and one with both sites mutated (*1B+Q4). When the wildtype and mutant *p57kip2* constructs were tested for their ability to respond to canonical Wnt signaling, only the wildtype *p57kip2* intron 2 sequence had a significant fold change of the luciferase

activity compared to the dominant negative TCF condition. When either or both sites are mutated, intron 2 could not respond to canonical Wnt signaling. The luciferase reporter results indicate that the 1B site and Q4 site are both necessary for the canonical Wnt response *in vitro*.

To test whether *p57kip2* is a direct target of canonical Wnt signaling *in vivo*, E15.5 renal interstitial cells including the Wnt7 target mural cells were isolated from the *Foxd1GC; ROSA*$^{mT/mG}$ mice. Then Chromatin Immunoprecipitation (ChIP) was performed using anti-β-catenin antibodies (**Figure 4-1C**). PCR was used to determine if the 1B and Q4 sites were pulled down by anti-β-catenin antibodies. Both the 1B and Q4 sites had a significant fold change over immunoprecipitation with IgG, showing that both sites bind with β-catenin. As a negative control, we also designed primers to amplify a region of *p57kip2* intron 2 that is 1kb away from the 1B and Q4 TCF/Lef binding sites, and we did not see a significant fold change over immunoprecipitation with IgG. Together, the results strongly suggest that p57kip2 expressed in mural cells is a direct target of canonical Wnt signaling via two TCF/Lef binding sites in intron 2.

4.3.2 p57kip2 action in peri-UB mural cells is necessary and sufficient for renal medulla elongation.

p57kip2 is expressed in both podocytes and renal medullary mural cells.[212] In order to specify the contribution of different p57kip2 expressing cell populations to renal medulla elongation, we took advantage of the *p57kip2NTAP* mouse model. The *p57kip2NTAP* allele has a stop site flanked by loxP sites inserted into Exon 2 of the *p57kip2* gene (**Figure 4-2A**). In the absence of Cre, *p57kip2 NTAP* produces a short transcript that gets degraded. In the presence of Cre, p57kip2 endogenous expression is

restored in the cells that express Cre and their progeny. Examination of the *p57kip2NTAP* kidneys confirmed that the allele behaved as designed, at least in the kidney. It did not express p57kip2 protein in either podocytes or mural cells, and the medulla length is shorter (**Figure4-2B**).

I then crossed *p57kip2NTAP* with *Sox2Cre* mice, where p57kip2 expression was restored in the entire embryo proper, and thus in the kidney p57kip2 expression was restored to both podocytes and Wnt7b target mural cells. A renal medulla of normal length formed, demonstrating that the *p57kip2NTAP* allele behaved as designed (**Figure 4-3A**). I then crossed *p57kip2NTAP* with *Six2Cre* mice (*p57kip2; Six2TCG*) to restore p57kip2 expression in the podocytes but not the Wnt7b target mural cells, and with *Foxd1GC* mice (*p57kip2NTAP;Foxd1GC*) to restore p57kip2 expression in the Wnt7b target mural cells but not podocytes (**Figure 4-3**). The medulla length was quantified as the distance starting directly below convoluted tubules and ending at the papilla tip, normalized over a distance starting at the same point and ending at the hilum. The resulting unit (M/M+P) is a reflection of the elongation of the medulla into the pelvic space. When p57kip2 endogenous expression was restored only to the podocytes, using *Six2Cre*, the medulla was short, similar to null mutants (**Figure 4-3B,J**). However when p57kip2 endogenous expression was restored to the peri-UB mural cells using *Foxd1GC*, the medulla is rescued to the wildtype length (**Figure 4-3C,J**). Together this indicates that p57kip2 expression in the peri-UB mural cells is both necessary and sufficient for renal medulla elongation, while its podocyte expression is not involved in the regulation of the renal medulla length.

4.3.3 Podocytes appear normal in *p57kip2* mutants.

Given that p57kip2 has known roles in proliferation, cell survival and differentiation, we examined whether p57kip2 had an effect on the development of the podocytes. We did not observe any obvious defect in glomerular structure in any of the *p57kip2NTAP* mouse strains (**Figure 4-3**). *In situ* hybridization showed mRNA expression of podocyte markers *Gsh1* and *Pod1* were also unchanged in *p57kip2NTAP* mutants, indicating that p57kip2 is not required for normal podocyte differentiation.

4.3.4 p57kip2 partially mediates Wnt7b's role in renal medulla elongation.

To resolve the mechanistic relationship between Wnt7b signal and p57kip2 in the renal medulla, we examined whether p57kip2 is a functional mediator ofWnt7b in regulating medulla elongation. We generated a mouse that allows Cre-mediated *p57kip2* expression, the *R26p57* mouse (**Figure 4-5A**). In the absence of Cre, no p57kip2 is expressed from this mouse, and in the presence of Cre, it will constitutively express p57kip2 in all progeny of Cre expressing cells. Unlike the *p57kip2NTAP* mouse or the endogenous expression of p57kip2 in the Wnt7b target mural cells, expression of p57kip2 from *R26p57* locus is not dependent on canonical Wnt signaling. We first performed a mouse cross to confirm that the protein expressed by *R26Rp57kip2* is functional, and that constitutive expression of p57kip2 throughout the interstitium beyond its endogenous expression domain does not interfere with renal medulla elongation. We crossed *R26p57* mice with the *Foxd1GC* mice, and with *p57kip2* null mice *(p57kip2$^{+/-m}$; Foxd1GC; R26Rp57*). These mice were in the *p57kip2* null background, but expressed p57kip2 constitutively in the interstitium. This expression rescues the medulla length defect in *p57kip2* mutants (**Figure 4-5B,C**), indicating that the protein expressed by *R26p57* in the

interstitium behaves similarly to the endogenous one and expressing p57kip2 in the interstitial cells that normally do not express p57kip2 does not interfere with renal medulla elongation.

To see if expression of p57kip2 in the renal interstitium including the Wnt7b target mural cell rescues the renal medulla elongation defect in the Wnt7b muants, we generated *Wnt7b*$^{+/-}$*; HoxB7Cre; Foxd1GC; R26Rp57kip2* embryos where p57kip2 is expressed in the Foxd1 descendant renal interstitium including mural cells, but in the UB epithelium as well due to the presence of Hoxb7Cre. The medulla length of *Wnt7b+/-; HoxB7 Cre; Foxd1GC; R26Rp57kip2* mice is greater than in that of Wnt7b mutants, or that of *Wnt7b*$^{+/-}$*; HoxB7Cre; R26Rp57kip2* kidneys, but was not completely restored to the wildtype length (**Figure 4-6**), indicating that p57kip2 expression in the interstitium is a partial mediator of Wnt7b function in renal medulla elongation.

4.3.5 p57kip2 regulates oriented cell division in the collecting duct.

Oriented cells division in the prospective medullary collecting ducts was disrupted in *Wnt7b* mutants and is likely to contribute to the renal medulla elongation defect. We therefore examined oriented cell division in the *p57kip2* mutant prospective medullary colleting ducts. We observed a disruption in the distribution of mitotic angles in the medullary UB as well (**Figure 4-7A**). In controls, there was a bias toward planar cell division along the longitudinal axis of the elongating UB epithelium. In *p57kip2* mutant the direction of cell division was randomized. Consistent with our medulla length observations, the *p57kip2* mutants oriented cell division defect was milder than that of *Wnt7b* mutants.[70] Similar to *Wnt7b* mutants, proliferation in the UB was unchanged in *p57kip2* mutants (**Figure 4-7B**).

4.3.6 *Wnt11* expression is greatly reduced in *p57kip2* mutants.

Wnt11 is downregulated in the interstitial cells neighboring the prospective medullary collecting ducts of *Wnt7b* mutants.[70] Wnt11 is primarily associated with signaling through the planar cell polarity pathway. Further, Wnt11 has been shown to regulate oriented cell division in the kidney.[266] To determine whether *Wnt11* expression is regulated by p57kip2, we examined the mRNA expression of *Wnt11* in *p57kip2* mutants. We observed a decrease in *Wnt11* mRNA level in the cells neighboring the medullary UB epithelium, though not as severe as that in the *Wnt7b* mutants (**Figure 4-8A**). *Wnt4* is also downregulated in the medullary interstitium of *Wnt7b* mutants, however *Wnt4* expression was unchanged in the *p57kip2* mutants **(Figure 4-8B).**

4.3.7 The role of p57kip2 in capillary development.

We showed in Chapter 3 that both p57kip2 and Wntb7 inhibits Wnt7b target mural cell proliferation. Wnt7b also regulates endothelial cell proliferation and vascular lumen formation (Chapter3). Thus, we examined whether p57kip2 mutants had vasculature defects similar to Wnt7b mutants. Proliferation of endothelial cells were increased in p57kip2 mutants, although the change in proliferation was not as great as in *Wnt7b* mutants (**Figure 4-9**). However p57kip2 mutants did not have changes in VE-cadherin expression in the peri-UB medullary capillaries (**Figure 4-10**). Thus, p57kip2 regulates neighboring endothelial cells proliferation, but likely not capillary lumen formation.

4.4 Discussion

Our work has started to uncover the molecular mechanisms regulating renal medulla formation, by identifying p57kip2 in the mural cells as a direct target of canonical Wnt signaling from the UB and a mediator of a part of Wnt7b functions in regulating renal medulla elongation. In addition, my work showed that the p57kip2 expressing Wnt7b target mural cells regulate some aspects of renal medulla elongation and development.

We demonstrated that p57kip2 is a direct target of canonical Wnt signal. Even though canonical Wnt target Lef1 is expressed in both cortical and medullary interstitium, p57kip2 expression is restricted to the medulla (Chapter 3). This shows that canonical Wnt promotion of p57kip2 expression is cell type specific, and that the cortical and medullary mural cells are indeed different cell types. The p57kip2 expressing cells in the medulla are older than the cortical interstitial cells,[111] so p57kip2 expression in the peri-UB mural cells may indicate a more differentiated cell type, consistent with the role of p57kip2 in promoting cell differentiation as a CKI.

p57kip2 mutants have increased proliferation of both endothelial cells and mural cells. That p57kip2 regulated proliferation in the mural cells where it is expressed is not surprising given its CKI function. Here we show that p57kip2 is also necessary to inhibit proliferation in the neighboring endothelial cells. Co-culture experiments showed that mural cells can inhibit endothelial cell proliferation by a mechanism likely dependent on contact or close proximity.[267] My data suggests p57kip2 mediates mural cell inhibition of endothelial cell proliferation.

p57kip2 mutants appear to have a lower density of epithelia in the medulla. This could be due to there being fewer UB trunks in *p57kip2* kidneys, fewer LOH, or an

increase in non-epithelial cell types. *Wnt7b* mutants have a defect in LOH elongation, and an increase in UB apoptosis at E17.5. Preliminary data for the *p57kip2* mutant indicate that LOH elongation is not completely disrupted, yet there does appear to be fewer LOH in *p57kip2* mutant. Future experiment will include measurements of LOH and UB trunk number/density, as well as measurements of apoptosis in the epithelia from E15.5 to E18.5, in both *p57kip2* mutants and in rescue mice.

Renal medulla development can be impaired due to placental defects,[90] and p57kip2 has been shown to regulate placental development.[221, 268] However when we crossed the *p57kipNTAP* mouse with *Sox2Cre*, which is specific for all embryonic tissue, the renal medulla looked fully extended, with normal morphology (**Fig4-3A**), indicating loss of p57kip2 in extraembryonic tissues does not affect renal medulla elongation.

We have shown that peri-UB mural cells in the renal medulla can regulate endothelial cell proliferation, oriented cell division in the UB epithelium, and renal medulla elongation. Increased proliferation in cells that have lost p57kip2 expression can cause defective or delayed differentiation in many cell types.[117, 212] However peri-UB mural cells in *p57kip2* mutants did not lose PDGFRβ expression (Chapter 3), which indicates they have kept mural cell identity. Podocyte differentiation is normal as well despite the loss of p57kip2.

Removal of Wnt7b from the collecting duct, and removal of β-catenin from the interstitium result in failure to form renal medulla,[70] while removal of p57kip2 results in a drastically shortened renal medulla.[117] Consistent with this difference, the *p57kip2* rescue in *Wnt7b* mutant background partially rescued medulla length. Additionally the oriented cell division defect was not as strong in *p57kip2* mutants as it was in *Wnt7b*

mutants. This indicates there is at least another Wnt7b regulated pathway that directs oriented cell division and renal medulla elongation.

How could mural cells regulate oriented cell division in the UB epithelium? Wnt11 is known to signal through the planar cell polarity pathway. Furthermore, PCP pathway can regulate oriented cell division in the kidney.[266] We observed a decrease in *Wnt11* expression in *p57kip2* mutants that is a milder reduction than that in the *Wnt7b* mutants, suggesting that p57kip2 could promote a PCP signal from the peri-UB mural cells to the UB epithelium to regulate oriented cell division.

Together, our results start to outline a pathway whereby Wnt7b promotes p57kip2 expression via the canonical Wnt pathway, to regulate renal medulla elongation. We identified *p57kip2* as a direct target of canonical Wnt signaling and showed that p57kip2 mediates, at least in part, Wnt7b's role in renal medulla elongation. There is much work still required to understand the downstream components of this pathway.

4.5 Figures

A

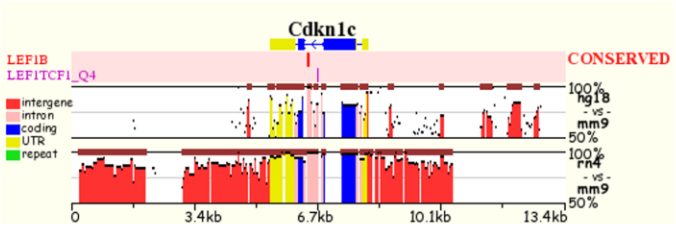

Human	AGGTCCGCGGCGGGTCAGCTTTGTTTACGTCGCCGCGCAATGTGCTGTGTAAGCATTTCC
Rat	AGGTCCGCGGCGGGTCAGCTTTGTTTACGTCGCCGCGCAATGTGCTGTGTAAGCATTTCC
Mouse	AGGTCCGCGGCGGGTCAGCTTTGTTTACGTCGCCGCGCAATGTGCTGTGTAAGCATTTCC

LEF1B

Human	GGGGAGGGGGGTAAGGGCGCAGCCGCGCCCTGAGCGCTGCGGGCCCTTTAATGCCA
Rat	TAGGAAAGGGGTGCGGGCGCAACCGCGCCCTAAGCGCCGCGGGCCCTTTAATGCCA
Mouse	TAGGAAAGGGGTGCGGGCGCAACCGCGCCCTAAGCGCCGCGGGCCCTTTAATGCCA

LEF1TCF1-Q4

B

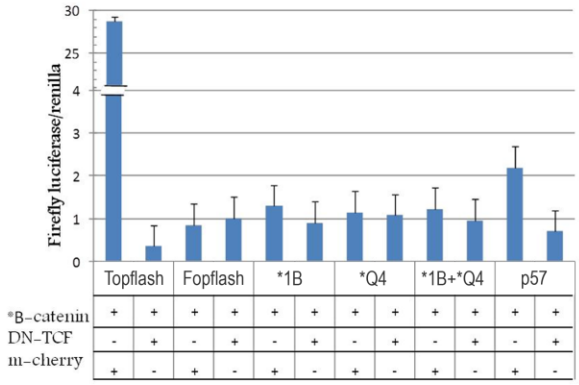

C

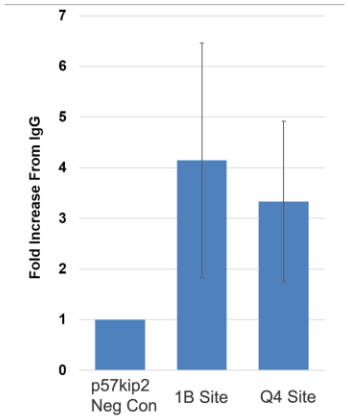

Figure 4-1 p57kip2 expressed in the Wnt7b target mural cells is a direct target of canonical Wnt signal

(A) Predicted conserved TCF/Lef binding sites in intron 2 of the *Cdkn1c* gene of the human rat and mouse genomes. The exons were marked in blue and the introns in pink. (B) The luciferase reporter assay in NIH3T3 Cells. When the 8x-Topflash vector was co-transfected with a dominant active β-catenin, robust luciferase activity is produced. This response is ablated when a dominant negative TCF is co-transfected. No luciferase is produced from transfection of 8x-Fopflash with a dominant active β–catenin with or without a dominant negative TCF. When both 1B and Q4 sites are intact, p57kip intron 2 (p57) has a 2 fold response compared to Fopflash, and a 3.5 fold response compared to p57kip2 intron2 in the absence of Wnt signaling (p=0.0123). When either (1B* and Q4*) or both (1B+Q4*) sites are mutated, there is no statistically significant response to canonical Wnt signaling (p=0.6820, p=0.4336, p=09226). (C) Chromatin ImmunoPrecipitation (ChIP) on E15.5 Foxd1-descendant renal interstitial cells. Both the 1B site and Q4 site were enriched with anti-β-catenin antibody pull-down, compared to an unrelated region of p57kip2 intron 2. (1B p=0.036) (Q4 p=0.034)

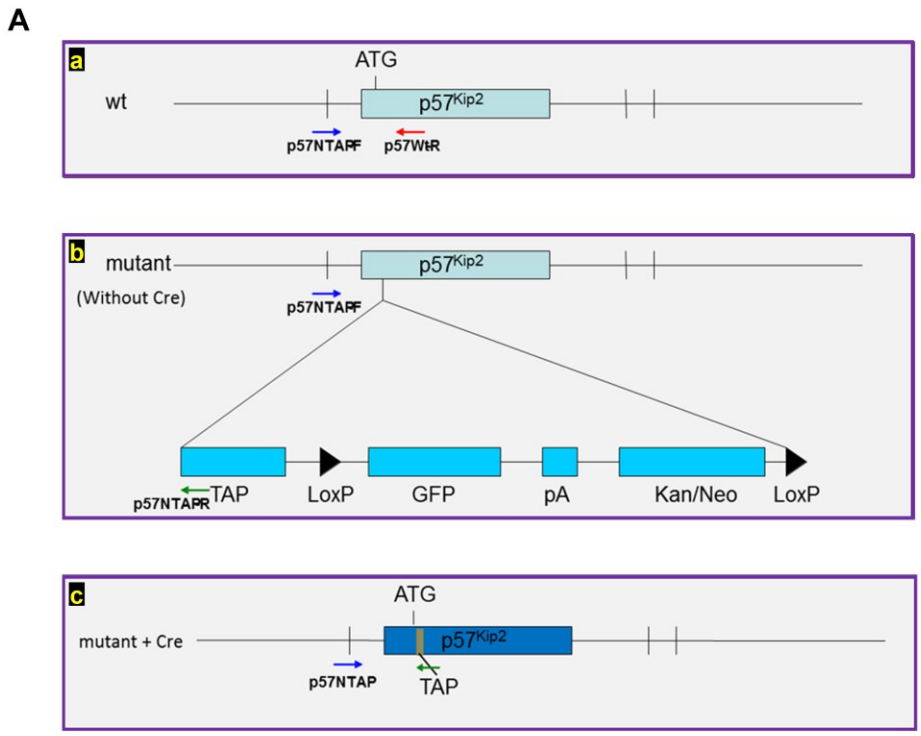
A
a
ATG
wt
p57Kip2
p57NTAPF
p57WtR
b
mutant
(Without Cre)
p57Kip2
p57NTAPF
p57NTAPR
TAP
LoxP
GFP
pA
Kan/Neo
LoxP
c
ATG
mutant + Cre
p57Kip2
p57NTAP
TAP

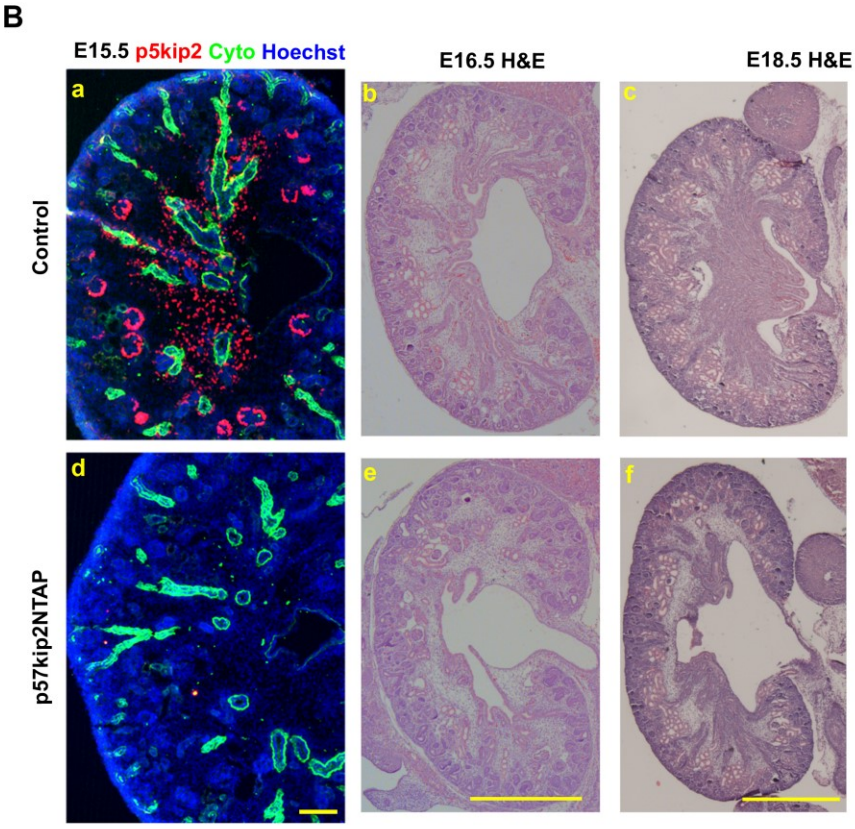
B
E15.5 p5kip2 Cyto Hoechst
E16.5 H&E
E18.5 H&E
Control
p57kip2NTAP
a
b
c
d
e
f

Figure 4-2 *p57kip2NTAP* mouse
(A) Schematic of the *p57kip2NTAP* mouse. (a) the wild type allele (b) the *NTAP* allele without Cre recombination. A stop site flanked by loxP sites is inserted into exon 2, producing a shortened transcript. (c) *NTAP* allele after Cre recombination. *p57kip2* is transcribed by its endogenous promoter. (B) Characterization of the kidney of the *p57kip2NTAP* mouse. (a-c) wildtype littermates of *p57kip2NTAP* mice have normal expression of p57kip2 protein and normal medulla elongation. (d-f) *p57kip2NTAP* mice do not express p57kip2 protein and have shorter renal medulla. Scale bar= 100µm fir panels (a and d), and 500 µm for panels (b-c and e-f)

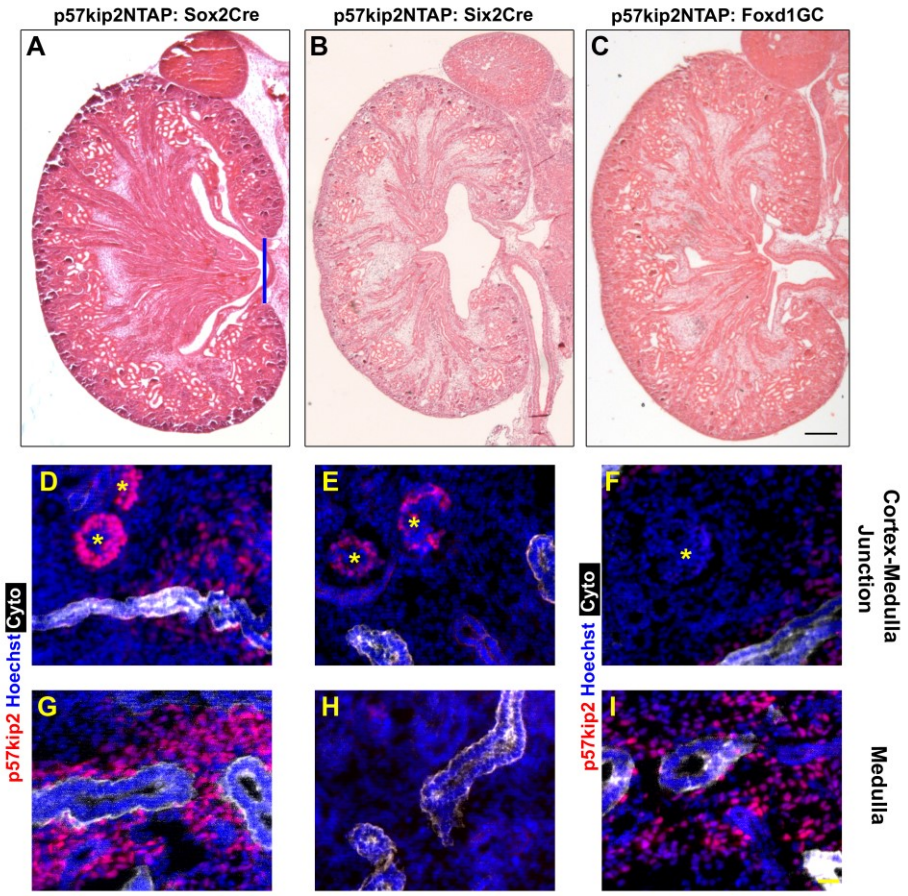
p57kip2NTAP: Sox2Cre
p57kip2NTAP: Six2Cre
p57kip2NTAP: Foxd1GC
A
B
C
D
E
F
G
H
I
Cyto
Hoechst
p57kip2
Cortex-Medulla Junction
Medulla

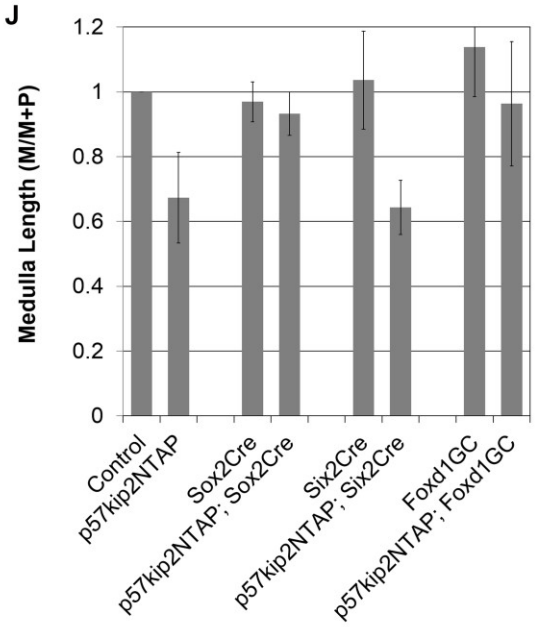
J
Medulla Length (M/M+P)
1.2
1
0.8
0.6
0.4
0.2
0
Control
p57kip2NTAP
Sox2Cre
p57kip2NTAP; Sox2Cre
Six2Cre
p57kip2NTAP; Six2Cre
Foxd1GC
p57kip2NTAP; Foxd1GC

Figure 4-3 p57kip2 endogenous expression in peri-UB mural cells, but not podocytes, restores medulla length

(A-C) the medulla length is restored at E18.5 with restoration of expression in the Wnt7b target mural cells. Scale bar = 100 µm (D-I) expression of p57kip2 restored at E15.5 in the progeny of Cre-expressing cells that normally express p57kip2. Asterisks mark the location of renal corpuscles. Scale bar = 20 µm (J) Quantification of the medulla length. The medulla length was normalized over the length from the cortico-medullary border to the hilum, represented by the blue line in (A). (*p57NTAP* vs *p57NTAP; Six2Cre* p=0.6141)(*p57NTAP vs p57NTAP;Foxd1GC* p=0.0039)(*p57NTAP* vs *P57NTAP;Sox2Cre* p=0.0004)

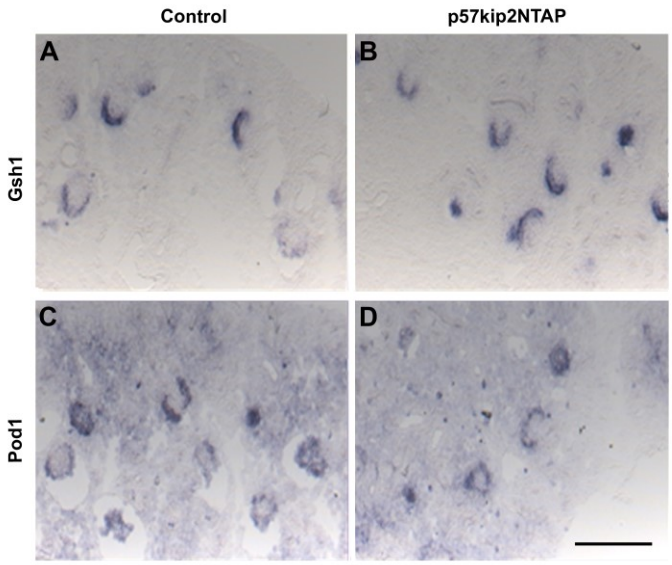

Figure 4-4 Expression of podocyte markers *Gsh1* and *Pod1* is unchanged in *p57kip2* mutants
Scale bar=100µm

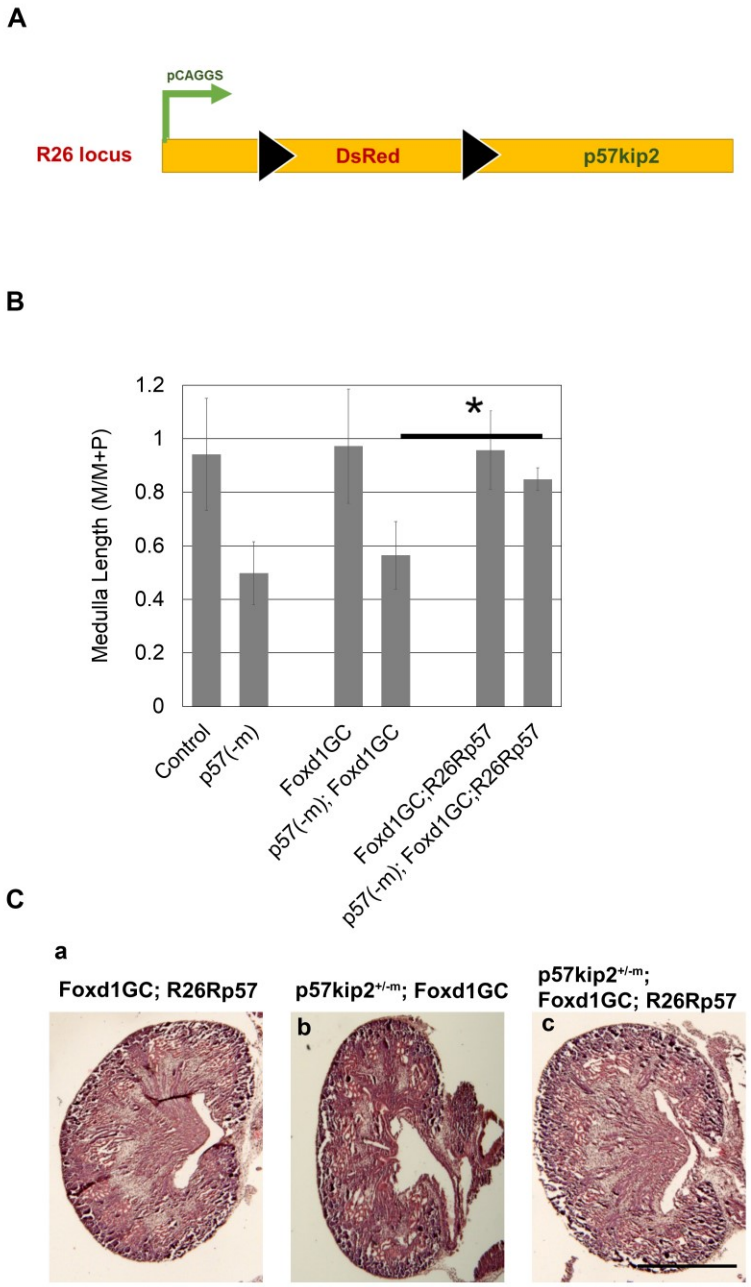

Figure 4-5 Expression of p57kip2 from the *Rosa26* locus in the Foxd1 lineage rescues the renal medulla elongation defect of *p57kip2* mutants
(A) A schematic diagram of *R26Rp57* mouse. *p57kip2* cDNA is introduced in the *ROSA26* locus downstream of a transcriptional stop site flanked by loxP sites. *p57kip2* will be expressed in any tissues that have expressed Cre in their history. (B) In the *p57kip2* mutant background, *R26Rp57kip2* allele rescues medulla elongation defect. (*p57kip2*$^{+/-m}$*;Foxd1GC* vs *p57kip2*$^{+/-m}$*;Foxd1GC;R26Rp57* p=0.0050) (C) Representative images of control, *p57kip2* mutant, and *p57kip2* rescue ((a)*Foxd1GC;R26R57* (b)*p57kip2*$^{+/-m}$*;Foxd1GC* (c)*p57kip2*$^{+/-m}$*;Foxd1GC;R26Rp57*) kidney sections showing the normal medulla length in the *p57kip2* rescue mouse kidney. Scale bar = 500µm.

A

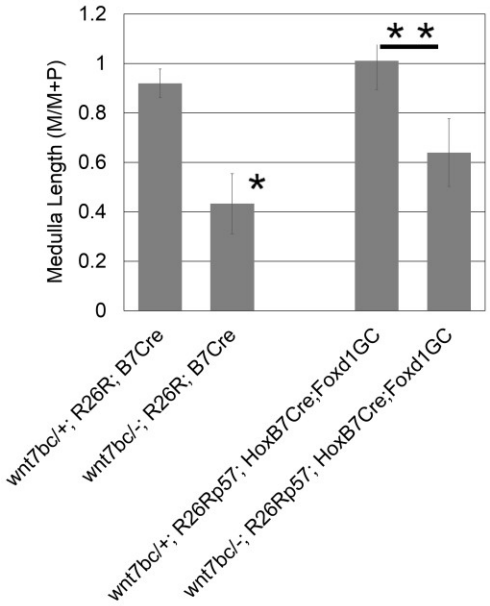
1.2
1
0.8
0.6
0.4
0.2
0
Medulla Length (M/M+P)
* *
*
wnt7bc/+; R26R; B7Cre
wnt7bc/-; R26R; B7Cre
wnt7bc/+; R26Rp57; HoxB7Cre;Foxd1GC
wnt7bc/-; R26Rp57; HoxB7Cre;Foxd1GC

B

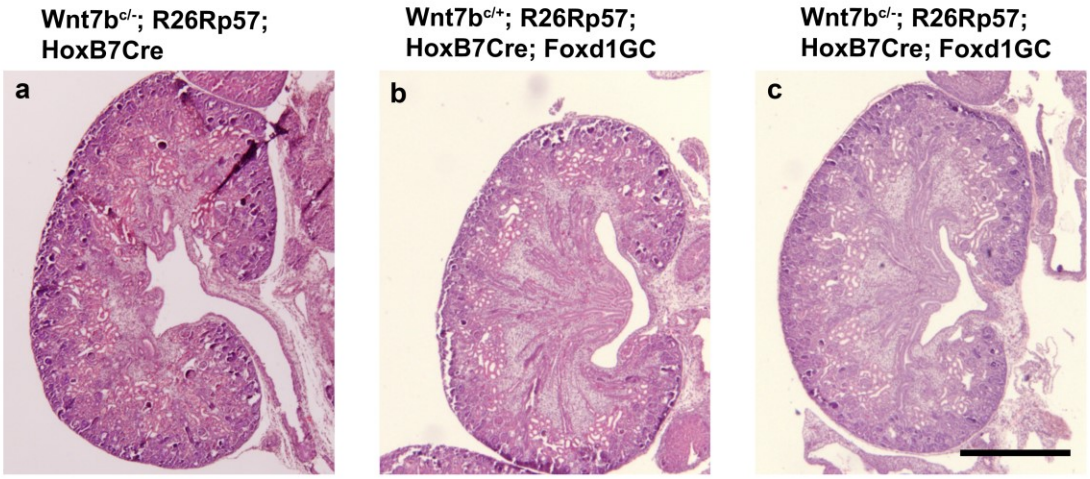
Wnt7b$^{c/-}$; R26Rp57; HoxB7Cre
Wnt7b$^{c/+}$; R26Rp57; HoxB7Cre; Foxd1GC
Wnt7b$^{c/-}$; R26Rp57; HoxB7Cre; Foxd1GC
a
b
c

Figure 4-6 Expression of p57kip2 from the *Rosa26* locus in the Foxd1 lineage partially rescues the medulla elongation defect of Wnt7b mutants
(A) Quantification of the renal medulla length showing a partial rescue of the renal medulla elongation defect in the *Wnt7b* mutants(*Wnt7b*$^{c/-}$*; R26Rp57kip2; Hoxb7Cre*), in rescue (*Wnt7b*$^{c/-}$*;R26Rp57kip2;Foxd1GC;Hoxb7Cre*) kidneys.(p=0.0126) The rescue mice renal medulla length is a partial rescue and not a long as control (*Wnt7b*$^{c/+}$*;R26Rp57kip2;Foxd1GC;Hoxb7Cre*) renal medulla. (p=0.0012) (B) Representative images of kidney sections of *Wnt7b* mutant (*Wnt7b*$^{c/-}$*; R26Rp57kip2; Hoxb7Cre*), positive control (*Wnt7b*$^{c/+}$*;R26Rp57kip2;Foxd1GC;Hoxb7Cre*), and Wnt7b rescue (*Wnt7b*$^{c/-}$*;R26Rp57kip2;Foxd1GC;Hoxb7Cre*) (a) mutant kidneys have very little renal medulla. (b)positive control kidneys look normal. (c) rescue mice have some medulla elongation. Scale bar = 500µm.

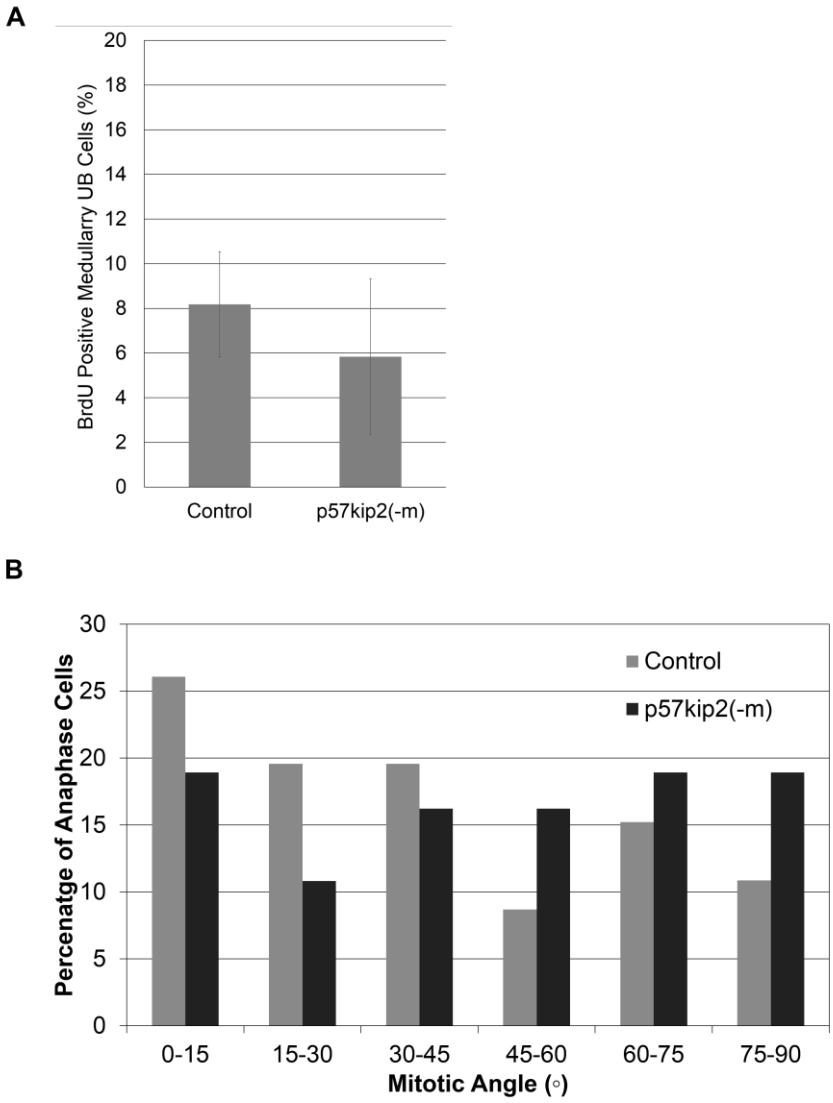

Figure 4-7 Medullary UB cells in *p57kip2* mutants do not have changed proliferation but have a defect in oriented cell division
(A)No change in proliferation in the medullary UB of *p57kip2* mutants. (p=0.3781) (B) Oriented Cell Division is disrupted in *p57kip2* mutants. (U-test p value =0.025)

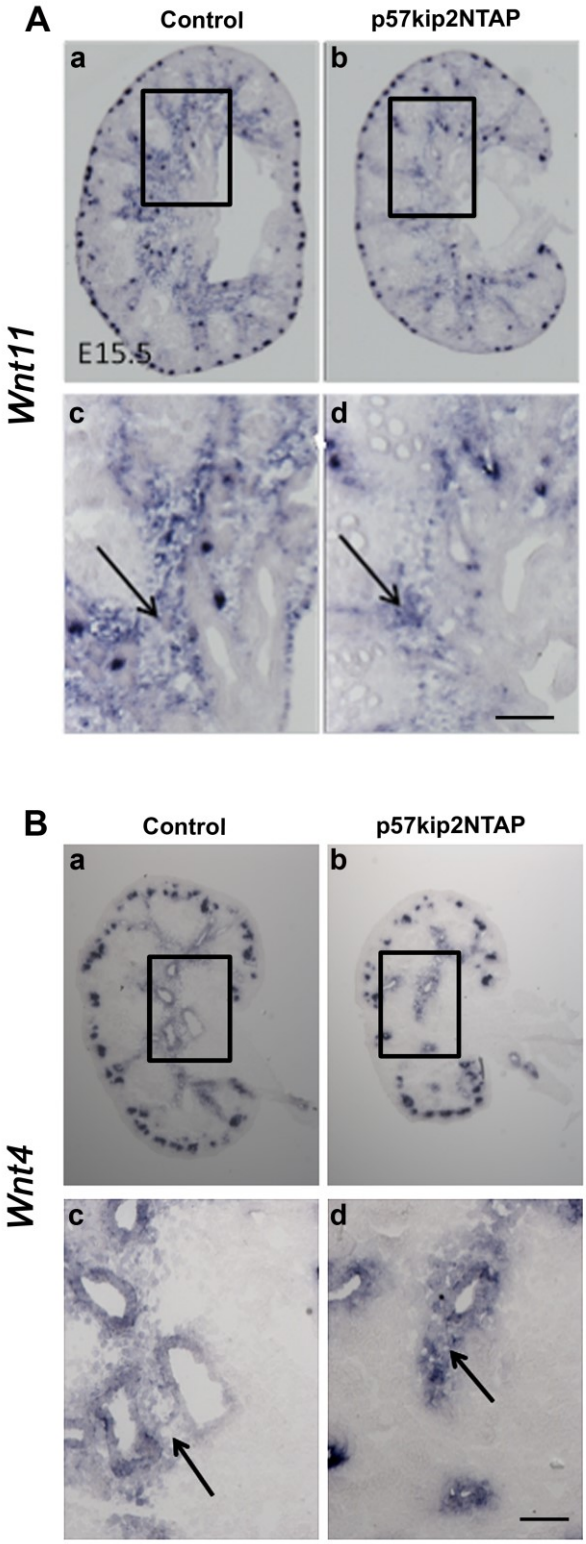
A
Control
p57kip2NTAP
a
b
E15.5
Wnt11
c
d
B
Control
p57kip2NTAP
a
b
Wnt4
c
d

Figure 4-8 Expression of PCP pathway Wnts in the renal interstitium of *p57kip2* mutants
(A) *Wnt11* expression is decreased in *p57kip2* mutants. (B) *Wnt4* expression is unchanged in *p57kip2* mutants. Scale bar=50µm

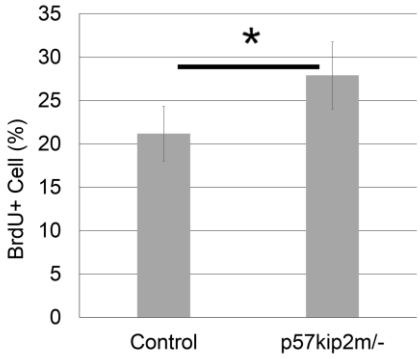

Figure 4-9 Proliferation of peri-UB medullary endothelial cells is increased in *p57kip2* mutants
(p=0.0364)

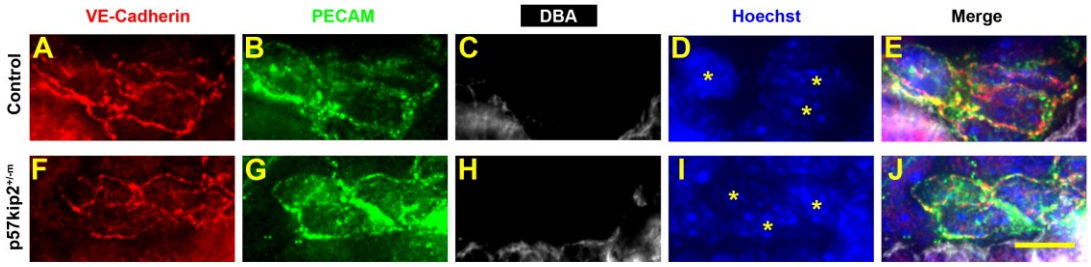

Figure 4-10 VE-Cadherin expression is unchanged in peri-UB endothelial cells of *p57kip2* mutants
Scale bar = 5µm

Chapter 5

Conserved and tissue specific roles of Wnt7b in embryonic lung vasculature

5.1 Abstract

The vasculature is an integral component of the kidney and lungs for their physiological function in the regulation of blood contents. The close interrelationship of capillaries and the epithelium is key to the physiology of the two organs. Our previous and others' work showed that Wnt7b signaling shares similarity in these two organs during development. In both organs Wnt7b is expressed in the epithelium and activates canonical Wnt signaling in the surrounding mesenchyme where the capillaries reside. In Chapter 3, I examined the role of Wnt7b in the renal medullary vasculature in detail. This chapter describes an analysis of Wnt7b's role in embryonic lungs. In embryonic lungs, Wnt7b is expressed in the distal lung bud tip. Wnt7b signaling targets mural cells of the capillaries surrounding the lung bud tip, and promotes their PDGFRβ expression. These findings identify a conserved role of Wnt7b, and the epithelium, in capillary development in both lung and kidney. On the other hand, our analysis of Wnt7b's function also revealed tissue-specific roles of Wnt7b in capillary formation. Unlike in the kidney, Wnt7b promotes proliferation in the lungs, possibly due to the differential expression of p57Kip2 (*Cdkn1c*), a cyclin-dependent kinase inhibitor, in the two populations of Wnt7b target mural cells. Further, in lungs Wnt7b does not regulate lumen formation and cell cycle exit of the capillary endothelium. Our study presents the common and tissue-specific action of Wnt7b signaling in lungs.

5.2 Introduction

A capillary blood vessel is composed of an endothelial tube with a lumen of less than 10 μm and pericytes associated at its abluminal surface.[256, 257] In the lungs, capillaries localizing around the alveolar epithelium are an integral component of the blood-air barrier and perform the pulmonary function of gas exchange.[269] In the kidney, the capillary bed is a two-portal system consisting of glomerular capillaries and peritubular capillaries connected by efferent arterioles.[7, 8] These capillaries facilitate the kidney's physiological role in removing metabolic waste and reserving nutrients in the bloodstream, and in maintaining body water, electrolyte, and acid-base homeostasis. In both organs, the capillaries cooperate intimately with the epithelium to achieve their physiological functions. While our understanding of the formation of the larger-caliber blood vessels in the kidneys and lungs has been accumulating in recent years, the timing, morphogenesis, and molecular control of capillary formation in these organs have been little explored.

Wnt7b is a Wnt family ligand important for the proper formation of a number of organs and tissues including the placenta, the eye, the bones, the lungs, the kidney, the central nervous system (CNS), neurons, hair, the pancreas, and olfactory receptor neuron axon connectivity.[70, 166, 168-170, 172-182] Notably, *Wnt7b* has been reported to regulate vasculature development in the eyes, the brain, and the lungs, by different cellular mechanisms. In the eye, it signals to the endothelial cells of the hyaloid vasculature and activates their apoptosis.[166] In the CNS, it also acts on the endothelial cells but promotes angiogenesis and blood-brain barrier formation.[180, 182] In the lungs, it signals to the

mesenchyme and regulates the differentiation/maintenance of vascular smooth muscles surrounding the major pulmonary vessels.[179]

In both the embryonic kidneys and lungs, *Wnt7b* is expressed in the epithelium and activates Wnt/β-catenin signaling in the surrounding mesenchyme.[70, 170, 179, 202] Here we demonstrate that, similar to kidney, the *Wnt7b* target cells in the lung mesenchyme are mural cells associated with capillaries. However the effect of Wnt7b signal on the proliferation of lung mural cells and the capillary endothelial cells they surround is opposite from kidney. Further, in the lungs *Wnt7b* does not regulate lumen formation or endothelial cell shape of the capillaries.

5.3 Results

5.3.1 *Wnt7b* regulates lung mural cell proliferation

Similar to the kidney, *Wnt7b* is expressed in the lung bud epithelium.[167, 179, 191] and activates canonical Wnt signaling in the surrounding mesenchyme in embryonic lungs.[167, 170] Furthermore, a vascular defect in *Wnt7b* mutant lungs has been observed, though unlike what we reported in the kidney, the lung vascular defect reported lies in the large-caliber blood vessels.[179, 202] To compare and contrast the role and mode of actions of *Wnt7b* in the embryonic lungs and the kidneys, we characterized the *Wnt7b*-responsive lung mesenchymal cells in detail. As shown in **Figure 5-1A-E**, canonical Wnt target cells in the lungs were PDGFRβ-positive, consistent with previous studies,[202] and although they were PECAM-negative, they were adjacent to the PECAM+ capillaries, thereby demonstrating that like those in the renal medulla, the *Wnt7b*-responsive

mesenchymal cells in the embryonic lungs are capillary mural cells. In contrast, our examination of p57kip2 expression in the lungs showed that unlike those in the kidney, the Lef1+ mural cells surrounding the lung buds do not express p57Kip2.(**Figure 5-1F-J**)

Previously published studies have reported a global decrease in proliferation in the *Wnt7b* mutant lung mesenchyme[170, 179] and a reduction in PDGFRβ expression[202]. To determine whether the mural cells exhibited decreased cell proliferation in *Wnt7b* mutant lungs, we quantified BrdU incorporation in PDGFRβ-positive (mural cells in *Wnt7b* mutant lungs still expressed PDGFRβ, albeit at reduced levels [202]), PECAM-negative mesenchyme.(**Figure 5-2**) This analysis showed that the cell proliferation rate of the *Wnt7b* mutant lung mural cells was significantly reduced. The difference between the mural cell proliferation phenotype in the lungs and the kidney may be due to their organ-specific expression of p57kip2.

5.3.2 *Wnt7b* regulates lung endothelial cell proliferation but not lumen formation

To determine whether lumen formation occurred normally in the capillaries lining lung buds in the absence of *Wnt7b* functions, we examined lung capillary morphology with TEM. Lung development initiates one day ahead of the kidney, and correspondingly, capillaries surrounding lung buds developed one day ahead of the peri-UB capillaries in the renal medulla. From E14.5, lumenized capillaries were extensively observed lining lung buds. Unlike the kidneys, there was no discernible difference in lumen formation, EC cell flattening, or luminal junctions between control and *Wnt7b* mutant lung capillaries (**Figure 5-3A,G**). Consistent with this observation, VE-cadherin localization in these capillaries appeared normal in *Wnt7b* mutants (**Figure 5-3B-F, H-L**). Furthermore, in agreement with normal endothelial cell flattening, endothelial cell

density surrounding the *Wnt7b* mutant lung buds was similar to that of controls (**Figure 5-4A**). Moreover, when proliferation of the endothelial cells lining the lung buds was measured at E14.5 by BrdU incorporation (**Figure 5-4B**), a decrease in cell proliferation was observed in *Wnt7b* mutant lungs at E14.5, unlike in the kidney.

5.4 Discussion

Here we have shown that while the signaling and target cell types are conserved between the developing kidneys and the lungs, *Wnt7b* exerts organ-specific effects on its target capillaries, on both the mural and the endothelial components.

The organ-specific effect of *Wnt7b* on mural cell proliferation likely results from the distinct downstream target genes that *Wnt7b* regulates, one of which is p57kip2. p57kip2 is normally expressed in the *Wnt7b* target mural cells in the renal medulla, but absent in those in the lungs. As p57kip2 is a cell-cycle inhibitor and has was shown in Chapter 3 to negatively regulate mural cell proliferation in the renal medulla, the difference in its expression in the mural cells of the two organs may contribute significantly to the differential regulation of mural cell proliferation by *Wnt7b* in the two organs.

The molecular mechanisms underlying the organ-specific effects of *Wnt7b* on endothelial cell morphogenesis and proliferation in the kidney and lung remain elusive, but likely lie in the distinct effect of *Wnt7b* on mural cells. That the changes in endothelial cell proliferation went parallel to the changes in the proliferation of mural cells associated with them in both organs is consistent with this notion. It could be that the expression of p57kip2 triggers a cascade of changes in mural cells that relay Wnt7b's

effect to the endothelium. Alternatively, some unidentified kidney-specific *Wnt7b* target genes in the mural cells are responsible for the endothelial phenotype.

In both the kidneys and the lungs, the close relationship between the epithelium and the vasculature is critical for their functions as modifiers of blood contents. Our study showed that despite differences in mechanisms and effects, the epithelium plays a crucial role in the formation of its physiological partner, the capillary bed, in both organs. This mechanism probably serves to coordinate their development to establish the structural basis serving postnatal physiological needs.

5.5 Figures

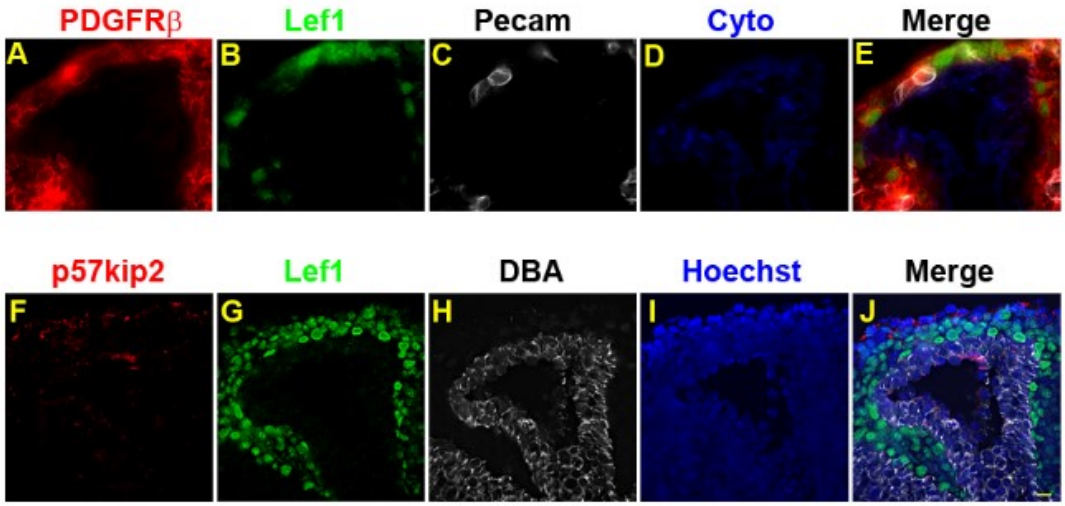

Figure 5-1 Characterization of canonical Wnt responsive mesenchyme lining the embryonic lung bud
(A – E) Lef1 positive cells make up most of the mesenchyme adjacent to the lung bud. (A) Lef1+ cells express PDGFRβ. Pecam expressing endothelial cells do not express Lef1. (F - J) The Lef1+ cells are not p57kip2 positive. Scale bar=10µm.

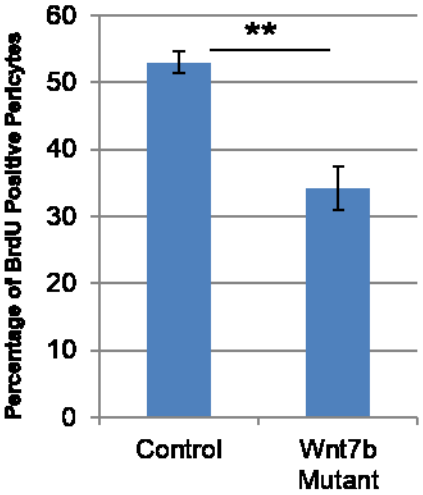

Figure 5-2 Mural cell proliferation surrounding the lung bud tips is decreased in *Wnt7b* mutant lungs
(p=0.0037)

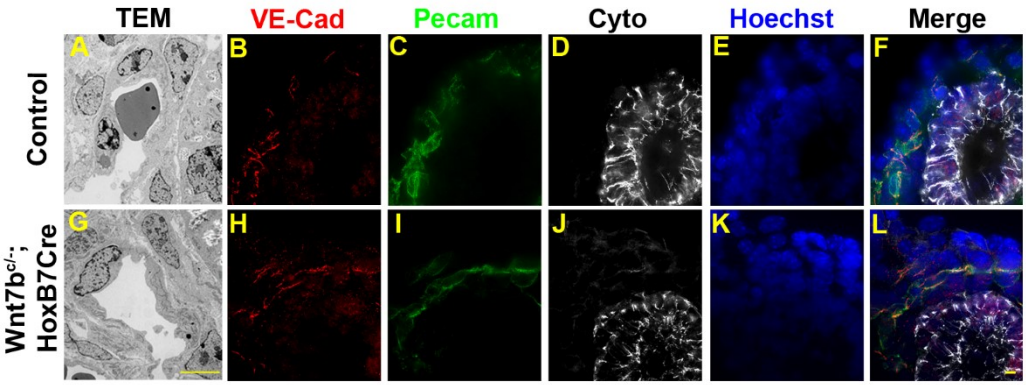

Figure 5-3 No lumen formation defect in the capillaries of E14.5 *Wnt7b* mutant lungs

Both VE-Cadherin expression and endothelial cell morphology appear unchanged in *Wnt7b* mutants. Scale bar 5µm.

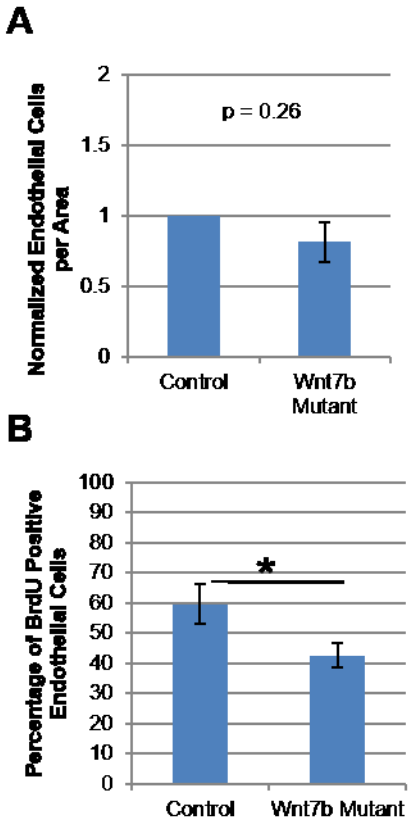

Figure 5-4 Endothelial Cell Density and Proliferation in *Wnt7b* Mutant Lungs
(A) Endothelial Cell Density is not affected in *Wnt7b* mutant lungs(p=0.26). (B) *Wnt7b* mutant lung endothelial cells proliferation rate is reduced at E14.5 (p=0.0234)

Chapter 6
Discussion and Future Directions

6.1 Summary

In order to understand how the reciprocal signaling between the UB epithelium and the interstitium direct renal medulla development, I analyzed the function of two genes necessary for normal renal medulla formation, *Wnt7b*, and *p57kip2*.

My work has revealed a novel role for *Wnt7b* in the kidney, regulation of the medullary microvasculature. I identified peri-UB mural cells as the target of canonical Wnt signaling in the renal medulla, and demonstrated that Wnt7b can regulate capillary lumen formation. Furthermore, I have shown that peri-UB mural cells can regulate oriented cell division and renal medulla elongation, and they mediate Wnt7b's role in these processes. I also analyzed the lungs, the one other organ where *Wnt7b* regulates *Pdgfrβ* expression in mural cells, and demonstrated that *Wnt7b's* role in capillary lumen formation is tissue specific. Together, my work has described several cell types regulated by *Wnt7b*, and has begun to uncover the pathways involved in regulating renal medulla formation **(Figure 6-1)**. One pathway is a p57kip2 mediated pathway that directs UB elongation through oriented cell division. Second, a non-p57kip2 mediated pathway regulates the mural cell expression of PDGFRβ and medullary capillary lumen formation.

There are still many questions regarding the mechanism by which Wnt7b regulates proliferation, lumen formation and oriented cell division. How does Wnt7b signal to the endothelial cells to regulate capillary lumen formation? How do the changes in peri-UB mural cells affect the endothelium? What is the signal received by the UB epithelial to regulate its elongation, and which cell is it coming from. How does Wnt7b promote LOH elongation? What do the tissue specific differences tell us about Wnt7b

function? In this chapter I examine these questions and suggest some ways to address them.

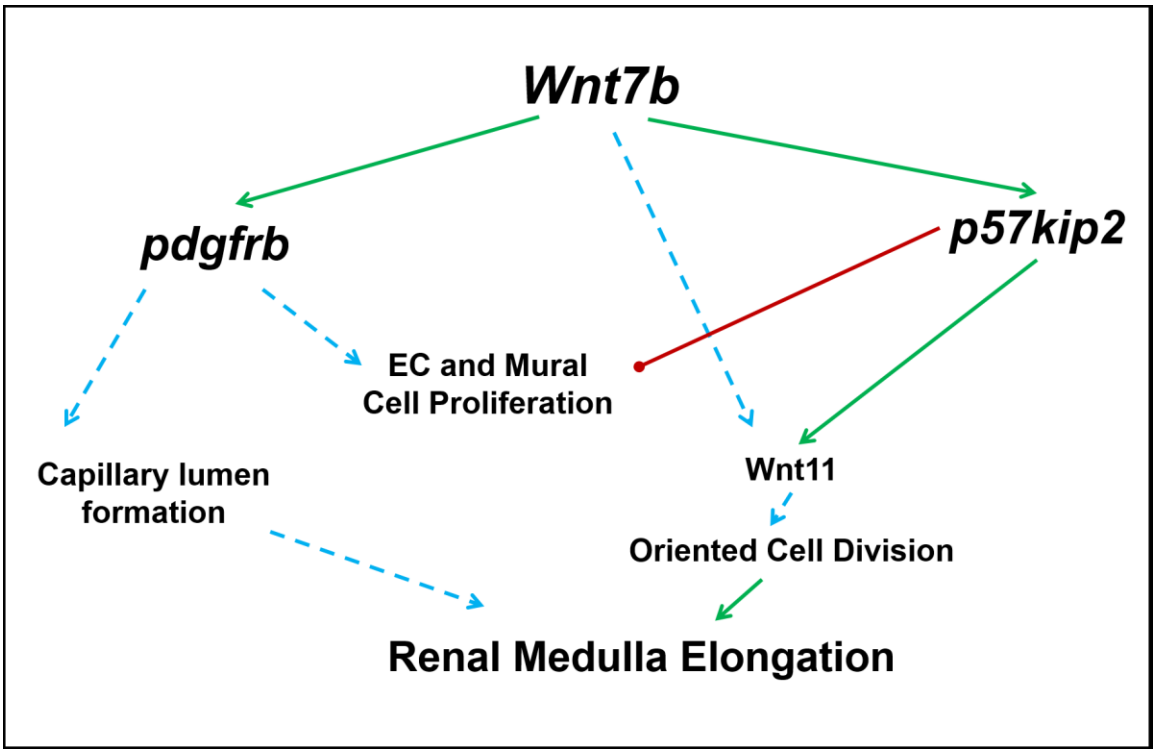

Figure 6-1 Wnt7b directs renal medulla development via a *p57kip2* mediated pathway and at least one other pathway involving *pdgfrb*
Green arrows represent activation, red lines represent inhibition. Blue arrows represent possible signaling to be examined in future experiments.

6.2 The role of Wnt7b in mural cells in the renal medulla and in the lungs

Wnt7b regulates the expression of *Pdgfrβ* in both kidney and in lung. Deletion of *Wnt7b* in lungs caused a decrease in mural cell expression of *Pdgfrβ*.[202] In the kidneys of *Wnt7b* mutants, loss of *Pdgfrβ* was restricted to the subset of mural cells that lost Lef1 expression. The mural cells that surround the LOH do not express Lef1, but do express *Pdgfrβ*. Together, this indicates that in the cells that do express Lef1, *Pdgfrβ* expression is downstream of canonical Wnt signaling. In cells that are not canonical Wnt signaling

targets, *Pdgfrβ* is regulated by some other signaling pathway. *p57kip2* mutants do not lose *Pdgfrβ* expression, indicating that *p57kip2* and *Pdgfrβ* function in parallel pathways.

Wnt7b regulation of peri-UB mural cell proliferation in the renal medulla is likely primarily mediated by p57kip2. In the lungs, where p57kip2 is not expressed in the Wnt7b target cells, proliferation of the mural cells was decreased in *Wnt7b* mutants. In *Wnt7b* mutant kidneys, which lose expression of p57kip2 and PDGFRβ, proliferation of the mural cells was increased. In *p57kip2* mutants, which lose expression of p57kip2 but not PDGFRβ, the increase in mural cell proliferation was even greater than in Wnt7b mutants. Together this indicates that Wnt7b has both positive and negative effects on mural cell proliferation. Wnt7b inhibits proliferation via p57kip2, and promotes proliferation through a parallel pathway. Both signaling pathways are needed to maintain a specific level of proliferation during development.

The proliferation promoting pathway could be mediated by PDGFRβ or some other factor. PDGFB, the ligand for PDGFRβ signaling, has been shown to promote proliferation of mural cells.[251, 252] Additionally, canonical Wnt signaling has been shown to promote proliferation via upregulation of Cyclin D1 and c-Myc in skeletal muscle[270], hence these factors could be working in conjunction with or instead of PDGFRβ to promote proliferation of peri-UB mural cells in the renal medulla. Cyclin D1 gene (*Ccnd1*) is expressed in the medullary interstitium at E15.5.[94] Analysis of *Ccnd1* expression in *Wnt7b* and *p57kip2* mutants at this stage would be informative, as would analysis of medullary peri-UB mural cells' proliferation in *PDGFRβ* mutant kidneys.

6.3 Wnt7b-directed mural cell-endothelial cell signaling and regulation of endothelial cell proliferation

In the renal medulla, proliferation of the peri-UB endothelial cells is increased in *Wnt7b* mutants, while in the lungs endothelial cell proliferation is decreased. In both organs endothelial cell proliferation is changed in the same direction as the mural cell proliferation, indicating that endothelial cell proliferation is regulated by the mural cells. However, the increase in endothelial cell proliferation in *Wnt7b* mutants is greater than that of *p57kip* mutants, despite the increase in proliferation in mural cells being greater in *p57kip2* mutants. The ratio of endothelial cells to mural cells is important for their ability to make contacts and their signaling.[267] Hence, some of the differences observed between *Wnt7b* mutants and *p57kip2* mutants could be influenced by their proliferation rates.

Using TEM, I observed that mural cell recruitment to the vessels appeared normal in *Wnt7b* mutants. However, I did not use any markers to examine the mural cell – endothelial cell interaction. N-cadherin is expressed at the sites of endothelial- mural cell contacts, and it can regulate endothelial proliferation.[271, 272] Examination of N-cadherin expression in control animals and *Wnt7b* mutants as well as *p57kip2* mutants might tell us if mural-endothelial cell interaction is impaired.

6.4 Capillary formation and stability

Wnt7b regulates the capillary lumen formation in the renal medulla, most likely via VE-Cadherin. Whether the signal directing lumen formation comes from the mural cells or from the epithelium is unclear. Future work in finding the upstream promotors for VE-cadherin will help us bridge the gap between canonical Wnt signaling and capillary lumen formation. It is currently unknown whether VE- cadherin in the peri-UB

endothelial cells of the renal medulla is regulated at the DNA or protein level. This question can be answered using *in situ* hybridization.

VE-cadherin expression can be induced by FGF signaling, and is regulated by transcription factors of the Ets and Sp1 families.[273, 274] At the protein level, VE-cadherin endocytosis is mediated by VEGF. It could be upregulated in *Wnt7b* mutants, thereby decreasing VE-cadherin expression at the cell membrane. Conversely VEGF could be decreased in *Wnt7b* mutants, thus impairing junction remodeling. However in Lammert's model of lumen formation VEGF acts downstream of VE-cadherin, regulating MyosinII role in cell flattening.[152] Additionally, N-cadherin was also shown to regulate VE-cadherin expression,[272] and is a likely candidate to mediate Wnt7b function because of its role in mural cell-endothelial cell interactions.

The established role of PDGFRβ signaling is recruitment of mural cells to the endothelium and support and maintenance of the capillary structure. *Pdgfrβ* mutant's reported kidney phenotype is failure of the mesangial cells to associate with the glomerular capillary, resulting in absent mesangium and dilated capillary.[131, 254] Correspondingly, *Wnt7b* mutant lungs can exhibit hemorrhage in both the large vessels and capillaries resulting from the lack of proper mural cell function.[170, 179] However in *Wnt7b* mutant kidneys, which lost PDGFRβ expression, we did not see a change in recruitment of peri-UB mural cells, structure of endothelial cell junctions by TEM, or permeability of the capillary. It is possible that in the kidney, there is a compensatory mechanism that prevented these phenotypes despite the decrease of PDGFRβ. Additionally, the presence of a compensatory mechanism in the lungs could explain why

the lung hypomorph has a stronger and more prevalent hemorrhage phenotype than in the lungs where *Wnt7b* is completely deleted.[170, 179]

6.5 The role of Wnt7b target peri-UB mural cells in renal medulla elongation

My characterization of the role of p57kip2 in the kidney demonstrates that Wnt7b target peri-UB mural cells regulate medulla elongation and oriented cell division in the trunks of the UB epithelium, or the future collecting ducts. Although p57kip2 is not the sole mediator of Wnt7b function, it is a key player downstream of Wnt7b in renal medulla elongation, as evidenced by the ability of *p57kip2* to partially rescue medulla length in *Wnt7b* mutant background. Interestingly, both the oriented cell division defect and the decrease in *Wnt11* expression was not as strong in *p57kip2* mutants as it was in *Wnt7b* mutants. One model for pericyte regulation of renal medulla elongation is that p57kip2, along with some unidentified target of *Wnt7b*, promotes the expression of *Wnt11*. Then Wnt11, a known non-canonical Wnt, signals through the PCP pathway to regulate oriented cell division. PCP pathway has been implicated in regulation of oriented cell division in UB epithelium acting via the Fat-Ds-Fj cassette.[266] Mice with a deletion of Fat4 exhibited disruption of oriented cell division and tube elongation in UB and in LOH, and neither *Wnt7b* nor *Wnt11* expression was changed in *Fat4* mutants.[266] Together these findings suggest that p57kip2 could promote a PCP signal from the pericytes to the UB epithelium to regulate oriented cell division.

What is the other signal from Wnt7b that is acting in parallel to p57kip2 mediated pathway? I have already shown that *Pdgfrβ* is also a target of Wnt7b. However, no medullary defect is reported in *Pdgfrβ* or *Pdgfb* mutants. If *p57kip2* and *Pdgfrβ* are

acting in parallel, loss of both genes may produce a phenotype stronger than that of *p57kip2* alone.

Another signaling molecule with differential expression between *Wnt7b* mutants and *p57kip2* mutants is Wnt5a. *Wnt5a* is expressed in the peri-UB interstitial cells and is slightly decreased in *Wnt7b* mutants,[70] but unchanged in *p57kip2* mutants. *Wnt5a* mutants have a malformed basement membrane and various defects in the UB epithelium.[92] *Wnt7b* mutants did not exhibit changed laminin expression, nor were there any obvious defects in the basement membrane of *Wnt7b* mutants UB epithelial observable by TEM. Therefore, it is unlikely that Wnt5a is a mediator of Wnt7b regulation of renal medulla elongation.

6.6 How vasculature could affect renal medulla elongation

The difference between medulla lengths in *Wnt7b* vs *p57kip2* mutants could also be attributed to contributions from the vasculature. A role for hypoxia seems less likely in *Wnt7b* mutant kidneys, since they did not have hemorrhage, and we observed injected fluorescent dextran located inside the blood vessels throughout the medulla of *Wnt7b* mutant mice. However the higher percentage of capillaries with smaller lumenal space in *Wnt7b* mutant mice could presumably cause a defect in the amount of nutrients able to reach the medulla tissues over time. Additionally, hypoxia has been shown to affect renal medulla length in a mouse model with placental insuffiecieny.[90] Expression of hypoxia inducible factors may have increased expression in *Wnt7b* mutant kidneys at E15.5.

6.7 Loop of Henle elongation

The mechanism by which Wnt7b promotes proliferation in the LOH is still unclear. In the lung, Wnt7b likely promotes BMP signaling in the lung bud epithelium to promote its proliferation.[170] Because Wnt ligands are highly insoluble and cannot signal over long distances,[166] it is highly unlikely that the LOH is receiving a direct signal from Wnt7b in the UB to promote its proliferation. The mural cells surrounding the UB epithelial in the renal medulla are also neighboring the LOH, and are the likely mediators of Wnt7b regulation of LOH elongation. Some elongated LOH are still present in *p57kip2* mutants at E18.5, indicating the decrease in LOH proliferation in *Wnt7b* mutants cannot be completely due to p57kip2 loss. A screen for genes that are decreased in the nephron lineage cells of *Wnt7b* mutants may uncover some other candidates for regulation of LOH elongation.

6.8 Conclusion

In this work, I have demonstrated crosstalk between the vasculature and the UB-epithelium that regulates the development of both structures. I have shown that Wnt7b expression in the UB epithelium is required for normal development of the microvascular endothelium in the renal medulla. Furthermore, I have identified that the pericytes, through expression of p57kip2, regulate oriented cell division and thus direct renal medulla elongation. Finally I have shown that the role of Wnt7b in the microvasculature is tissue specific. Together, this work contributes to our understanding of how an essential renal compartment, the renal medulla, is formed.

Chapter 7
Literature Cited

1. Schrier, RW: Biochemical, Structural, and Functional Correlations in the Kidney. In: *Diseases of the kidney & urinary tract.* 8th ed. edited by SCHRIER, R. W., Philadelphia, Wolters Kluwer Health/Lippincott Williams & Wilkins, 2007.
2. Gerich, JE: Role of the kidney in normal glucose homeostasis and in the hyperglycaemia of diabetes mellitus: therapeutic implications. *Diabet Med,* 27**:** 136-142, 2010.
3. Silbernagl, S: The renal handling of amino acids and oligopeptides. *Physiol Rev,* 68**:** 911-1007, 1988.
4. Nielsen, S, Kwon, TH, Fenton, RA, Praetorious, J: Anatomy of the Kidney. In: *Brenner & Rector's The Kidney.* 9th ed. edited by TAAL, M. W., CHERTOW, G. M., MARSDEN, P. A., SKORECKI, K., YU, A. S. L., BRENNER, B. M., Philadelphia, Elsevier, 2012.
5. Bulger, RE: The Urinary System. In: *Cell and tissue biology : a textbook of histology.* 6th ed. edited by WEISS, L., Baltimore, Urban & Schwarzenberg, 1988, pp xii, 1158 p., [1116] p. of plates.
6. Madsen, KM, Verlander, JW, Tisher, CC: Relationship between structure and function in distal tubule and collecting duct. *J Electron Microsc Tech,* 9**:** 187-208, 1988.
7. Sands, JM, Verlander, JW: Anatomy and Physiology of the Kidneys. In: *Toxicology of the Kidney, 3rd Edition.* edited by TARLOFF, J., LASH, L., Informa Healthcare, 2004, pp 3-56.
8. Munger, KA, Kost, CK, Brenner, BA, Maddox, DA: The Renal Circulation and Glomerular Ultrafiltration. In: *Brenner & Rector's The Kidney.* 9th ed. edited by TAAL, M. W., CHERTOW, G. M., MARSDEN, P. A., SKORECKI, K., YU, A. S. L., BRENNER, B. M., Philadelphia, Elsevier, 2012.
9. Schlondorff, D: The glomerular mesangial cell: an expanding role for a specialized pericyte. *FASEB J,* 1**:** 272-281, 1987.
10. De Martino, C, Allen, DJ, Accinni, L: Microsopic stucture of the kidney. In: *Basic, Clinical and Surgical Nephrology.* edited by DIDIO, L. J., MOTTA, P., Boston, Martinus Nijhoff Publishers, 1985, pp 53-59.
11. Abrahamson, DR: Recent studies on the structure and pathology of basement membranes. *J Pathol,* 149**:** 257-278, 1986.
12. Rodewald, R, Karnovsky, MJ: Porous substructure of the glomerular slit diaphragm in the rat and mouse. *J Cell Biol,* 60**:** 423-433, 1974.
13. Reiser, J, Kriz, W, Kretzler, M, Mundel, P: The glomerular slit diaphragm is a modified adherens junction. *J Am Soc Nephrol,* 11**:** 1-8, 2000.
14. Schnabel, E, Anderson, JM, Farquhar, MG: The tight junction protein ZO-1 is concentrated along slit diaphragms of the glomerular epithelium. *J Cell Biol,* 111**:** 1255-1263, 1990.
15. Kawachi, H, Miyauchi, N, Suzuki, K, Han, GD, Orikasa, M, Shimizu, F: Role of podocyte slit diaphragm as a filtration barrier. *Nephrology (Carlton),* 11**:** 274-281, 2006.
16. Mundel, P, Kriz, W: Structure and function of podocytes: an update. *Anat Embryol (Berl),* 192**:** 385-397, 1995.
17. Smoyer, WE, Mundel, P: Regulation of podocyte structure during the development of nephrotic syndrome. *J Mol Med (Berl),* 76**:** 172-183, 1998.

18. Kerjaschki, D, Sharkey, DJ, Farquhar, MG: Identification and characterization of podocalyxin--the major sialoprotein of the renal glomerular epithelial cell. *J Cell Biol,* 98**:** 1591-1596, 1984.
19. Schnabel, E, Dekan, G, Miettinen, A, Farquhar, MG: Biogenesis of podocalyxin--the major glomerular sialoglycoprotein--in the newborn rat kidney. *Eur J Cell Biol,* 48**:** 313-326, 1989.
20. Brown, LF, Berse, B, Tognazzi, K, Manseau, EJ, Van de Water, L, Senger, DR, Dvorak, HF, Rosen, S: Vascular permeability factor mRNA and protein expression in human kidney. *Kidney Int,* 42**:** 1457-1461, 1992.
21. Chen, J, Braet, F, Brodsky, S, Weinstein, T, Romanov, V, Noiri, E, Goligorsky, MS: VEGF-induced mobilization of caveolae and increase in permeability of endothelial cells. *Am J Physiol Cell Physiol,* 282**:** C1053-1063, 2002.
22. Esser, S, Wolburg, K, Wolburg, H, Breier, G, Kurzchalia, T, Risau, W: Vascular endothelial growth factor induces endothelial fenestrations in vitro. *J Cell Biol,* 140**:** 947-959, 1998.
23. Roberts, WG, Palade, GE: Increased microvascular permeability and endothelial fenestration induced by vascular endothelial growth factor. *J Cell Sci,* 108 (Pt 6)**:** 2369-2379, 1995.
24. Simon, M, Grone, HJ, Johren, O, Kullmer, J, Plate, KH, Risau, W, Fuchs, E: Expression of vascular endothelial growth factor and its receptors in human renal ontogenesis and in adult kidney. *Am J Physiol,* 268**:** F240-250, 1995.
25. Wang, T: Flow-activated transport events along the nephron. *Curr Opin Nephrol Hypertens,* 15**:** 530-536, 2006.
26. Good, DW, Burg, MB: Ammonia production by individual segments of the rat nephron. *J Clin Invest,* 73**:** 602-610, 1984.
27. Good, DW, Knepper, MA: Ammonia transport in the mammalian kidney. *Am J Physiol,* 248**:** F459-471, 1985.
28. Du, Z, Yan, Q, Duan, Y, Weinbaum, S, Weinstein, AM, Wang, T: Axial flow modulates proximal tubule NHE3 and H-ATPase activities by changing microvillus bending moments. *Am J Physiol Renal Physiol,* 290**:** F289-296, 2006.
29. Dieterich, HJ, Barrett, JM, Kriz, W, Bulhoff, JP: The ultrastructure of the thin loop limbs of the mouse kidney. *Anat Embryol (Berl),* 147**:** 1-18, 1975.
30. Ecelbarger, CA, Terris, J, Hoyer, JR, Nielsen, S, Wade, JB, Knepper, MA: Localization and regulation of the rat renal Na(+)-K(+)-2Cl- cotransporter, BSC-1. *Am J Physiol,* 271**:** F619-628, 1996.
31. Obermuller, N, Kunchaparty, S, Ellison, DH, Bachmann, S: Expression of the Na-K-2Cl cotransporter by macula densa and thick ascending limb cells of rat and rabbit nephron. *J Clin Invest,* 98**:** 635-640, 1996.
32. Yang, T, Huang, YG, Singh, I, Schnermann, J, Briggs, JP: Localization of bumetanide- and thiazide-sensitive Na-K-Cl cotransporters along the rat nephron. *Am J Physiol,* 271**:** F931-939, 1996.
33. Gottschalk, CW, Mylle, M: Micropuncture study of the mammalian urinary concentrating mechanism: evidence for the countercurrent hypothesis. *Am J Physiol,* 196**:** 927-936, 1959.
34. Ellison, DH, Velazquez, H, Wright, FS: Thiazide-sensitive sodium chloride cotransport in early distal tubule. *Am J Physiol,* 253**:** F546-554, 1987.

35. Dorup, J: Ultrastructure of distal nephron cells in rat renal cortex. *J Ultrastruct Res,* 92**:** 101-118, 1985.
36. Marunaka, Y: Hormonal and osmotic regulation of NaCl transport in renal distal nephron epithelium. *Jpn J Physiol,* 47**:** 499-511, 1997.
37. Peti-Peterdi, J, Harris, RC: Macula densa sensing and signaling mechanisms of renin release. *J Am Soc Nephrol,* 21**:** 1093-1096, 2010.
38. Kon, Y, Hashimoto, Y, Murakami, K, Sugimura, M: An immunoelectron-microscopical observation of mouse juxtaglomerular cells in the case of experimental hydronephrosis. *Acta Anat (Basel),* 144**:** 354-362, 1992.
39. Ice, KS, Geary, KM, Gomez, RA, Johns, DW, Peach, MJ, Carey, RM: Cell and molecular studies of renin secretion. *Clin Exp Hypertens A,* 10**:** 1169-1187, 1988.
40. Pearce, D, Soundararajan, R, Trimpert, C, Kashlan, OB, Deen, PM, Kohan, DE: Collecting duct principal cell transport processes and their regulation. *Clin J Am Soc Nephrol,* 10**:** 135-146, 2015.
41. Wang, WH, Giebisch, G: Regulation of potassium (K) handling in the renal collecting duct. *Pflugers Arch,* 458**:** 157-168, 2009.
42. Garty, H, Palmer, LG: Epithelial sodium channels: function, structure, and regulation. *Physiol Rev,* 77**:** 359-396, 1997.
43. Alper, SL, Natale, J, Gluck, S, Lodish, HF, Brown, D: Subtypes of intercalated cells in rat kidney collecting duct defined by antibodies against erythroid band 3 and renal vacuolar H+-ATPase. *Proc Natl Acad Sci U S A,* 86**:** 5429-5433, 1989.
44. Madsen, KM, Verlander, JW, Kim, J, Tisher, CC: Morphological adaptation of the collecting duct to acid-base disturbances. *Kidney Int Suppl,* 33**:** S57-63, 1991.
45. Kriz, W: Structural organization of the renal medulla: comparative and functional aspects. *Am J Physiol,* 241**:** R3-16, 1981.
46. Ren, H, Gu, L, Andreasen, A, Thomsen, JS, Cao, L, Christensen, EI, Zhai, XY: Spatial organization of the vascular bundle and the interbundle region: three-dimensional reconstruction at the inner stripe of the outer medulla in the mouse kidney. *Am J Physiol Renal Physiol,* 306**:** F321-326, 2014.
47. Nielsen, S, Frokiaer, J, Marples, D, Kwon, TH, Agre, P, Knepper, MA: Aquaporins in the kidney: from molecules to medicine. *Physiol Rev,* 82**:** 205-244, 2002.
48. Nielsen, S, Pallone, T, Smith, BL, Christensen, EI, Agre, P, Maunsbach, AB: Aquaporin-1 water channels in short and long loop descending thin limbs and in descending vasa recta in rat kidney. *Am J Physiol,* 268**:** F1023-1037, 1995.
49. Xu, Y, Olives, B, Bailly, P, Fischer, E, Ripoche, P, Ronco, P, Cartron, JP, Rondeau, E: Endothelial cells of the kidney vasa recta express the urea transporter HUT11. *Kidney Int,* 51**:** 138-146, 1997.
50. Mattson, DL, Bellehumeur, TG: Neural nitric oxide synthase in the renal medulla and blood pressure regulation. *Hypertension,* 28**:** 297-303, 1996.
51. Mattson, DL, Lu, S, Cowley, AW, Jr.: Role of nitric oxide in the control of the renal medullary circulation. *Clin Exp Pharmacol Physiol,* 24**:** 587-590, 1997.
52. Mattson, DL, Wu, F: Control of arterial blood pressure and renal sodium excretion by nitric oxide synthase in the renal medulla. *Acta Physiol Scand,* 168**:** 149-154, 2000.

53. Miyata, N, Zou, AP, Mattson, DL, Cowley, AW, Jr.: Renal medullary interstitial infusion of L-arginine prevents hypertension in Dahl salt-sensitive rats. *Am J Physiol,* 275**:** R1667-1673, 1998.
54. Parekh, N, Zou, AP: Role of prostaglandins in renal medullary circulation: response to different vasoconstrictors. *Am J Physiol,* 271**:** F653-658, 1996.
55. Wei, G, Rosen, S, Dantzler, WH, Pannabecker, TL: Architecture of the human renal inner medulla and functional implications. *Am J Physiol Renal Physiol,* 309**:** F627-637, 2015.
56. Lemley, KV, Kriz, W: Anatomy of the renal interstitium. *Kidney Int,* 39**:** 370-381, 1991.
57. Kaissling, B, Le Hir, M: The renal cortical interstitium: morphological and functional aspects. *Histochem Cell Biol,* 130**:** 247-262, 2008.
58. Takahashi-Iwanaga, H: The three-dimensional cytoarchitecture of the interstitial tissue in the rat kidney. *Cell Tissue Res,* 264**:** 269-281, 1991.
59. Humphreys, BD, Lin, SL, Kobayashi, A, Hudson, TE, Nowlin, BT, Bonventre, JV, Valerius, MT, McMahon, AP, Duffield, JS: Fate tracing reveals the pericyte and not epithelial origin of myofibroblasts in kidney fibrosis. *Am J Pathol,* 176**:** 85-97, 2010.
60. Qi, W, Chen, X, Poronnik, P, Pollock, CA: The renal cortical fibroblast in renal tubulointerstitial fibrosis. *Int J Biochem Cell Biol,* 38**:** 1-5, 2006.
61. Lacombe, C, Da Silva, JL, Bruneval, P, Fournier, JG, Wendling, F, Casadevall, N, Camilleri, JP, Bariety, J, Varet, B, Tambourin, P: Peritubular cells are the site of erythropoietin synthesis in the murine hypoxic kidney. *J Clin Invest,* 81**:** 620-623, 1988.
62. Cahan, C, Hoekje, PL, Goldwasser, E, Decker, MJ, Strohl, KP: Assessing the characteristic between length of hypoxic exposure and serum erythropoietin levels. *Am J Physiol,* 258**:** R1016-1021, 1990.
63. Jelkmann, W: Regulation of erythropoietin production. *J Physiol,* 589**:** 1251-1258, 2011.
64. Nangaku, M, Eckardt, KU: Hypoxia and the HIF system in kidney disease. *J Mol Med (Berl),* 85**:** 1325-1330, 2007.
65. Artunc, F, Risler, T: Serum erythropoietin concentrations and responses to anaemia in patients with or without chronic kidney disease. *Nephrol Dial Transplant,* 22**:** 2900-2908, 2007.
66. Berg, AC, Chernavvsky-Sequeira, C, Lindsey, J, Gomez, RA, Sequeira-Lopez, ML: Pericytes synthesize renin. *World J Nephrol,* 2**:** 11-16, 2013.
67. Castrop, H, Hocherl, K, Kurtz, A, Schweda, F, Todorov, V, Wagner, C: Physiology of kidney renin. *Physiol Rev,* 90**:** 607-673, 2010.
68. Sequeira Lopez, ML, Pentz, ES, Nomasa, T, Smithies, O, Gomez, RA: Renin cells are precursors for multiple cell types that switch to the renin phenotype when homeostasis is threatened. *Dev Cell,* 6**:** 719-728, 2004.
69. Little, M, Georgas, K, Pennisi, D, Wilkinson, L: Kidney development: two tales of tubulogenesis. *Curr Top Dev Biol,* 90**:** 193-229, 2010.
70. Yu, J, Carroll, TJ, Rajagopal, J, Kobayashi, A, Ren, Q, McMahon, AP: A Wnt7b-dependent pathway regulates the orientation of epithelial cell division and

establishes the cortico-medullary axis of the mammalian kidney. *Development,* 136**:** 161-171, 2009.
71. Lin, EE, Sequeira-Lopez, ML, Gomez, RA: RBP-J in FOXD1+ renal stromal progenitors is crucial for the proper development and assembly of the kidney vasculature and glomerular mesangial cells. *Am J Physiol Renal Physiol,* 306**:** F249-258, 2014.
72. Hum, S, Rymer, C, Schaefer, C, Bushnell, D, Sims-Lucas, S: Ablation of the renal stroma defines its critical role in nephron progenitor and vasculature patterning. *PLoS One,* 9**:** e88400, 2014.
73. Combes, AN, Davies, JA, Little, MH: Cell-cell interactions driving kidney morphogenesis. *Curr Top Dev Biol,* 112**:** 467-508, 2015.
74. Costantini, F, Kopan, R: Patterning a complex organ: branching morphogenesis and nephron segmentation in kidney development. *Dev Cell,* 18**:** 698-712, 2010.
75. Dressler, GR: Advances in early kidney specification, development and patterning. *Development,* 136**:** 3863-3874, 2009.
76. Little, MH, McMahon, AP: Mammalian kidney development: principles, progress, and projections. *Cold Spring Harb Perspect Biol,* 4, 2012.
77. Saxen, L, Sariola, H: Early organogenesis of the kidney. *Pediatr Nephrol,* 1**:** 385-392, 1987.
78. Durbec, P, Marcos-Gutierrez, CV, Kilkenny, C, Grigoriou, M, Wartiowaara, K, Suvanto, P, Smith, D, Ponder, B, Costantini, F, Saarma, M, et al.: GDNF signalling through the Ret receptor tyrosine kinase. *Nature,* 381**:** 789-793, 1996.
79. Pachnis, V, Mankoo, B, Costantini, F: Expression of the c-ret proto-oncogene during mouse embryogenesis. *Development,* 119**:** 1005-1017, 1993.
80. Sariola, H, Saarma, M: GDNF and its receptors in the regulation of the ureteric branching. *Int J Dev Biol,* 43**:** 413-418, 1999.
81. Vega, QC, Worby, CA, Lechner, MS, Dixon, JE, Dressler, GR: Glial cell line-derived neurotrophic factor activates the receptor tyrosine kinase RET and promotes kidney morphogenesis. *Proc Natl Acad Sci U S A,* 93**:** 10657-10661, 1996.
82. Cacalano, G, Farinas, I, Wang, LC, Hagler, K, Forgie, A, Moore, M, Armanini, M, Phillips, H, Ryan, AM, Reichardt, LF, Hynes, M, Davies, A, Rosenthal, A: GFRalpha1 is an essential receptor component for GDNF in the developing nervous system and kidney. *Neuron,* 21**:** 53-62, 1998.
83. Enomoto, H, Araki, T, Jackman, A, Heuckeroth, RO, Snider, WD, Johnson, EM, Jr., Milbrandt, J: GFR alpha1-deficient mice have deficits in the enteric nervous system and kidneys. *Neuron,* 21**:** 317-324, 1998.
84. Sanchez, MP, Silos-Santiago, I, Frisen, J, He, B, Lira, SA, Barbacid, M: Renal agenesis and the absence of enteric neurons in mice lacking GDNF. *Nature,* 382**:** 70-73, 1996.
85. Schuchardt, A, D'Agati, V, Larsson-Blomberg, L, Costantini, F, Pachnis, V: Defects in the kidney and enteric nervous system of mice lacking the tyrosine kinase receptor Ret. *Nature,* 367**:** 380-383, 1994.
86. Schuchardt, A, D'Agati, V, Pachnis, V, Costantini, F: Renal agenesis and hypodysplasia in ret-k- mutant mice result from defects in ureteric bud development. *Development,* 122**:** 1919-1929, 1996.

87. Majumdar, A, Vainio, S, Kispert, A, McMahon, J, McMahon, AP: Wnt11 and Ret/Gdnf pathways cooperate in regulating ureteric branching during metanephric kidney development. *Development,* 130**:** 3175-3185, 2003.
88. Cebrian, C, Borodo, K, Charles, N, Herzlinger, DA: Morphometric index of the developing murine kidney. *Dev Dyn,* 231**:** 601-608, 2004.
89. Hartwig, S, Bridgewater, D, Di Giovanni, V, Cain, J, Mishina, Y, Rosenblum, ND: BMP receptor ALK3 controls collecting system development. *J Am Soc Nephrol,* 19**:** 117-124, 2008.
90. Sparrow, DB, Boyle, SC, Sams, RS, Mazuruk, B, Zhang, L, Moeckel, GW, Dunwoodie, SL, de Caestecker, MP: Placental insufficiency associated with loss of Cited1 causes renal medullary dysplasia. *J Am Soc Nephrol,* 20**:** 777-786, 2009.
91. Matsui, T, Kanai-Azuma, M, Hara, K, Matoba, S, Hiramatsu, R, Kawakami, H, Kurohmaru, M, Koopman, P, Kanai, Y: Redundant roles of Sox17 and Sox18 in postnatal angiogenesis in mice. *J Cell Sci,* 119**:** 3513-3526, 2006.
92. Pietila, I, Prunskaite-Hyyrylainen, R, Kaisto, S, Tika, E, van Eerde, AM, Salo, AM, Garma, L, Miinalainen, I, Feitz, WF, Bongers, EM, Juffer, A, Knoers, NV, Renkema, KY, Myllyharju, J, Vainio, SJ: Wnt5a Deficiency Leads to Anomalies in Ureteric Tree Development, Tubular Epithelial Cell Organization and Basement Membrane Integrity Pointing to a Role in Kidney Collecting Duct Patterning. *PLoS One,* 11**:** e0147171, 2016.
93. Yang, DH, McKee, KK, Chen, ZL, Mernaugh, G, Strickland, S, Zent, R, Yurchenco, PD: Renal collecting system growth and function depend upon embryonic gamma1 laminin expression. *Development,* 138**:** 4535-4544, 2011.
94. McMahon, AP, Aronow, BJ, Davidson, DR, Davies, JA, Gaido, KW, Grimmond, S, Lessard, JL, Little, MH, Potter, SS, Wilder, EL, Zhang, P: GUDMAP: the genitourinary developmental molecular anatomy project. *J Am Soc Nephrol,* 19**:** 667-671, 2008.
95. Kobayashi, A, Valerius, MT, Mugford, JW, Carroll, TJ, Self, M, Oliver, G, McMahon, AP: Six2 defines and regulates a multipotent self-renewing nephron progenitor population throughout mammalian kidney development. *Cell Stem Cell,* 3**:** 169-181, 2008.
96. Mugford, JW, Sipila, P, McMahon, JA, McMahon, AP: Osr1 expression demarcates a multi-potent population of intermediate mesoderm that undergoes progressive restriction to an Osr1-dependent nephron progenitor compartment within the mammalian kidney. *Dev Biol,* 324**:** 88-98, 2008.
97. Kobayashi, T, Tanaka, H, Kuwana, H, Inoshita, S, Teraoka, H, Sasaki, S, Terada, Y: Wnt4-transformed mouse embryonic stem cells differentiate into renal tubular cells. *Biochem Biophys Res Commun,* 336**:** 585-595, 2005.
98. Stark, K, Vainio, S, Vassileva, G, McMahon, AP: Epithelial transformation of metanephric mesenchyme in the developing kidney regulated by Wnt-4. *Nature,* 372**:** 679-683, 1994.
99. Carroll, TJ, Park, JS, Hayashi, S, Majumdar, A, McMahon, AP: Wnt9b plays a central role in the regulation of mesenchymal to epithelial transitions underlying organogenesis of the mammalian urogenital system. *Dev Cell,* 9**:** 283-292, 2005.

100. Karner, CM, Das, A, Ma, Z, Self, M, Chen, C, Lum, L, Oliver, G, Carroll, TJ: Canonical Wnt9b signaling balances progenitor cell expansion and differentiation during kidney development. *Development,* 138**:** 1247-1257, 2011.
101. Park, JS, Ma, W, O'Brien, LL, Chung, E, Guo, JJ, Cheng, JG, Valerius, MT, McMahon, JA, Wong, WH, McMahon, AP: Six2 and Wnt regulate self-renewal and commitment of nephron progenitors through shared gene regulatory networks. *Dev Cell,* 23**:** 637-651, 2012.
102. Park, JS, Valerius, MT, McMahon, AP: Wnt/beta-catenin signaling regulates nephron induction during mouse kidney development. *Development,* 134**:** 2533-2539, 2007.
103. Boyle, S, Misfeldt, A, Chandler, KJ, Deal, KK, Southard-Smith, EM, Mortlock, DP, Baldwin, HS, de Caestecker, M: Fate mapping using Cited1-CreERT2 mice demonstrates that the cap mesenchyme contains self-renewing progenitor cells and gives rise exclusively to nephronic epithelia. *Dev Biol,* 313**:** 234-245, 2008.
104. Brunskill, EW, Aronow, BJ, Georgas, K, Rumballe, B, Valerius, MT, Aronow, J, Kaimal, V, Jegga, AG, Yu, J, Grimmond, S, McMahon, AP, Patterson, LT, Little, MH, Potter, SS: Atlas of gene expression in the developing kidney at microanatomic resolution. *Dev Cell,* 15**:** 781-791, 2008.
105. Mugford, JW, Yu, J, Kobayashi, A, McMahon, AP: High-resolution gene expression analysis of the developing mouse kidney defines novel cellular compartments within the nephron progenitor population. *Dev Biol,* 333**:** 312-323, 2009.
106. Lee, MP, DeBaun, M, Randhawa, G, Reichard, BA, Elledge, SJ, Feinberg, AP: Low frequency of p57KIP2 mutation in Beckwith-Wiedemann syndrome. *Am J Hum Genet,* 61**:** 304-309, 1997.
107. Surendran, K, Boyle, S, Barak, H, Kim, M, Stomberski, C, McCright, B, Kopan, R: The contribution of Notch1 to nephron segmentation in the developing kidney is revealed in a sensitized Notch2 background and can be augmented by reducing Mint dosage. *Dev Biol,* 337**:** 386-395, 2010.
108. Cheng, HT, Kim, M, Valerius, MT, Surendran, K, Schuster-Gossler, K, Gossler, A, McMahon, AP, Kopan, R: Notch2, but not Notch1, is required for proximal fate acquisition in the mammalian nephron. *Development,* 134**:** 801-811, 2007.
109. Barker, N, Rookmaaker, MB, Kujala, P, Ng, A, Leushacke, M, Snippert, H, van de Wetering, M, Tan, S, Van Es, JH, Huch, M, Poulsom, R, Verhaar, MC, Peters, PJ, Clevers, H: Lgr5(+ve) stem/progenitor cells contribute to nephron formation during kidney development. *Cell Rep,* 2**:** 540-552, 2012.
110. Hartman, HA, Lai, HL, Patterson, LT: Cessation of renal morphogenesis in mice. *Dev Biol,* 310**:** 379-387, 2007.
111. Kobayashi, A, Mugford, JW, Krautzberger, AM, Naiman, N, Liao, J, McMahon, AP: Identification of a multipotent self-renewing stromal progenitor population during mammalian kidney organogenesis. *Stem Cell Reports,* 3**:** 650-662, 2014.
112. Sequeira-Lopez, ML, Lin, EE, Li, M, Hu, Y, Sigmund, CD, Gomez, RA: The earliest metanephric arteriolar progenitors and their role in kidney vascular development. *Am J Physiol Regul Integr Comp Physiol,* 308**:** R138-149, 2015.
113. Mendelsohn, C, Batourina, E, Fung, S, Gilbert, T, Dodd, J: Stromal cells mediate retinoid-dependent functions essential for renal development. *Development,* 126**:** 1139-1148, 1999.

114. Yosypiv, IV, Boh, MK, Spera, MA, El-Dahr, SS: Downregulation of Spry-1, an inhibitor of GDNF/Ret, causes angiotensin II-induced ureteric bud branching. *Kidney Int,* 74**:** 1287-1293, 2008.
115. Hatini, V, Huh, SO, Herzlinger, D, Soares, VC, Lai, E: Essential role of stromal mesenchyme in kidney morphogenesis revealed by targeted disruption of Winged Helix transcription factor BF-2. *Genes Dev,* 10**:** 1467-1478, 1996.
116. Levinson, RS, Batourina, E, Choi, C, Vorontchikhina, M, Kitajewski, J, Mendelsohn, CL: Foxd1-dependent signals control cellularity in the renal capsule, a structure required for normal renal development. *Development,* 132**:** 529-539, 2005.
117. Zhang, P, Liegeois, NJ, Wong, C, Finegold, M, Hou, H, Thompson, JC, Silverman, A, Harper, JW, DePinho, RA, Elledge, SJ: Altered cell differentiation and proliferation in mice lacking p57KIP2 indicates a role in Beckwith-Wiedemann syndrome. *Nature,* 387**:** 151-158, 1997.
118. Quaggin, SE, Schwartz, L, Cui, S, Igarashi, P, Deimling, J, Post, M, Rossant, J: The basic-helix-loop-helix protein pod1 is critically important for kidney and lung organogenesis. *Development,* 126**:** 5771-5783, 1999.
119. Cui, S, Schwartz, L, Quaggin, SE: Pod1 is required in stromal cells for glomerulogenesis. *Dev Dyn,* 226**:** 512-522, 2003.
120. Robert, B, St John, PL, Hyink, DP, Abrahamson, DR: Evidence that embryonic kidney cells expressing flk-1 are intrinsic, vasculogenic angioblasts. *Am J Physiol,* 271**:** F744-753, 1996.
121. Abrahamson, DR, Robert, B, Hyink, DP, St John, PL, Daniel, TO: Origins and formation of microvasculature in the developing kidney. *Kidney Int Suppl,* 67**:** S7-11, 1998.
122. Robert, B, St John, PL, Abrahamson, DR: Direct visualization of renal vascular morphogenesis in Flk1 heterozygous mutant mice. *Am J Physiol,* 275**:** F164-172, 1998.
123. Sequeira Lopez, ML, Gomez, RA: Development of the renal arterioles. *J Am Soc Nephrol,* 22**:** 2156-2165, 2011.
124. Sims-Lucas, S, Schaefer, C, Bushnell, D, Ho, J, Logar, A, Prochownik, E, Gittes, G, Bates, CM: Endothelial Progenitors Exist within the Kidney and Lung Mesenchyme. *PLoS One,* 8**:** e65993, 2013.
125. Lancrin, C, Sroczynska, P, Serrano, AG, Gandillet, A, Ferreras, C, Kouskoff, V, Lacaud, G: Blood cell generation from the hemangioblast. *J Mol Med (Berl),* 88**:** 167-172, 2010.
126. Hu, Y, Li, M, Gothert, JR, Gomez, RA, Sequeira-Lopez, ML: Hemovascular Progenitors in the Kidney Require Sphingosine-1-Phosphate Receptor 1 for Vascular Development. *J Am Soc Nephrol*, 2015.
127. Tufro-McReddie, A, Romano, LM, Harris, JM, Ferder, L, Gomez, RA: Angiotensin II regulates nephrogenesis and renal vascular development. *Am J Physiol,* 269**:** F110-115, 1995.
128. Tufro, A: VEGF spatially directs angiogenesis during metanephric development in vitro. *Dev Biol,* 227**:** 558-566, 2000.
129. Boyle, SC, Liu, Z, Kopan, R: Notch signaling is required for the formation of mesangial cells from a stromal mesenchyme precursor during kidney development. *Development,* 141**:** 346-354, 2014.

130. Leveen, P, Pekny, M, Gebre-Medhin, S, Swolin, B, Larsson, E, Betsholtz, C: Mice deficient for PDGF B show renal, cardiovascular, and hematological abnormalities. *Genes Dev,* 8**:** 1875-1887, 1994.
131. Lindahl, P, Hellstrom, M, Kalen, M, Karlsson, L, Pekny, M, Pekna, M, Soriano, P, Betsholtz, C: Paracrine PDGF-B/PDGF-Rbeta signaling controls mesangial cell development in kidney glomeruli. *Development,* 125**:** 3313-3322, 1998.
132. Lindahl, P, Johansson, BR, Leveen, P, Betsholtz, C: Pericyte loss and microaneurysm formation in PDGF-B-deficient mice. *Science,* 277**:** 242-245, 1997.
133. Madsen, K, Marcussen, N, Pedersen, M, Kjaersgaard, G, Facemire, C, Coffman, TM, Jensen, BL: Angiotensin II promotes development of the renal microcirculation through AT1 receptors. *J Am Soc Nephrol,* 21**:** 448-459, 2010.
134. Rohn, DA, Stewart, RH, Elk, JR, Laine, GA, Drake, RE: Renal lymphatic function following venous pressure elevation. *Lymphology,* 29**:** 67-75, 1996.
135. Ishikawa, Y, Akasaka, Y, Kiguchi, H, Akishima-Fukasawa, Y, Hasegawa, T, Ito, K, Kimura-Matsumoto, M, Ishiguro, S, Morita, H, Sato, S, Soh, S, Ishii, T: The human renal lymphatics under normal and pathological conditions. *Histopathology,* 49**:** 265-273, 2006.
136. Tenstad, O, Heyeraas, KJ, Wiig, H, Aukland, K: Drainage of plasma proteins from the renal medullary interstitium in rats. *J Physiol,* 536**:** 533-539, 2001.
137. Risau, W, Flamme, I: Vasculogenesis. *Annu Rev Cell Dev Biol,* 11**:** 73-91, 1995.
138. Drake, CJ, Fleming, PA: Vasculogenesis in the day 6.5 to 9.5 mouse embryo. *Blood,* 95**:** 1671-1679, 2000.
139. Drake, CJ, LaRue, A, Ferrara, N, Little, CD: VEGF regulates cell behavior during vasculogenesis. *Dev Biol,* 224**:** 178-188, 2000.
140. Shalaby, F, Ho, J, Stanford, WL, Fischer, KD, Schuh, AC, Schwartz, L, Bernstein, A, Rossant, J: A requirement for Flk1 in primitive and definitive hematopoiesis and vasculogenesis. *Cell,* 89**:** 981-990, 1997.
141. Shalaby, F, Rossant, J, Yamaguchi, TP, Gertsenstein, M, Wu, XF, Breitman, ML, Schuh, AC: Failure of blood-island formation and vasculogenesis in Flk-1-deficient mice. *Nature,* 376**:** 62-66, 1995.
142. Ribatti, D, Nico, B, Crivellato, E: Morphological and molecular aspects of physiological vascular morphogenesis. *Angiogenesis,* 12**:** 101-111, 2009.
143. Pardanaud, L, Yassine, F, Dieterlen-Lievre, F: Relationship between vasculogenesis, angiogenesis and haemopoiesis during avian ontogeny. *Development,* 105**:** 473-485, 1989.
144. van Hinsbergh, VW, Koolwijk, P: Endothelial sprouting and angiogenesis: matrix metalloproteinases in the lead. *Cardiovasc Res,* 78**:** 203-212, 2008.
145. Carmeliet, P, De Smet, F, Loges, S, Mazzone, M: Branching morphogenesis and antiangiogenesis candidates: tip cells lead the way. *Nat Rev Clin Oncol,* 6**:** 315-326, 2009.
146. Gerhardt, H: VEGF and endothelial guidance in angiogenic sprouting. *Organogenesis,* 4**:** 241-246, 2008.
147. Ruhrberg, C, Gerhardt, H, Golding, M, Watson, R, Ioannidou, S, Fujisawa, H, Betsholtz, C, Shima, DT: Spatially restricted patterning cues provided by heparin-

binding VEGF-A control blood vessel branching morphogenesis. *Genes Dev,* 16**:** 2684-2698, 2002.
148. Horowitz, A, Simons, M: Branching morphogenesis. *Circ Res,* 103**:** 784-795, 2008.
149. Suchting, S, Freitas, C, le Noble, F, Benedito, R, Breant, C, Duarte, A, Eichmann, A: The Notch ligand Delta-like 4 negatively regulates endothelial tip cell formation and vessel branching. *Proc Natl Acad Sci U S A,* 104**:** 3225-3230, 2007.
150. Zovein, AC, Luque, A, Turlo, KA, Hofmann, JJ, Yee, KM, Becker, MS, Fassler, R, Mellman, I, Lane, TF, Iruela-Arispe, ML: Beta1 integrin establishes endothelial cell polarity and arteriolar lumen formation via a Par3-dependent mechanism. *Dev Cell,* 18**:** 39-51, 2010.
151. Lubarsky, B, Krasnow, MA: Tube morphogenesis: making and shaping biological tubes. *Cell,* 112**:** 19-28, 2003.
152. Strilic, B, Kucera, T, Eglinger, J, Hughes, MR, McNagny, KM, Tsukita, S, Dejana, E, Ferrara, N, Lammert, E: The molecular basis of vascular lumen formation in the developing mouse aorta. *Dev Cell,* 17**:** 505-515, 2009.
153. Santiago-Martinez, E, Soplop, NH, Patel, R, Kramer, SG: Repulsion by Slit and Roundabout prevents Shotgun/E-cadherin-mediated cell adhesion during Drosophila heart tube lumen formation. *J Cell Biol,* 182**:** 241-248, 2008.
154. Andrae, J, Gallini, R, Betsholtz, C: Role of platelet-derived growth factors in physiology and medicine. *Genes Dev,* 22**:** 1276-1312, 2008.
155. Dumont, DJ, Yamaguchi, TP, Conlon, RA, Rossant, J, Breitman, ML: tek, a novel tyrosine kinase gene located on mouse chromosome 4, is expressed in endothelial cells and their presumptive precursors. *Oncogene,* 7**:** 1471-1480, 1992.
156. Wakui, S, Yokoo, K, Muto, T, Suzuki, Y, Takahashi, H, Furusato, M, Hano, H, Endou, H, Kanai, Y: Localization of Ang-1, -2, Tie-2, and VEGF expression at endothelial-pericyte interdigitation in rat angiogenesis. *Lab Invest,* 86**:** 1172-1184, 2006.
157. Davis, S, Aldrich, TH, Jones, PF, Acheson, A, Compton, DL, Jain, V, Ryan, TE, Bruno, J, Radziejewski, C, Maisonpierre, PC, Yancopoulos, GD: Isolation of angiopoietin-1, a ligand for the TIE2 receptor, by secretion-trap expression cloning. *Cell,* 87**:** 1161-1169, 1996.
158. Sundberg, C, Kowanetz, M, Brown, LF, Detmar, M, Dvorak, HF: Stable expression of angiopoietin-1 and other markers by cultured pericytes: phenotypic similarities to a subpopulation of cells in maturing vessels during later stages of angiogenesis in vivo. *Lab Invest,* 82**:** 387-401, 2002.
159. Dumont, DJ, Gradwohl, G, Fong, GH, Puri, MC, Gertsenstein, M, Auerbach, A, Breitman, ML: Dominant-negative and targeted null mutations in the endothelial receptor tyrosine kinase, tek, reveal a critical role in vasculogenesis of the embryo. *Genes Dev,* 8**:** 1897-1909, 1994.
160. Patan, S: TIE1 and TIE2 receptor tyrosine kinases inversely regulate embryonic angiogenesis by the mechanism of intussusceptive microvascular growth. *Microvasc Res,* 56**:** 1-21, 1998.
161. Goumans, MJ, Valdimarsdottir, G, Itoh, S, Rosendahl, A, Sideras, P, ten Dijke, P: Balancing the activation state of the endothelium via two distinct TGF-beta type I receptors. *EMBO J,* 21**:** 1743-1753, 2002.

162. Seki, T, Yun, J, Oh, SP: Arterial endothelium-specific activin receptor-like kinase 1 expression suggests its role in arterialization and vascular remodeling. *Circ Res,* 93**:** 682-689, 2003.
163. Urness, LD, Sorensen, LK, Li, DY: Arteriovenous malformations in mice lacking activin receptor-like kinase-1. *Nat Genet,* 26**:** 328-331, 2000.
164. Domenga, V, Fardoux, P, Lacombe, P, Monet, M, Maciazek, J, Krebs, LT, Klonjkowski, B, Berrou, E, Mericskay, M, Li, Z, Tournier-Lasserve, E, Gridley, T, Joutel, A: Notch3 is required for arterial identity and maturation of vascular smooth muscle cells. *Genes Dev,* 18**:** 2730-2735, 2004.
165. Jin, S, Hansson, EM, Tikka, S, Lanner, F, Sahlgren, C, Farnebo, F, Baumann, M, Kalimo, H, Lendahl, U: Notch signaling regulates platelet-derived growth factor receptor-beta expression in vascular smooth muscle cells. *Circ Res,* 102**:** 1483-1491, 2008.
166. Lobov, IB, Rao, S, Carroll, TJ, Vallance, JE, Ito, M, Ondr, JK, Kurup, S, Glass, DA, Patel, MS, Shu, W, Morrisey, EE, McMahon, AP, Karsenty, G, Lang, RA: WNT7b mediates macrophage-induced programmed cell death in patterning of the vasculature. *Nature,* 437**:** 417-421, 2005.
167. Wang, Z, Shu, W, Lu, MM, Morrisey, EE: Wnt7b activates canonical signaling in epithelial and vascular smooth muscle cells through interactions with Fzd1, Fzd10, and LRP5. *Mol Cell Biol,* 25**:** 5022-5030, 2005.
168. Rosso, SB, Sussman, D, Wynshaw-Boris, A, Salinas, PC: Wnt signaling through Dishevelled, Rac and JNK regulates dendritic development. *Nature neuroscience,* 8**:** 34-42, 2005.
169. Tu, X, Joeng, KS, Nakayama, KI, Nakayama, K, Rajagopal, J, Carroll, TJ, McMahon, AP, Long, F: Noncanonical Wnt signaling through G protein-linked PKCdelta activation promotes bone formation. *Dev Cell,* 12**:** 113-127, 2007.
170. Rajagopal, J, Carroll, TJ, Guseh, JS, Bores, SA, Blank, LJ, Anderson, WJ, Yu, J, Zhou, Q, McMahon, AP, Melton, DA: Wnt7b stimulates embryonic lung growth by coordinately increasing the replication of epithelium and mesenchyme. *Development,* 135**:** 1625-1634, 2008.
171. Liu, Y, Chattopadhyay, N, Qin, S, Szekeres, C, Vasylyeva, T, Mahoney, ZX, Taglienti, M, Bates, CM, Chapman, HA, Miner, JH, Kreidberg, JA: Coordinate integrin and c-Met signaling regulate Wnt gene expression during epithelial morphogenesis. *Development,* 136**:** 843-853, 2009.
172. Afelik, S, Pool, B, Schmerr, M, Penton, C, Jensen, J: Wnt7b is required for epithelial progenitor growth and operates during epithelial-to-mesenchymal signaling in pancreatic development. *Dev Biol,* 399**:** 204-217, 2015.
173. Brynczka, C, Merrick, BA: The p53 transcriptional target gene wnt7b contributes to NGF-inducible neurite outgrowth in neuronal PC12 cells. *Differentiation; research in biological diversity,* 76**:** 795-808, 2008.
174. Chen, J, Tu, X, Esen, E, Joeng, KS, Lin, C, Arbeit, JM, Ruegg, MA, Hall, MN, Ma, L, Long, F: WNT7B promotes bone formation in part through mTORC1. *PLoS Genet,* 10**:** e1004145, 2014.
175. Kandyba, E, Kobielak, K: Wnt7b is an important intrinsic regulator of hair follicle stem cell homeostasis and hair follicle cycling. *Stem Cells,* 32**:** 886-901, 2014.

176. Miller, MF, Cohen, ED, Baggs, JE, Lu, MM, Hogenesch, JB, Morrisey, EE: Wnt ligands signal in a cooperative manner to promote foregut organogenesis. *Proc Natl Acad Sci U S A,* 109**:** 15348-15353, 2012.
177. Parr, BA, Cornish, VA, Cybulsky, MI, McMahon, AP: Wnt7b regulates placental development in mice. *Dev Biol,* 237**:** 324-332, 2001.
178. Pietila, I, Ellwanger, K, Railo, A, Jokela, T, Barrantes Idel, B, Shan, J, Niehrs, C, Vainio, SJ: Secreted Wnt antagonist Dickkopf-1 controls kidney papilla development coordinated by Wnt-7b signalling. *Dev Biol,* 353**:** 50-60, 2011.
179. Shu, W, Jiang, YQ, Lu, MM, Morrisey, EE: Wnt7b regulates mesenchymal proliferation and vascular development in the lung. *Development,* 129**:** 4831-4842, 2002.
180. Stenman, JM, Rajagopal, J, Carroll, TJ, Ishibashi, M, McMahon, J, McMahon, AP: Canonical Wnt signaling regulates organ-specific assembly and differentiation of CNS vasculature. *Science,* 322**:** 1247-1250, 2008.
181. Zaghetto, AA, Paina, S, Mantero, S, Platonova, N, Peretto, P, Bovetti, S, Puche, A, Piccolo, S, Merlo, GR: Activation of the Wnt-beta catenin pathway in a cell population on the surface of the forebrain is essential for the establishment of olfactory axon connections. *J Neurosci,* 27**:** 9757-9768, 2007.
182. Zhou, Y, Nathans, J: Gpr124 controls CNS angiogenesis and blood-brain barrier integrity by promoting ligand-specific canonical wnt signaling. *Dev Cell,* 31**:** 248-256, 2014.
183. Kreidberg, JA, Donovan, MJ, Goldstein, SL, Rennke, H, Shepherd, K, Jones, RC, Jaenisch, R: Alpha 3 beta 1 integrin has a crucial role in kidney and lung organogenesis. *Development,* 122**:** 3537-3547, 1996.
184. Perrimon, N: Serpentine proteins slither into the wingless and hedgehog fields. *Cell,* 86**:** 513-516, 1996.
185. He, X, Semenov, M, Tamai, K, Zeng, X: LDL receptor-related proteins 5 and 6 in Wnt/beta-catenin signaling: arrows point the way. *Development,* 131**:** 1663-1677, 2004.
186. Travis, A, Amsterdam, A, Belanger, C, Grosschedl, R: LEF-1, a gene encoding a lymphoid-specific protein with an HMG domain, regulates T-cell receptor alpha enhancer function [corrected]. *Genes Dev,* 5**:** 880-894, 1991.
187. van de Wetering, M, Oosterwegel, M, Dooijes, D, Clevers, H: Identification and cloning of TCF-1, a T lymphocyte-specific transcription factor containing a sequence-specific HMG box. *EMBO J,* 10**:** 123-132, 1991.
188. Waterman, ML, Fischer, WH, Jones, KA: A thymus-specific member of the HMG protein family regulates the human T cell receptor C alpha enhancer. *Genes Dev,* 5**:** 656-669, 1991.
189. Behrens, J, von Kries, JP, Kuhl, M, Bruhn, L, Wedlich, D, Grosschedl, R, Birchmeier, W: Functional interaction of beta-catenin with the transcription factor LEF-1. *Nature,* 382**:** 638-642, 1996.
190. Pepicelli, CV, Lewis, PM, McMahon, AP: Sonic hedgehog regulates branching morphogenesis in the mammalian lung. *Curr Biol,* 8**:** 1083-1086, 1998.
191. Weidenfeld, J, Shu, W, Zhang, L, Millar, SE, Morrisey, EE: The WNT7b promoter is regulated by TTF-1, GATA6, and Foxa2 in lung epithelium. *J Biol Chem,* 277**:** 21061-21070, 2002.

192. Hogan, BL, Yingling, JM: Epithelial/mesenchymal interactions and branching morphogenesis of the lung. *Curr Opin Genet Dev,* 8**:** 481-486, 1998.
193. Morrisey, EE, Hogan, BL: Preparing for the first breath: genetic and cellular mechanisms in lung development. *Dev Cell,* 18**:** 8-23, 2010.
194. Metzger, RJ, Klein, OD, Martin, GR, Krasnow, MA: The branching programme of mouse lung development. *Nature,* 453**:** 745-750, 2008.
195. Alanis, DM, Chang, DR, Akiyama, H, Krasnow, MA, Chen, J: Two nested developmental waves demarcate a compartment boundary in the mouse lung. *Nat Commun,* 5**:** 3923, 2014.
196. Treutlein, B, Brownfield, DG, Wu, AR, Neff, NF, Mantalas, GL, Espinoza, FH, Desai, TJ, Krasnow, MA, Quake, SR: Reconstructing lineage hierarchies of the distal lung epithelium using single-cell RNA-seq. *Nature,* 509**:** 371-375, 2014.
197. Thurlbeck, WM: Postnatal growth and development of the lung. *Am Rev Respir Dis,* 111**:** 803-844, 1975.
198. Kauffman, SL: Cell proliferation in the mammalian lung. *Int Rev Exp Pathol,* 22**:** 131-191, 1980.
199. Hall, SM, Hislop, AA, Pierce, CM, Haworth, SG: Prenatal origins of human intrapulmonary arteries: formation and smooth muscle maturation. *Am J Respir Cell Mol Biol,* 23**:** 194-203, 2000.
200. deMello, DE, Sawyer, D, Galvin, N, Reid, LM: Early fetal development of lung vasculature. *Am J Respir Cell Mol Biol,* 16**:** 568-581, 1997.
201. Partanen, J, Puri, MC, Schwartz, L, Fischer, KD, Bernstein, A, Rossant, J: Cell autonomous functions of the receptor tyrosine kinase TIE in a late phase of angiogenic capillary growth and endothelial cell survival during murine development. *Development,* 122**:** 3013-3021, 1996.
202. Cohen, ED, Ihida-Stansbury, K, Lu, MM, Panettieri, RA, Jones, PL, Morrisey, EE: Wnt signaling regulates smooth muscle precursor development in the mouse lung via a tenascin C/PDGFR pathway. *J Clin Invest,* 119**:** 2538-2549, 2009.
203. De Langhe, SP, Sala, FG, Del Moral, PM, Fairbanks, TJ, Yamada, KM, Warburton, D, Burns, RC, Bellusci, S: Dickkopf-1 (DKK1) reveals that fibronectin is a major target of Wnt signaling in branching morphogenesis of the mouse embryonic lung. *Dev Biol,* 277**:** 316-331, 2005.
204. Jho, EH, Zhang, T, Domon, C, Joo, CK, Freund, JN, Costantini, F: Wnt/beta-catenin/Tcf signaling induces the transcription of Axin2, a negative regulator of the signaling pathway. *Mol Cell Biol,* 22**:** 1172-1183, 2002.
205. Tebar, M, Destree, O, de Vree, WJ, Ten Have-Opbroek, AA: Expression of Tcf/Lef and sFrp and localization of beta-catenin in the developing mouse lung. *Mech Dev,* 109**:** 437-440, 2001.
206. Eblaghie, MC, Reedy, M, Oliver, T, Mishina, Y, Hogan, BL: Evidence that autocrine signaling through Bmpr1a regulates the proliferation, survival and morphogenetic behavior of distal lung epithelial cells. *Dev Biol,* 291**:** 67-82, 2006.
207. Yeo, EJ, Cassetta, L, Qian, BZ, Lewkowich, I, Li, JF, Stefater, JA, 3rd, Smith, AN, Wiechmann, LS, Wang, Y, Pollard, JW, Lang, RA: Myeloid WNT7b mediates the angiogenic switch and metastasis in breast cancer. *Cancer Res,* 74**:** 2962-2973, 2014.

208. Sherr, CJ, Roberts, JM: Inhibitors of mammalian G1 cyclin-dependent kinases. *Genes Dev,* 9**:** 1149-1163, 1995.
209. Chang, TS, Kim, MJ, Ryoo, K, Park, J, Eom, SJ, Shim, J, Nakayama, KI, Nakayama, K, Tomita, M, Takahashi, K, Lee, MJ, Choi, EJ: p57KIP2 modulates stress-activated signaling by inhibiting c-Jun NH2-terminal kinase/stress-activated protein Kinase. *J Biol Chem,* 278**:** 48092-48098, 2003.
210. Jadasz, JJ, Rivera, FJ, Taubert, A, Kandasamy, M, Sandner, B, Weidner, N, Aktas, O, Hartung, HP, Aigner, L, Kury, P: p57kip2 regulates glial fate decision in adult neural stem cells. *Development,* 139**:** 3306-3315, 2012.
211. Yokoo, T, Toyoshima, H, Miura, M, Wang, Y, Iida, KT, Suzuki, H, Sone, H, Shimano, H, Gotoda, T, Nishimori, S, Tanaka, K, Yamada, N: p57Kip2 regulates actin dynamics by binding and translocating LIM-kinase 1 to the nucleus. *J Biol Chem,* 278**:** 52919-52923, 2003.
212. Yan, Y, Frisen, J, Lee, MH, Massague, J, Barbacid, M: Ablation of the CDK inhibitor p57Kip2 results in increased apoptosis and delayed differentiation during mouse development. *Genes Dev,* 11**:** 973-983, 1997.
213. Hatada, I, Ohashi, H, Fukushima, Y, Kaneko, Y, Inoue, M, Komoto, Y, Okada, A, Ohishi, S, Nabetani, A, Morisaki, H, Nakayama, M, Niikawa, N, Mukai, T: An imprinted gene p57KIP2 is mutated in Beckwith-Wiedemann syndrome. *Nat Genet,* 14**:** 171-173, 1996.
214. Lee, MH, Reynisdottir, I, Massague, J: Cloning of p57KIP2, a cyclin-dependent kinase inhibitor with unique domain structure and tissue distribution. *Genes Dev,* 9**:** 639-649, 1995.
215. Mannens, M, Hoovers, JM, Redeker, E, Verjaal, M, Feinberg, AP, Little, P, Boavida, M, Coad, N, Steenman, M, Bliek, J, et al.: Parental imprinting of human chromosome region 11p15.3-pter involved in the Beckwith-Wiedemann syndrome and various human neoplasia. *Eur J Hum Genet,* 2**:** 3-23, 1994.
216. Matsuoka, S, Edwards, MC, Bai, C, Parker, S, Zhang, P, Baldini, A, Harper, JW, Elledge, SJ: p57KIP2, a structurally distinct member of the p21CIP1 Cdk inhibitor family, is a candidate tumor suppressor gene. *Genes Dev,* 9**:** 650-662, 1995.
217. Matsuoka, S, Thompson, JS, Edwards, MC, Bartletta, JM, Grundy, P, Kalikin, LM, Harper, JW, Elledge, SJ, Feinberg, AP: Imprinting of the gene encoding a human cyclin-dependent kinase inhibitor, p57KIP2, on chromosome 11p15. *Proc Natl Acad Sci U S A,* 93**:** 3026-3030, 1996.
218. Potikha, T, Kassem, S, Haber, EP, Ariel, I, Glaser, B: p57Kip2 (cdkn1c): sequence, splice variants and unique temporal and spatial expression pattern in the rat pancreas. *Lab Invest,* 85**:** 364-375, 2005.
219. Reynaud, EG, Guillier, M, Leibovitch, MP, Leibovitch, SA: Dimerization of the amino terminal domain of p57Kip2 inhibits cyclin D1-cdk4 kinase activity. *Oncogene,* 19**:** 1147-1152, 2000.
220. Gomez Lahoz, E, Liegeois, NJ, Zhang, P, Engelman, JA, Horner, J, Silverman, A, Burde, R, Roussel, MF, Sherr, CJ, Elledge, SJ, DePinho, RA: Cyclin D- and E-dependent kinases and the p57(KIP2) inhibitor: cooperative interactions in vivo. *Mol Cell Biol,* 19**:** 353-363, 1999.

221. Ullah, Z, Kohn, MJ, Yagi, R, Vassilev, LT, DePamphilis, ML: Differentiation of trophoblast stem cells into giant cells is triggered by p57/Kip2 inhibition of CDK1 activity. *Genes Dev,* 22**:** 3024-3036, 2008.
222. Gardner, RL, Davies, TJ: Lack of coupling between onset of giant transformation and genome endoreduplication in the mural trophectoderm of the mouse blastocyst. *J Exp Zool,* 265**:** 54-60, 1993.
223. MacAuley, A, Cross, JC, Werb, Z: Reprogramming the cell cycle for endoreduplication in rodent trophoblast cells. *Mol Biol Cell,* 9**:** 795-807, 1998.
224. Nakayama, H, Scott, IC, Cross, JC: The transition to endoreduplication in trophoblast giant cells is regulated by the mSNA zinc finger transcription factor. *Dev Biol,* 199**:** 150-163, 1998.
225. Hattori, N, Davies, TC, Anson-Cartwright, L, Cross, JC: Periodic expression of the cyclin-dependent kinase inhibitor p57(Kip2) in trophoblast giant cells defines a G2-like gap phase of the endocycle. *Mol Biol Cell,* 11**:** 1037-1045, 2000.
226. Westbury, J, Watkins, M, Ferguson-Smith, AC, Smith, J: Dynamic temporal and spatial regulation of the cdk inhibitor p57(kip2) during embryo morphogenesis. *Mech Dev,* 109**:** 83-89, 2001.
227. Heinen, A, Kremer, D, Hartung, HP, Kury, P: p57 kip2's role beyond Schwann cell cycle control. *Cell Cycle,* 7**:** 2781-2786, 2008.
228. Heinen, A, Kremer, D, Gottle, P, Kruse, F, Hasse, B, Lehmann, H, Hartung, HP, Kury, P: The cyclin-dependent kinase inhibitor p57kip2 is a negative regulator of Schwann cell differentiation and in vitro myelination. *Proc Natl Acad Sci U S A,* 105**:** 8748-8753, 2008.
229. Kavanagh, E, Vlachos, P, Emourgeon, V, Rodhe, J, Joseph, B: p57(KIP2) control of actin cytoskeleton dynamics is responsible for its mitochondrial pro-apoptotic effect. *Cell Death Dis,* 3**:** e311, 2012.
230. Vlachos, P, Joseph, B: The Cdk inhibitor p57(Kip2) controls LIM-kinase 1 activity and regulates actin cytoskeleton dynamics. *Oncogene,* 28**:** 4175-4188, 2009.
231. Arboleda, VA, Lee, H, Parnaik, R, Fleming, A, Banerjee, A, Ferraz-de-Souza, B, Delot, EC, Rodriguez-Fernandez, IA, Braslavsky, D, Bergada, I, Dell'Angelica, EC, Nelson, SF, Martinez-Agosto, JA, Achermann, JC, Vilain, E: Mutations in the PCNA-binding domain of CDKN1C cause IMAGe syndrome. *Nat Genet,* 44**:** 788-792, 2012.
232. Brioude, F, Oliver-Petit, I, Blaise, A, Praz, F, Rossignol, S, Le Jule, M, Thibaud, N, Faussat, AM, Tauber, M, Le Bouc, Y, Netchine, I: CDKN1C mutation affecting the PCNA-binding domain as a cause of familial Russell Silver syndrome. *J Med Genet,* 50**:** 823-830, 2013.
233. Borges, KS, Arboleda, VA, Vilain, E: Mutations in the PCNA-binding site of CDKN1C inhibit cell proliferation by impairing the entry into S phase. *Cell Div,* 10**:** 2, 2015.
234. Engstrom, W, Lindham, S, Schofield, P: Wiedemann-Beckwith syndrome. *Eur J Pediatr,* 147**:** 450-457, 1988.
235. Weksberg, R, Shuman, C, Smith, AC: Beckwith-Wiedemann syndrome. *Am J Med Genet C Semin Med Genet,* 137C**:** 12-23, 2005.
236. Cooper, WN, Luharia, A, Evans, GA, Raza, H, Haire, AC, Grundy, R, Bowdin, SC, Riccio, A, Sebastio, G, Bliek, J, Schofield, PN, Reik, W, Macdonald, F, Maher,

ER: Molecular subtypes and phenotypic expression of Beckwith-Wiedemann syndrome. *Eur J Hum Genet,* 13**:** 1025-1032, 2005.
237. Enklaar, T, Zabel, BU, Prawitt, D: Beckwith-Wiedemann syndrome: multiple molecular mechanisms. *Expert Rev Mol Med,* 8**:** 1-19, 2006.
238. Maher, ER, Reik, W: Beckwith-Wiedemann syndrome: imprinting in clusters revisited. *J Clin Invest,* 105**:** 247-252, 2000.
239. Li, M, Squire, J, Shuman, C, Fei, YL, Atkin, J, Pauli, R, Smith, A, Nishikawa, J, Chitayat, D, Weksberg, R: Imprinting status of 11p15 genes in Beckwith-Wiedemann syndrome patients with CDKN1C mutations. *Genomics,* 74**:** 370-376, 2001.
240. O'Keefe, D, Dao, D, Zhao, L, Sanderson, R, Warburton, D, Weiss, L, Anyane-Yeboa, K, Tycko, B: Coding mutations in p57KIP2 are present in some cases of Beckwith-Wiedemann syndrome but are rare or absent in Wilms tumors. *Am J Hum Genet,* 61**:** 295-303, 1997.
241. Hayashi, S, Lewis, P, Pevny, L, McMahon, AP: Efficient gene modulation in mouse epiblast using a Sox2Cre transgenic mouse strain. *Gene Expr Patterns,* 2**:** 93-97, 2002.
242. Yu, J, Carroll, TJ, McMahon, AP: Sonic hedgehog regulates proliferation and differentiation of mesenchymal cells in the mouse metanephric kidney. *Development,* 129**:** 5301-5312, 2002.
243. Muzumdar, MD, Tasic, B, Miyamichi, K, Li, L, Luo, L: A global double-fluorescent Cre reporter mouse. *Genesis,* 45**:** 593-605, 2007.
244. Nagalakshmi, VK, Ren, Q, Pugh, MM, Valerius, MT, McMahon, AP, Yu, J: Dicer regulates the development of nephrogenic and ureteric compartments in the mammalian kidney. *Kidney Int,* 79**:** 317-330, 2011.
245. Schindelin, J, Arganda-Carreras, I, Frise, E, Kaynig, V, Longair, M, Pietzsch, T, Preibisch, S, Rueden, C, Saalfeld, S, Schmid, B, Tinevez, JY, White, DJ, Hartenstein, V, Eliceiri, K, Tomancak, P, Cardona, A: Fiji: an open-source platform for biological-image analysis. *Nat Methods,* 9**:** 676-682, 2012.
246. Ben-Zvi, A, Lacoste, B, Kur, E, Andreone, BJ, Mayshar, Y, Yan, H, Gu, C: Mfsd2a is critical for the formation and function of the blood-brain barrier. *Nature,* 509**:** 507-511, 2014.
247. Veeman, MT, Slusarski, DC, Kaykas, A, Louie, SH, Moon, RT: Zebrafish prickle, a modulator of noncanonical Wnt/Fz signaling, regulates gastrulation movements. *Curr Biol,* 13**:** 680-685, 2003.
248. Dimke, H, Sparks, MA, Thomson, BR, Frische, S, Coffman, TM, Quaggin, SE: Tubulovascular cross-talk by vascular endothelial growth factor a maintains peritubular microvasculature in kidney. *J Am Soc Nephrol,* 26**:** 1027-1038, 2015.
249. Armulik, A, Genove, G, Betsholtz, C: Pericytes: developmental, physiological, and pathological perspectives, problems, and promises. *Dev Cell,* 21**:** 193-215, 2011.
250. Yu, X, Liu, P, Min, J, Chen, Q: [Regression on order statistics and its application in estimating nondetects for food exposure assessment]. *Wei Sheng Yan Jiu,* 38**:** 89-91, 2009.
251. Hirschi, KK, Rohovsky, SA, Beck, LH, Smith, SR, D'Amore, PA: Endothelial cells modulate the proliferation of mural cell precursors via platelet-derived growth factor-BB and heterotypic cell contact. *Circ Res,* 84**:** 298-305, 1999.

252. Floege, J, Topley, N, Hoppe, J, Barrett, TB, Resch, K: Mitogenic effect of platelet-derived growth factor in human glomerular mesangial cells: modulation and/or suppression by inflammatory cytokines. *Clin Exp Immunol,* 86**:** 334-341, 1991.
253. Hellstrom, M, Kalen, M, Lindahl, P, Abramsson, A, Betsholtz, C: Role of PDGF-B and PDGFR-beta in recruitment of vascular smooth muscle cells and pericytes during embryonic blood vessel formation in the mouse. *Development,* 126**:** 3047-3055, 1999.
254. Soriano, P: Abnormal kidney development and hematological disorders in PDGF beta-receptor mutant mice. *Genes Dev,* 8**:** 1888-1896, 1994.
255. Armulik, A, Abramsson, A, Betsholtz, C: Endothelial/pericyte interactions. *Circ Res,* 97**:** 512-523, 2005.
256. Rhodin, JAG: *Histology,* New York, Oxford University Press, 1974.
257. Siminescu, N, Simionescu, M: (Eds.) *Endothelial Cell Biology In Health and Disease,* New York, Plenum Press, 1988.
258. Carmeliet, P, Lampugnani, MG, Moons, L, Breviario, F, Compernolle, V, Bono, F, Balconi, G, Spagnuolo, R, Oosthuyse, B, Dewerchin, M, Zanetti, A, Angellilo, A, Mattot, V, Nuyens, D, Lutgens, E, Clotman, F, de Ruiter, MC, Gittenberger-de Groot, A, Poelmann, R, Lupu, F, Herbert, JM, Collen, D, Dejana, E: Targeted deficiency or cytosolic truncation of the VE-cadherin gene in mice impairs VEGF-mediated endothelial survival and angiogenesis. *Cell,* 98**:** 147-157, 1999.
259. Lagendijk, AK, Hogan, BM: VE-cadherin in vascular development: a coordinator of cell signaling and tissue morphogenesis. *Curr Top Dev Biol,* 112**:** 325-352, 2015.
260. Wang, Y, Kaiser, MS, Larson, JD, Nasevicius, A, Clark, KJ, Wadman, SA, Roberg-Perez, SE, Ekker, SC, Hackett, PB, McGrail, M, Essner, JJ: Moesin1 and Ve-cadherin are required in endothelial cells during in vivo tubulogenesis. *Development,* 137**:** 3119-3128, 2010.
261. Yang, S, Graham, J, Kahn, JW, Schwartz, EA, Gerritsen, ME: Functional roles for PECAM-1 (CD31) and VE-cadherin (CD144) in tube assembly and lumen formation in three-dimensional collagen gels. *Am J Pathol,* 155**:** 887-895, 1999.
262. Strilic, B, Eglinger, J, Krieg, M, Zeeb, M, Axnick, J, Babal, P, Muller, DJ, Lammert, E: Electrostatic cell-surface repulsion initiates lumen formation in developing blood vessels. *Curr Biol,* 20**:** 2003-2009, 2010.
263. Hurtado, R, Zewdu, R, Mtui, J, Liang, C, Aho, R, Kurylo, C, Selleri, L, Herzlinger, D: Pbx1-dependent control of VMC differentiation kinetics underlies gross renal vascular patterning. *Development,* 142**:** 2653-2664, 2015.
264. Little, MH, Brennan, J, Georgas, K, Davies, JA, Davidson, DR, Baldock, RA, Beverdam, A, Bertram, JF, Capel, B, Chiu, HS, Clements, D, Cullen-McEwen, L, Fleming, J, Gilbert, T, Herzlinger, D, Houghton, D, Kaufman, MH, Kleymenova, E, Koopman, PA, Lewis, AG, McMahon, AP, Mendelsohn, CL, Mitchell, EK, Rumballe, BA, Sweeney, DE, Valerius, MT, Yamada, G, Yang, Y, Yu, J: A high-resolution anatomical ontology of the developing murine genitourinary tract. *Gene Expr Patterns,* 7**:** 680-699, 2007.
265. Schuster, VL: Function and regulation of collecting duct intercalated cells. *Annu Rev Physiol,* 55**:** 267-288, 1993.
266. Saburi, S, Hester, I, Fischer, E, Pontoglio, M, Eremina, V, Gessler, M, Quaggin, SE, Harrison, R, Mount, R, McNeill, H: Loss of Fat4 disrupts PCP signaling and

oriented cell division and leads to cystic kidney disease. *Nat Genet,* 40**:** 1010-1015, 2008.
267. Orlidge, A, D'Amore, PA: Inhibition of capillary endothelial cell growth by pericytes and smooth muscle cells. *J Cell Biol,* 105**:** 1455-1462, 1987.
268. Matsuura, T, Takahashi, K, Nakayama, K, Kobayashi, T, Choi-Miura, NH, Tomita, M, Kanayama, N: Increased expression of vascular endothelial growth factor in placentas of p57(Kip2) null embryos. *FEBS Lett,* 532**:** 283-288, 2002.
269. West, JB: Thoughts on the pulmonary blood-gas barrier. *Am J Physiol Lung Cell Mol Physiol,* 285**:** L501-513, 2003.
270. Tanaka, S, Terada, K, Nohno, T: Canonical Wnt signaling is involved in switching from cell proliferation to myogenic differentiation of mouse myoblast cells. *J Mol Signal,* 6**:** 12, 2011.
271. Gerhardt, H, Betsholtz, C: Endothelial-pericyte interactions in angiogenesis. *Cell Tissue Res,* 314**:** 15-23, 2003.
272. Luo, Y, Radice, GL: N-cadherin acts upstream of VE-cadherin in controlling vascular morphogenesis. *J Cell Biol,* 169**:** 29-34, 2005.
273. Prandini, MH, Dreher, I, Bouillot, S, Benkerri, S, Moll, T, Huber, P: The human VE-cadherin promoter is subjected to organ-specific regulation and is activated in tumour angiogenesis. *Oncogene,* 24**:** 2992-3001, 2005.
274. Lelievre, E, Mattot, V, Huber, P, Vandenbunder, B, Soncin, F: ETS1 lowers capillary endothelial cell density at confluence and induces the expression of VE-cadherin. *Oncogene,* 19**:** 2438-2446, 2000.